Functional and genetic analysis of alpha-synuclein and huntingtin in *Drosophila melanogaster*

Gonçalo Manuel Poças

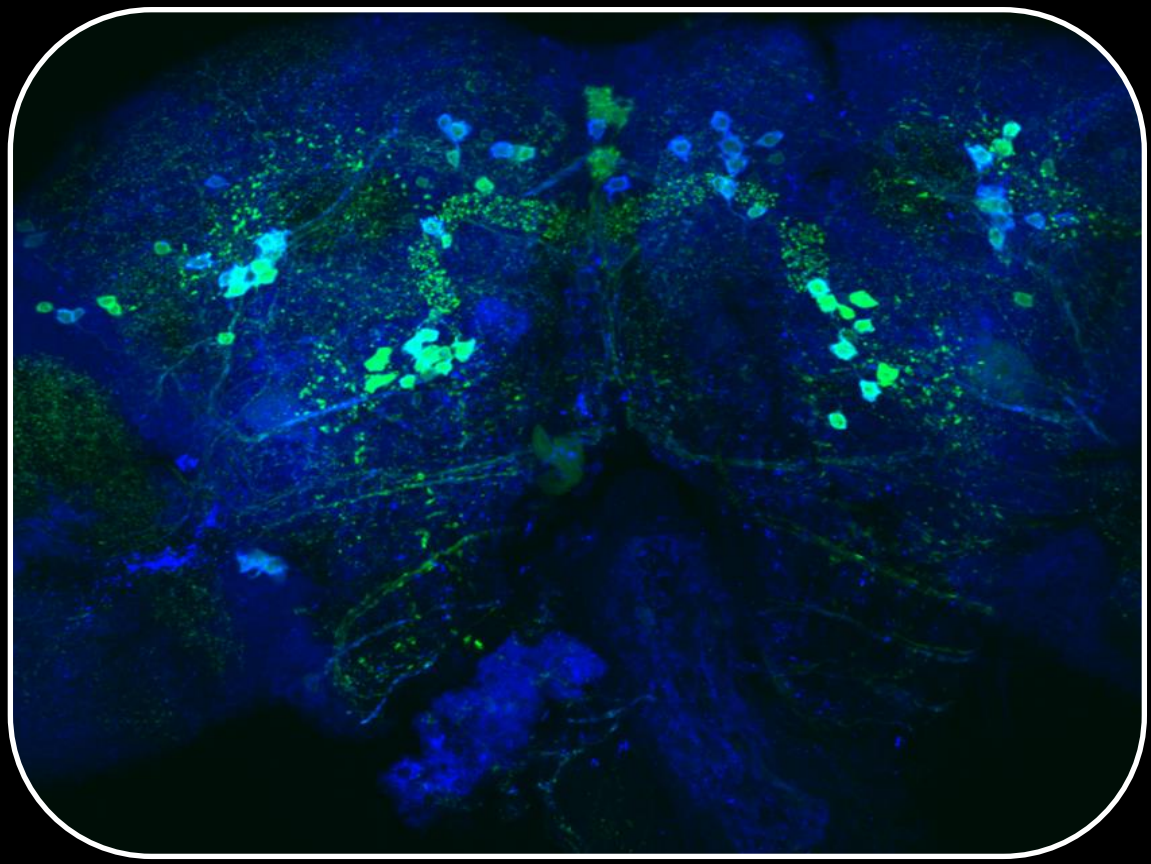

Dissertation presented to obtain the Ph.D degree in Biochemistry

Instituto de Tecnologia Química e Biológica António Xavier | Universidade Nova de Lisboa

Oeiras,
December, 2015

INSTITUTO
DE TECNOLOGIA
QUÍMICA E BIOLÓGICA
ANTÓNIO XAVIER /UNL

Knowledge Creation

ITQB-UNL | Av. da República, 2780-157 Oeiras, Portugal
Tel (+351) 214 469 100 | Fax (+351) 214 411 277

www.itqb.unl.pt

Functional and genetic analysis of alpha-synuclein and huntingtin in *Drosophila melanogaster*

Gonçalo Manuel Poças

Dissertation presented to obtain the Ph.D degree in Biochemistry

Instituto de Tecnologia Química e Biológica António Xavier | Universidade Nova de Lisboa

Oeiras, December, 2015

INSTITUTO
DE TECNOLOGIA
QUÍMICA E BIOLÓGICA
ANTÓNIO XAVIER /UNL

Knowledge Creation

Title: Functional and genetic analysis of alpha-synuclein and huntingtin in *Drosophila melanogaster*

Dissertation presented to obtain the Ph.D. degree in Biochemistry

Author: Gonçalo Manuel Poças

Cell Signaling in Drosophila Laboratory
Instituto de Tecnologia Química e Biológica
Universidade Nova de Lisboa
Av. da República
Estação Agronómica Nacional
2780-157 Oeiras
Portugal

Front cover picture: image obtained by confocal microscopy of a *Drosophila* brain expressing alpha-synuclein (green) in the dopaminergic neurons marked by a specific antibody for Tyrosine Hydroxylase (blue).

I declare that the work presented in this thesis, except where otherwise stated, is based on my own research and it was supervised by Doctor Pedro Manuel Domingos. The work was mainly performed in Instituto de Tecnologia Química e Biológica, Universidade Nova de Lisboa.

I am grateful for the financial support provided by Fundação para a Ciência e Tecnologia (grant reference SFRH/BD/61477/2009).

Aos meus pais

Table of contents

Acknowledgements

I would like to express my sincere gratitude to everyone who directly or indirectly helped me to complete this thesis.

To my supervisor, Pedro Domingos, for allowing me to join his group in 2008 when I was a master's student, introducing me to the wonderful world of *Drosophila*. Thank you for teaching me all the basics of *Drosophila* genetics and crucial tricks and for giving me the freedom of exploring it on my own during my PhD studies. Thank you for supporting me in the critical phases of my PhD, both at the scientific and personal levels.

To all the present and former members of the group "Cell Signaling in Drosophila" at ITQB. I would like to thank in particular to Fátima Cairrão, for guiding me in some of the molecular biology techniques used in the beginning of my PhD, to Vania Rasheva, for the support with *Drosophila* genetics, to Catarina Gaspar, for all the nice scientific discussions, friendship and companionship and to Yolanda Afonso, for helping me in the last 6 months in some of my PhD projects.

To my collaborators Federico Herrera and Tiago Outeiro, who strongly contributed to make the work in this thesis possible. I am also grateful to Maria Luísa Vasconcelos for being part of my PhD thesis committee, together with Tiago Outeiro, and for all the good scientific input and also for providing me some fly stocks which were extremely useful during my PhD studies.

I also acknowledge the Fundação para Ciência e a Tecnologia (FCT) of Ministry for Education and Science of Portugal for the indispensable financial support under my PhD grant SFRH/BD/61477/2009. To Instituto de Tecnologia Química e Biológica (ITQB) from Universidade Nova de Lisboa for giving me the opportunity of performing my PhD studies in a very good and stimulating environment, at the technical and intellectual levels. To Instituto Gulbenkian de Ciência (IGC) for allowing me to use its facilities, especially the imaging unit.

To all my colleagues and friends from the ITQB PhD program, especially to Cláudia Queiroga, Lia Domingues, Neuza Teixeira, Rui Pimpão and Margarida Saramago for the support and funny moments spent together. To all the people from the former Tiago Outeiro's group UNCM at IMM, especially to Joana Branco-Santos for collaborating with me in some of my PhD projects, to Patricia Guerreiro for helping me with the mass spectrometry experiments and to Leonor Fleming for all her support, nice scientific discussions and friendship.

To Diego Hartmann and Marija Petkovic for the friendship and companionship during this long journey. Thank you for all the lunches we had together, for all the funny moments, good conversations, advises and for supporting me throughout all the frustrations and less positive periods but also for sharing in the joy of the successes. To Luís Miguel Oliveira, who even from the other side of the Atlantic Ocean, finds a way of encourage and support me.

Finally, to all my dear friends and family for the love and support, with especial words to my mother and my father, who always supported and believed in me in all stages of my life, to my grandmother Deolinda, to my grandfather António Melo and to my brother. To my dear grandparents Maria do Carmo and Carlos Poças, who must be very proud, wherever they are. To Jaime for all his support and words full of positive energy. To Filipe Martins and Alpio James Aquilina for their great friendship and companionship. To Rui for the extremely good moments during this last year, making everything look a bit easier.

Muito obrigado a todos!

"Learn from yesterday, live for today, hope for tomorrow.
The important thing is not to stop questioning."

Albert Einstein

Summary

In this work we established new transgenic *Drosophila* models for Parkinson's (PD) and Huntington's disease (HD), two incurable devastating human neurodegenerative diseases, which strongly compromise the patients' motor abilities. Our *Drosophila* models are based on the transgenic overexpression of fluorescent-tagged versions of two human neuronal proteins extensively associated with these neuropathologies, but whose exact biological function is still unknown: alpha-synuclein (α-syn) for PD and huntingtin (Htt) for HD.

Here, we investigated whether the subcellular localization of α-syn and the defective axonal transport of this protein is relevant to the development of PD. Using a *Drosophila* model for PD based on the overexpression of EGFP-tagged versions of the wild-type and the familiar A30P mutant form of human α-syn, we observed a differential subcellular localization of the two versions of α-syn in the photoreceptors: while wild-type α-syn was enriched in pre-synaptic terminals, α-syn A30P was distributed throughout the cytoplasm of the photoreceptors, both in cell bodies and axons. We have identified, by immunoprecipitation and mass spectrometry, the specific neuronal proteins interacting with wild-type and A30P α-syn, and by knocking-down the genes of these proteins we identified three candidates as neuronal modulators of α-syn's axonal transport and subcellular localization: Tomosyn, Spaghetti Squash, and Synaptotagmin 4.

We also studied the role of N-terminal phosphorylation of mutant Htt in HD. We used our *Drosophila* model for HD, based on the overexpression of a mCherry-tagged version of the N-terminal truncated form of mutant human Htt, encoded by the exon 1 of Htt gene (Httex1). We analyzed the relative contribution of the phosphorylation state of each phosphorylatable residue in the first 17 amino acids of the N-terminal domain (NT17) towards Httex1 aggregation and toxicity in our *Drosophila* model and in mammalian cells in

culture. We demonstrated that single phosphorylation events in NT17 and specific protein phosphatases can modulate mutant Htt aggregation and neurotoxicity, depending on the biological context. Our findings suggest that single phosphorylation events at NT17 could be a more effective therapeutic approach against HD.

Taking advantage of our newly established *Drosophila* models for PD and HD, we also investigated the possible crosstalk between these two neuropathologies, by studying the interaction of α-syn and Htt, at the genetic and functional levels. We showed that α-syn and mutant Htt co-aggregate in vivo when co-expressed in *Drosophila* and produce a synergistic age-dependent increase in neurotoxicity associated to a decline in motor function and life span. Our results suggest that the co-existence of α-syn and Htt in the same neuronal cells worsens aggregation-related neuropathologies, accelerating the disease progression.

Finally, we wanted to test the therapeutic properties of mannosylglycerate (MG) in our *Drosophila* models for PD and HD. The biosynthesis of MG can be catalyzed by MG synthase (MGSD). We successfully generated transgenic lines expressing MGSD, but we could not detect the biosynthesis and accumulation of MG in *Drosophila*.

We hope this work will contribute for a better understanding of the molecular and cellular bases of PD and HD and that our new *Drosophila* models for these pathologies may constitute one more useful platform available to scientific community working in the area.

Sumário

Neste trabalho estabelecemos novos modelos transgénicos de *Drosophila* para as doenças de Parkinson (DP) e de Huntington (DH), duas doenças humanas neurodegenerativas devastadoras e incuráveis que afectam significativamente o controlo motor dos doentes. Os nossos modelos de *Drosophila* baseiam-se na sobrexpressão de duas proteínas neuronais humanas associadas a estas neuropatologias e para as quais a função biológica é desconhecida: alpha-synuclein (α-syn) para a DP e huntingtin (Htt) para a DH.

Um dos nossos objectivos consistia em investigar se a localização sub-celular da α-syn e o anormal transporte axonal desta proteína são relevantes no desenvolvimento da DP. Utilizando um modelo de *Drosophila* para a DP, baseado na sobrexpressão das formas "wild-type" e mutante A30P da α-syn fundidas com a "tag" fluorescente EGFP, observámos que o fenótipo relativo à localização sub-celular da α-syn é distinto para as duas formas da α-syn: a forma "wild-type" localiza-se predominantemente nos terminais pré-sinápticos, enquanto que a mutante A30P distribui-se por todo o citoplasma dos fotoreceptores, tanto nos corpos celulares como nos axónios. Através de imunoprecipitação e espectrometria de massa, foi possível identificar as proteínas que interagem especificamente com as versões "wild-type" e mutante da α-syn e através do "knocking-down" dos genes que codificam para estas proteínas conseguimos identificar três candidatos a moduladores da localização sub-celular e do transporte axonal da α-syn: Tomosyn, Spaghetti Squash, and Synaptotagmin 4.

Também estudámos o papel da fosforilação da porção N-terninal da Htt mutante na DH. Para isso, utilizámos o nosso modelo de *Drosophila* para a DH, baseado na sobrexpressão de uma versão truncada da porção N-terminal da Htt mutante, codificada pelo exão 1 do gene da Htt (Httex1). Assim, foi possível analisar, no nosso modelo de *Drosophila* e em células de mamífero em cultura, a contribuição relativa do estado de fosforilação de cada um dos

resíduos fosforiláveis nos primeiros 17 aminoácidos do domínio N-terminal (NT17) para os níveis de agregação e toxicidade da Httex1. Foi demonstrado que eventos únicos de fosforilação no NT17 e fosfatases especificas modulam efectivamente os níveis de agregação e neurotoxicidade da Htt mutante, de uma forma que é dependente do contexto biológico. Assim, os nossos resultados sugerem que eventos únicos de fosforilação no NT17 poderão constituir uma estratégia terapêutica mais eficaz contra a DH.

Tirando partido dos novos modelos de *Drosophila* para as DP e DH estabelecidos neste trabalho, o possível "crosstalk" entre estas duas doenças foi também investigado, através do estudo da interacção genética e funcional da α-syn e Htt. Desta forma, demonstrámos que a α-syn e a Htt mutante, quando co-expressas em *Drosophila*, co-agregam "in vivo" e aumentam, de uma forma sinergística e dependente da idade, a neurotoxicidade, disfunções motoras e mortalidade. Assim, os nossos resultados sugerem que a co-existência da α-syn e Htt nas mesmas células neuronais poderá exacerbar as neuropatologias relacionadas com a agregação de proteínas, podendo acelerar a progressão destas doenças.

Por último, também pretendiamos testar as propriedadades terapêuticas do manosilglicerato (MG) nos nossos modelos de *Drosophila* para as DP e DH. A biosíntese do MG pode ser catalizada pela MG sintetase (MGSD). Foi possível produzir linhas transgénicas a expressar MGSD, mas não conseguimos detectar a biosíntese e acumulação de MG em *Drosophila*.

Esperamos que este trabalho possa contribuir para um melhor conhecimento das bases moleculares e celulares das DP e DH e que os nossos novos modelos de *Drosophila* para estas patologias constituam mais uma plataforma disponível para a comunidade cientifica a trabalhar nesta área.

Thesis publications

Poças GM, Branco-Santos J, Herrera F, Outeiro TF, and Domingos P (2014) α-Synuclein modifies mutant Huntingtin aggregation and neurotoxicity in Drosophila. Human Molecular Genetics, 2015, 24(7):1898-907. DOI: 10.1093/hmg/ddu606

Manuscripts in preparation

Branco-Santos J*, Poças GM*, Herrera F, Domingos PM, Giorgini F, and Outeiro TF N-terminal phosphorylation modulates mutant huntingtin aggregation and neurotoxicity. * Equal contribution.

Poças GM, Afonso Y, Outeiro TF, Domingos PM Subcellular localization and axonal tranport of α-Synuclein in a Drosophila model for Parkinson's disease.

List of acronyms

aa – Amino acids

AD – Alzheimer's disease

BiFC – Bimolecular Fluorescence Complementation

CAG – Cytosine-adenine-guanine triplet repeats

CNS – Central nervous system

Co-IP – Co-immunoprecipitation

CS – Compatible solutes

DA – Dopaminergic

DMSO – Dimethylsulfoxide

EIF4G1 – Eukaryotic translation initiation factor 4-gamma 1

GAL4/UAS – GAL4-dependent upstream activating sequence

GFP – Green fluorescent protein

GO – Gene ontology

GWAS – Genome Wide Association Studies

HD – Huntington's disease

Htt – Huntingtin

Httex1 – Exon 1 of Htt gene

LDH – Lactate dehydrogenase

Lrrk2 – Leucine-rich repeat kinase 2

MG – Mannosylglycerate

MGSD – Mannosylglycerate synthase

MSN – Medium spiny neurons

NMR – Nuclear magnetic resonance

NT17 – First 17 amino acid residues in the Htt N-terminal

PBS – Phosphate-buffered saline

PD – Parkinson's disease

PolyQ – Polyglutamine

PRR – Proline-rich region

PTMs – Post-translational modifications

RP – Retinitis pigmentosa

S13 – Serine 13

S16 – Serine 16

SNCA – alpha-synuclein gene (non A4 component of amyloid precursor)

SNpc – Substantia nigra pars compacta

T3 – Threonine 3

TLC – Thin layer chromatography

UAS – Upstream activating sequence

VPS35 – Vacuolar protein sorting 35 homolog

VTA – Ventral tegmental area

α-syn – alpha-synuclein

Chapter I

General Introduction

1.1. Human neurodegenerative diseases

Human neurodegenerative diseases are a heterogeneous group of devastating age-dependent disorders for which there is no cure or effective symptomatic treatments.

These neuropathologies are characterized by the selective and progressive loss of specific neuronal cells. The clinical manifestations of each disease are determined by the region of the brain that degenerates (Table 1.1). Although most neurodegenerative disorders display an array of neural symptoms, they may be grouped and categorized in two major groups: movement disorders and dementias. Movement disorders are mainly characterized by the loss of motor control, in the form of tremor, chorea, akinesia, bradykinesia or ataxia, for example. Parkinson's disease (PD) and Huntington's disease (HD) belong to this category, although they frequently show cognitive deficits and psychiatric problems concomitant to motor deficits [1]. Dementias are mainly characterized by a severe loss of cognitive function, as it occurs in Alzheimer's disease (AD), fronto-temporal dementia or dementia with Lewy bodies (LB). However, dementias can also be accompanied by motor symptoms [2].

Table 1.1. Clinical, pathological and biochemical features of neurodegenerative diseases. Extracted from [3].

Disease	Mode of transmission	Clinical features	Affected regions of the brain	Protein involved	Cellular location of aggregates
Alzheimer's	Sporadic (95%) or inherited (5%)	Progressive dementia	Hippocampus, cerebral cotex	Amyloid-β and tau	Extracellular, cytoplasmic
Parkinson's	Mostly sporadic, rarely inherited	Movement disorder	Substantia nigra, hypothalamus	α-Synuclein	Cytoplasmic
Huntington's	Inherited (autosomal dominant)	Dementia, motor and psychiatric problems	Striatum, cerebral cortex	Huntingtin	Nuclear
Amyotrophic lateral sclerosis	Sporadic (90%) or inherited (10%)	Movement disorder	Motor cortex, brainstem	Superoxide dismutase	Cytoplasmic
Transmissible spongiform encephalopathies	Sporadic (90%), inherited (8%) or infectious (2%)	Dementia, ataxia, psychiatric problems or insomnia	Various regions depending on the disease	Prion protein	Extracellular

The genes responsible for many of the existing neurodegenerative diseases have been identified, and they can be genetically inherited in a recessive or dominant manner, depending on the disease. However, a high percentage of cases are sporadic, being their causes and the associated risks unclear. This is especially true for PD and AD, which are the two most frequent neurodegenerative disorders [4]. Approximately 95% of PD cases appear without a family history or a specific mutation [5].

The misfolding, aggregation and accumulation of neuronal proteins into protein inclusions constitutes a common hallmark to most human neurodegenerative diseases (Fig. 1.1).

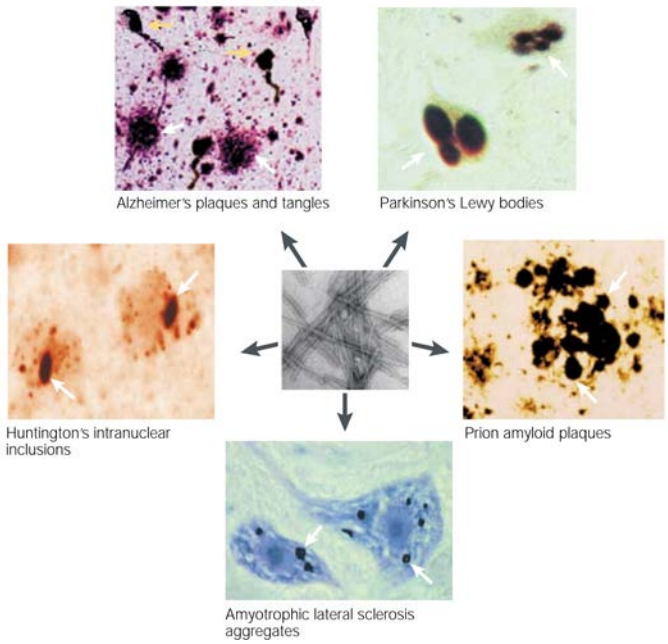

Figure 1.1. The formation of protein aggregates constitutes a common hallmark of human neurodegenerative diseases. Although the cellular and subcellular localization and the protein composition of these aggregates may be different, its ultrastructure seems to be similar and enriched in fibrillar polymers (center). Adapted from [3].

Protein aggregates are visible in cells and tissues with basic microscopic techniques, and still constitute the main post-mortem diagnostic tool for neurodegenerative disorders, including PD [6, 7].

However, protein aggregation is a dynamic process that involves seeding/nucleation mechanisms starting with the formation of small soluble oligomeric species. This intermediate state of aggregation has a high tendency to become stabilized by the formation of an oligomeric β-sheet structure, which by incorporation of additional monomers gives rise to protofibrils and finally to cross-β amyloid-like fibrils. Therefore protein oligomers constitute the nucleus material from which protein aggregates start forming and growing, giving rise to the typical protein amyloid-like inclusions observed in AD, PD and HD [8-10]. The generic term “amyloid” is commonly used to refer to the cross-β structure of the aggregates with binding affinities to Congo red and thioflavin S dies.

If large protein aggregates are the toxic entities responsible for neurodegeneration or a protective response against other toxic species is still widely debatable. There are several reports supporting a neurotoxic role for fibrillary aggregates, in which large aggregates containing misfolded proteins may interfere with the normal function of other neuronal proteins, by sequestering them in these aggregates.[11-16].

However, the hypothesis that the large protein aggregates may constitute a cellular defense mechanism against more toxic smaller aggregates, or monomers, dimers, oligomers and protofibrils, has lately gained great support by the scientific community (Fig. 1.2).

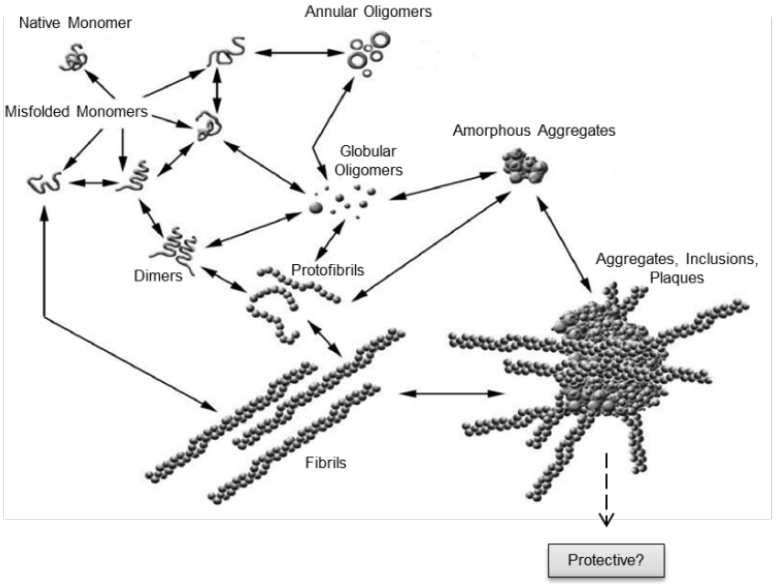

Figure 1.2. Schematic representation of the process involved in the formation of amyloid inclusions in human neurodegenerative diseases. Several factors (such as, mutations, environmental stress and aging) may contribute to the misfolding and aggregation of native soluble monomer proteins. These aggregated monomers can adopt abnormal conformational structures, generating different intermediate species of aggregates (dimers, oligomers and protofibrils). A variety of complex pathways eventually give rise to large amyloid plaques, enriched in β-sheet fibrils, a histopathological hallmark of most human neurodegenerative diseases. These large aggregates were originally considered neurotoxic but accumulating evidences suggest they may have a cytoprotective role. Adapted from [17].

For example, in AD the cognitive impairment is not correlated with the density of Aβ plaques [18, 19], being the concentration of soluble Aβ much strongly correlated with the severity of the disease [20-22]. Equivalently, in PD LB could have a protective role, since the neurons where these inclusions are mostly found are healthier than adjacent neurons with no inclusions [23]. Soluble oligomeric species are often able to cross membranes, move between cell compartments and outside the cell, interacting with several macromolecules and consequently interfering with normal cell functions [24, 25].

The role of protein aggregates in neuropathologies remains poorly understood and more studies are necessary to clarify if these aggregates and the correspondent molecular mechanisms associated to protein aggregation may be efficiently therapeutically targeted.

1.2. Parkinson's disease

1.2.1. Epidemiology, symptoms and general molecular features

PD was firstly described in 1817 by James Parkinson as the "shaking palsy" (Figure 1.3). The most prominent clinical symptoms are related to motor functions: tremor, bradykinesia (slowness of movement), rigidity and postural instability. In later stages, cognitive and behavioral functions may also be affected. Post-mortem analyses of PD brains revealed that PD is the second most frequent human neurodegenerative disease after AD, affecting approximately 10 million patients worldwide.

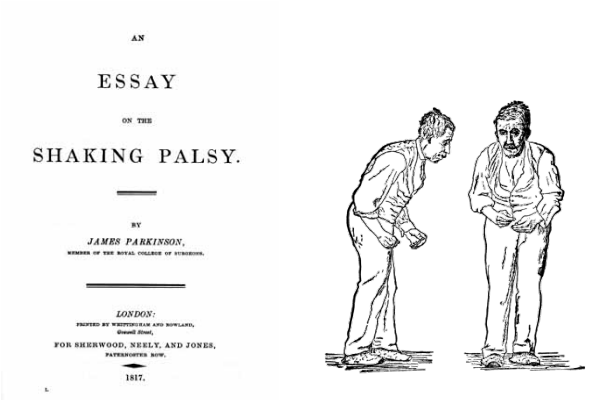
AN

ESSAY

ON THE

SHAKING PALSY.

BY

JAMES PARKINSON,

LONDON:

FOR SHERWOOD, NEELY, AND JONES,

1817.

Figure 1.3. First scientific description of Parkinson's disease (PD) by James Parkinson in "An essay on the shanking palsy, 1817" and the illustration of this pathology by William Richard Gowers published in "A manual of diseases of the nervous system, 1886".

PD is primarily an age-related disease and the number of affected individuals is expected to increase significantly in the next decades as global population ages (Figure 1.4).

PD, and neurodegenerative disorders in general, constitutes an enormous socio-economic burden. For example, the current cost of the treatments for patients with PD in United States is higher than 14 billion dollars per year [26].

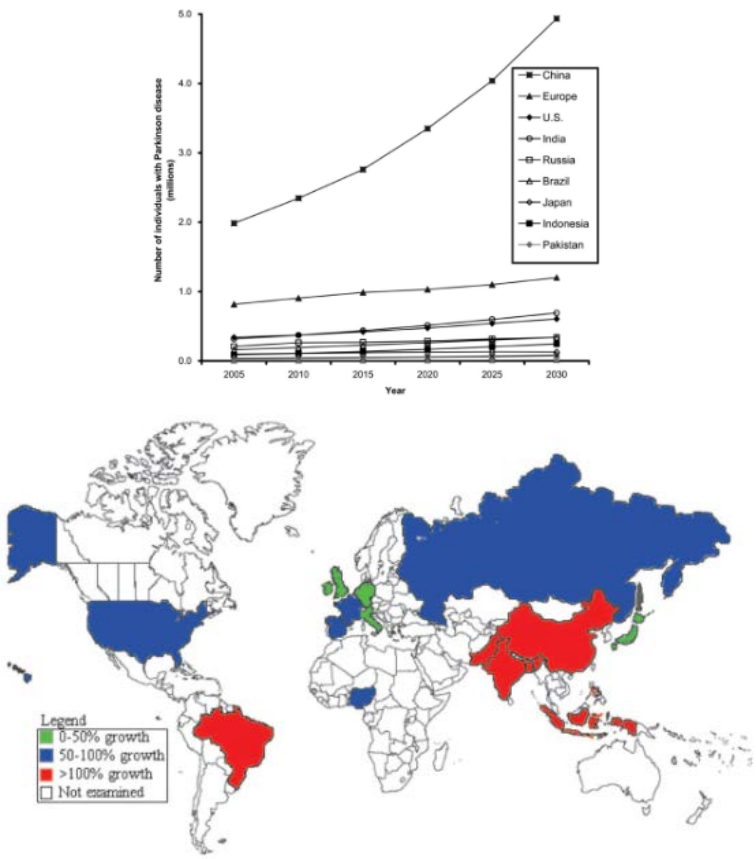

Figure 1.4. Projection of the grow rates (on the left) and of the number of patients suffering from Parkinson's disease (PD) (on the right) from 2005 until 2030. Extracted from [27].

The presence of intraneuronal inclusions in surviving neurons, called LB, constitutes one of the hallmarks of post-mortem brain analysis of patients suffering from PD (Fig. 1.5). In PD the region of the brain most affected by degeneration are the dopaminergic (DA) neurons from the *substantia nigra pars compacta* (SNpc).

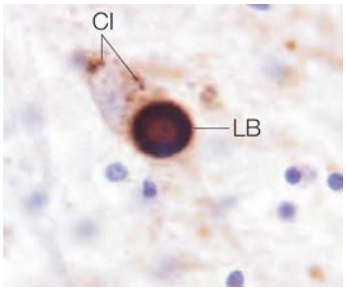

Figure 1.5. Lewy body (LB) and other cytoplasmic inclusions (CI) enriched in α-synuclein (α-syn) within the neurons of the dopaminergic neurons (DA) from substantia nigra pars compacta (SNpc) constitute an hallmark in Parkinson's disease (PD). Extracted from [28].

PD is mostly sporadic, with familial forms constituting approximately 10% of affected individuals. Eleven genes were associated to the familial forms of PD (Table 1.2).

Table 1.2. Genetic loci associated to Mendelian Parkinson's disease (PD). Extracted from [29].

Gene	Mutations	Inheritance (penetrance)	Gene product	Phenotype[a]
Autosomal dominant PD				
LRRK2, *Leucine-rich repeat kinase 2* (PARK 8)	G2019S, N1437H, R1441C/G/H, Y1699C, I2020T	AD (incomplete, age dependent)	Lrrk2 (dardarin)	PD
SNCA (PARK 1/4)	Triplication Duplication A53T, A30P, H50Q, G51D, E46K	AD (high)	α-synuclein	PD, MDD
VPS35	D620N	AD (incomplete)	Vacuolar protein sorting 35 homolog	PD
EIF4G1	R1205H	AD	Eukaryotic translation initiation factor 4-gamma 1	PD
Autosomal recessive PD				
PRKN (PARK2)	>100 different mutations	AR	Parkin, E3 protein ligase	EO PD
PINK1 (PARK6)	>40 different mutations	AR	PTEN-induced kinase 1	EO PD
DJ-1 (PARK7)	>10 different mutations	AR	Daisuke-Junko-1	EO PD
ATP13A2 (PARK9)	Duplications G877R, L1059, F182L, G504R	AR	Lysosomal P-type ATPase	EO PD, P-P
PLA2G6 (PARK14)	R741Q, R747W, Q452X, R635Q, R632W, D331Y	AR	Calcium-independent. phospholipase A2	EO PD, P-P
FBXO7 (PARK 15)	R378G, R498X, T22M	AR	F-box only protein 7	PD, P-P
DNAJC6		AR	Neuronal-specific clathrin-uncoating co-chaperone auxilin	CO P-P

[a] CO, childhood onset; EO, early onset; LO, late onset; MDD, myoclonus, dementia, dysautonomia (atypical forms); P-P, parkinsonism-pyramidal syndrome; PD, classical PD (levodopa-responsive parkinsonism).

Four of these loci are causative of autosomal dominant PD: SNCA, encoding α-synuclein (α-syn); LRRK2, encoding leucine-rich repeat kinase 2; VPS35, encoding Vacuolar protein sorting 35 homolog and EIF4G1, Eukaryotic translation initiation factor 4-gamma 1.

SNCA gene was the first to be identified as being associated to PD and encodes α-syn, a neuronal protein of unknown function. Because α-syn is the principal component of the LB, it is considered a major player in this neuropathology. Several mutations have been mapped to SNCA locus, including missense mutations and genomic duplications or triplications, which account for the second most common cause of dominant PD.

Mutations in LRRK2 are the most common genetic cause of dominant PD, accounting for 10% of all familial forms. Lrrk2 is a cytosolic protein with two predicted enzymatic domains, one with GTPase and another with kinase activity. Although the exact biological function is unknown, it has been associated with neurite formation and growth, maintenance of the cytoskeleton, vesicle trafficking and autophagy [30-

34]. More recently, mutant versions of VPS35 and EIF4G1 were linked to autosomal PD. VPS35 is one of the components of the tripartite complex retromer, involved in the endosomal-lysosomal trafficking. The mutant forms of VPS35 may affect the development of DA neurons through the Wnt pathway [35, 36] and abnormal iron accumulation in the brain by the DMT1 pathway [37, 38]. EIF4G1 is involved in mRNA translation [39].

Although the familial forms of PD constitute a minority, the identification of PD loci has enabled the study and characterization of some of the molecular mechanisms of idiopathic PD. For example, mutant forms of Parkin, Pink 1 and F-box only protein 7 have been implicated in the dysregulation of normal mitophagy [40-43], and mutations in the genes encoding Lrrk2 and VPS35 may disrupt normal processes of protein degradation by the autophagy/lysosomal pathway, ultimately leading to the accumulation of cytotoxic misfolded proteins and cell death [44-47].

Besides the classical linkage analysis, genome-wide association studies (GWAS) allowed to identify risk loci associated to sporadic forms of PD (Table 1.3). However, the specific roles of these genes in the molecular basis of PD remain unknown.

Whether PD is familiar or idiopathic, and regardless the mutations and genes involved, α-syn is the main constituent of LB in the brain, being for this reason considered a major player in PD.

Table 1.3. Risk loci identified by several genome-wide association studies (GWAS) as being associated with sporadic Parkinson's disease (PD). Adapted from [48].

MAPT	Microtubule-associated protein tau
RAB7L1	RAB7, member RAS oncogene family-like 1
BST1	Bone marrow stromal cell antigen 1
HLA-DRB5	Major histocompatibility complex, class II, DR beta 5
GAK/	Cyclin-G-associated kinase
ACMSD	Aminocarboxymuconate semialdehyde decarboxylase
STK39	Serine threonine kinase 39
SYT11	Synaptotagmin XI
FGF20	Fibroblast growth factor 20
STX1B	Syntaxin 1B
GPNMB	Glycoprotein (transmembrane) nmb
SIPA1L2	Signal-induced proliferation-associated 1 like 2
INPP5F	Inositol polyphosphate-5-phosphatase F
MIR4697HG	MIR4697 host gene (non-protein coding)
GCH1	GTP cyclohydrolase 1
VPS13C	Vacuolar protein sorting 13 homolog C (*S. cerevisiae*)
DDRGK1	DDRGK domain containing 1
MCCC1	Methylcrotonoyl-CoA carboxylase 1 (alpha)
SCARB2	Scavenger receptor class B, member 2
CCDC62	Coiled-coil domain containing 62
RIT2	Ras-like without CAAX 2
SREBF1	Sterol regulatory element binding transcription factor 1

1.2.2 α-Synuclein: a major player in Parkinson's disease

The synuclein family is constituted by α-, β- and γ-syn, but only α-syn has been found to be associated to human neurodegenerative diseases. α-Syn is a small neuronal protein composed by 140 amino acids, and encoded by the human SNCA gene in the chromosome 4 (Figure 1.6).

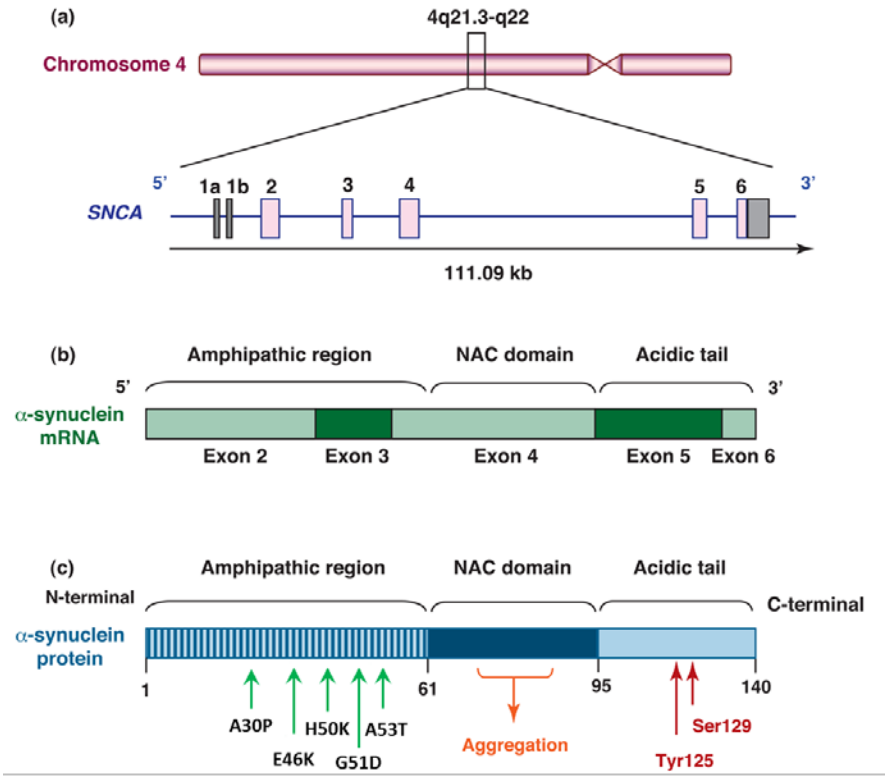

Figure 1.6. α-Synuclein (α-syn) is a major player in Parkinson's disease pathogenesis. (A) α-syn is encoded by SNCA gene, located on chromosome 4. (B) From the 6 exons comprising SNCA, only the last 5 encode for α-synuclein protein, which is composed by 140 amino acids. (C) Schematic representation of the different domains of α-syn and the localization of the familial mutations A30P, E46K, H50Q, G51D and A53T in the N-terminal domain. Adapted from [49].

Several mutations segregated with PD have been already mapped to the SNCA locus. The missense mutation A53T was mapped in 1997 [50]. Subsequently two additional missense mutations were mapped: A30P and E46K [51, 52]. These missense mutations are located in the N-terminal domain of α-syn, involved in the binding to membranes, and induce an increase in the propensity of this protein to misfold and form fibrillar aggregates enriched in β-sheet structure [53-55]. More recently, the H50Q [56] and G51D [57] missense mutations were also identified. The H50Q mutation stabilizes α-syn fibrils, significantly increasing the aggregation rate and the ability of this protein to form amyloid inclusions, while the G51D mutation slowdowns α-syn aggregation, but both mutations increased the toxicity [58-61]. Genomic duplication or triplication of the SNCA locus, which increases α-syn expression, also causes a form of autosomal dominant PD [62-64]. The SNCA dosage is inversely correlated with the age of onset and directly correlated with the severity of the disease [65-67]. Post-mortem analysis of sporadic PD midbrain tissues revealed that the total mRNA levels for α-syn were significantly increased, when compared to control brains, further highlighting the relevance of the levels of expression of this protein in PD [68].

GWAS indicated that variations at the SNCA locus are also strongly correlated with the sporadic forms of PD, corroborating the importance of α-syn in the etiology of this neuropathology (Fig. 1.7). In fact, hundreds of single nucleotide polymorphisms (SNPs) within the SNCA locus have been shown to increase susceptibility to PD (based on PDgene database – http://www.pdgene.org). Moreover, polymorphisms in the promoter region of SNCA have been also linked to PD [69]. The expansion of the polymorphic dinucleotide repeat REP1 increases α-syn expression, thus being related with an increased risk of sporadic PD [70, 71]. SNPs in

SNCA may also affect the stability and the alternative splicing of α-syn mRNA transcripts. Indeed, at least 6 different transcripts of this gene exist. Besides the transcript encoding the full-length protein (140 aa), 5 truncated forms have been described. One of these truncated forms (112 aa) has been associated to LB formation and neurotoxicity [72].

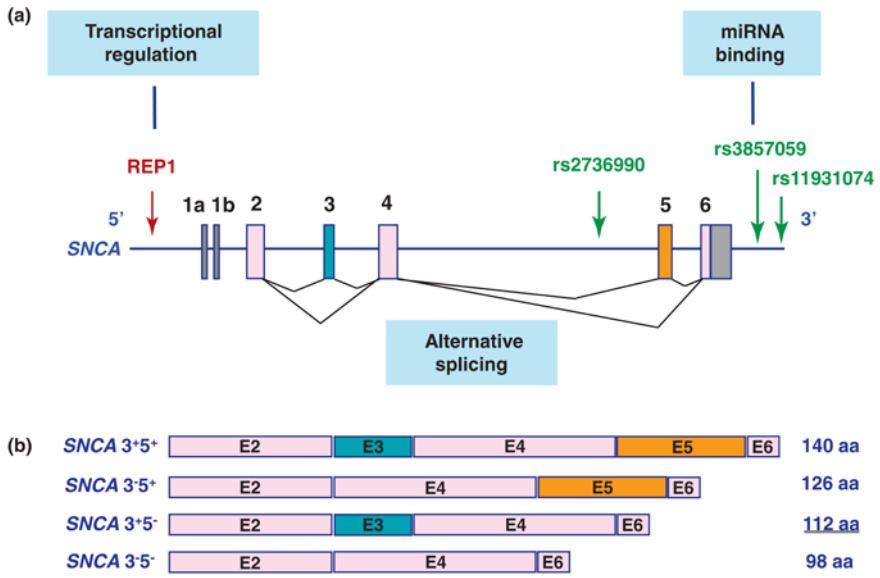

Figure 1.7. Variations at the SNCA locus, identified by genome-wide association studies (GWAS), associated to the sporadic forms of Parkinson's disease (PD). (A) The REP1 dinucleotide repeat, in the promoter region, regulates the levels of SNCA expression; Three single nucleotide polymorphisms (SNP) that may alter transcripts' splicing and stability, and that are highly associated with PD, are also indicated (in green). (B) Four isoforms of SNCA generated by alternative splicing and implicated in the formation of Lewy bodies (LB) and neurotoxicity. Adapted from [49].

1.2.3 The vulnerability of dopaminergic neurons in Parkinson's disease

The specificity of the neuronal subpopulations that are mostly affected and degenerate in each neurodegenerative disease raises a fundamental question: are the insults specifically induced in those neurons or are there specific cellular and molecular characteristics of the affected neuronal subpopulations that render them more vulnerable to the insults?
In the case of PD, the most affected neuronal population is the DA neurons from SNpc that project their axons to the striatum (Figure 1.8).

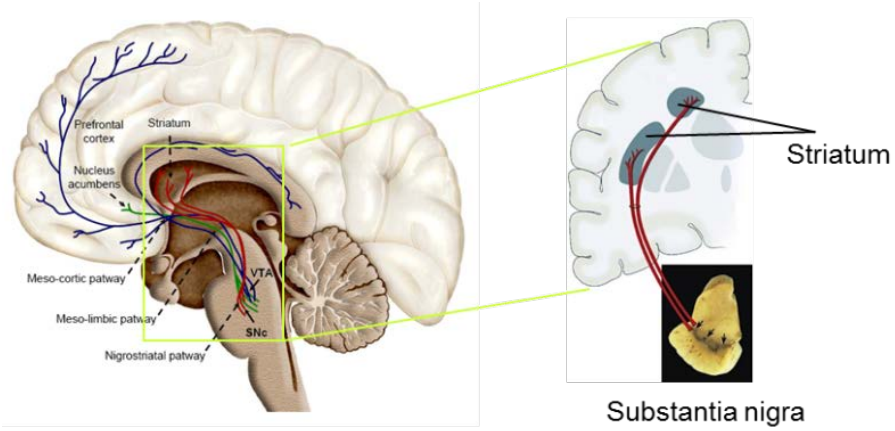

Figure 1.8. The dopaminergic (DA) system and the nigrostriatal pathway. The DA neurons from substantia nigra pars compacta (SNpc), the most vulnerable neuronal population in Parkinson's disease (PD), project their axons to the medium spiny neurons (MSN) from the striatum, constituting the nigrostriatal pathway, which plays a crucial role in the motor control.

The death of these neurons, and the consequent impairment of the nigrostriatal DA pathway, is the cause of the motor symptoms observed in PD. It is especially intriguing if we consider that from all the types of DA neurons present in the brain, including the molecularly very similar DA

neurons from ventral tegmental area (VTA), the DA neurons from SNpc are the most vulnerable in PD.

Protein misfolding and aggregation, dysregulation of the ubiquitin proteasome system, mitochondrial dysfunction and oxidative stress are not exclusive of DA neurons, but are present in most areas of the PD brain [73-75]. The difficulty in justifying the vulnerability of the DA neurons from SNpc also persists when considering the familial forms of PD. The expression of genes linked to this pathology is not specific and limited to the DA neurons. For example, SNCA is ubiquitously expressed in the central nervous system (CNS) at high levels, being also present in other non-neuronal tissues [76].

The exposure to the neurotoxins 6-OHDA and MPTP specifically induces neurodegeneration of the DA neurons from SNpc, and for this reason they have been largely used as pharmacological models of PD. The selectivity of these neurotoxins is explained by the fact that their internalization into the cells is dependent on Sodium-dependent dopamine transporter (DAT), which is only expressed in the DA neurons. Importantly, DAT is expressed at higher levels in SNpc than in the VTA [77]. However, this explanation cannot be applied to other drugs that induce PD-like pathology and symptoms, as is the case of the toxins rotenone and paraquat, widely used as pesticide and herbicide, respectively. Rotenone affects the mitochondrial function by inhibiting the mitochondrial complex I, while paraquat induces oxidative stress, both insults not being specifically targeted to the DA neurons from SNpc.

Bolan and Pissadaki [78] and by Brichta and Greengard [79] have previously reviewed several particular determinants that put the SNpc DA "on the edge" of the risk to degenerate in PD. Some of these characteristics are related with the neuroanatomy of the nigrostriatal pathway. The axons projecting from the SNpc DA neurons to the striatum

are unmyelinated and extremely long, having a total cumulative length of 70 cm [80] and the estimated number of synapses established by these axons is equally massive (200.000 – 400.000) [81, 82]. These unique morphological features impose extreme bioenergetic demands, increasing the metabolic needs of the SNpc DA neurons to maintain the membrane potential, generate action potentials and enable synaptic transmission [83]. These exceptional energetic demands could make them especially susceptible to insults of any sort, including environmental and genetic factors [78].

Another important risk factor inherent to the DA neurons is the oxidation of dopamine and the consequent generation of reactive oxygen species [84]. Dopamine is a potentially dangerous neurotransmitter within the cells, as it easily undergoes oxidation generating dopamine-derived quinones and other toxic molecules (Figure 1.9). Furthermore, cytoplasmic accumulations of misfolded α-syn may affect the secretory pathway by blocking the normal ER-Golgi traffic and thus exacerbating the deleterious effects induced by toxic molecules, namely dopamine-derived products [85].

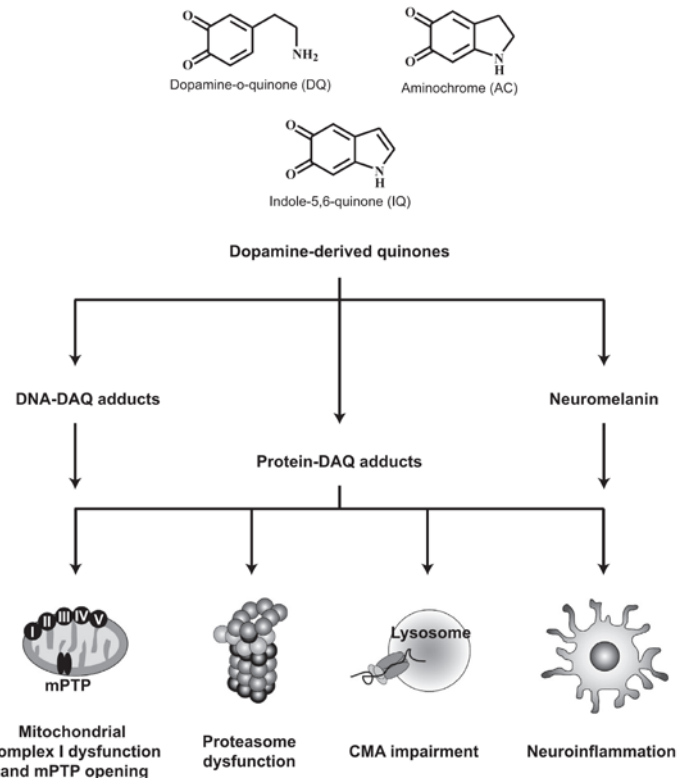

Figure 1.9. Schematic representation of the molecular mechanisms associated to the toxic properties of the dopamine-derived quinones (DAQ). Extracted from [86].

The investigation of the specific cellular and molecular determinants of the differential susceptibility of the DA neurons from SNpc in PD has proven to be very challenging but holds great potential for the discovery of new therapeutic targets.

1.3. Huntington's disease

1.3.1. Epidemiology, symptoms and general molecular features

HD is the most common genetically inherited neurodegenerative disease, belonging to the group of polyglutamine (polyQ) pathologies and affecting approximately 5 to 10 per 100.000 individuals in the Caucasian population [87-89]. It is caused by a mutation in the first exon of the unconventionally large IT-15 gene (67 exons), which encodes a protein called huntingtin (Htt).

Mutant Htt misfolds and accumulates into amyloid-like proteinaceous aggregates in the medium spiny neurons (MSN) from the striatum, being the most common post-mortem histopathological feature (Fig. 1.10).

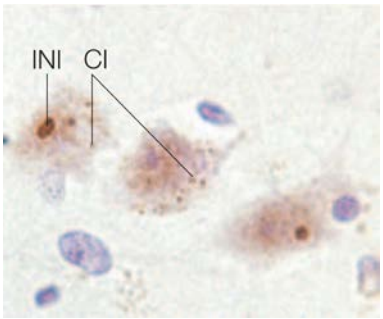

Figure 1.10. Post-mortem analysis of patients' brains with Huntington's disease (HD) show intranuclear inclusions (INI) and cytoplasmic inclusions (CI) containing mutant Huntingtin (Htt) accumulated. Extracted from [28].

Neurons from the thalamus, hippocampus and cortex also degenerate, accounting for the typical symptoms observed in patients: involuntary movements (chorea), dementia and psychiatric problems (depression, anxiety, irritability, sexual dysfunction and suicidal tendencies) [87].

1.3.2. Huntingtin: the monogenic cause of Huntington's disease

Since 1993, when the Htt gene was mapped to the short arm of chromosome 4, intense research has been conducted aiming to identify the biological function of Htt, as well as its role in the HD pathogenesis.

The disease-associated mutation of Htt occurs in the N-terminal region of Htt and consists of an abnormally high number of cytosine-adenine-guanine (CAG) triplet repeats. The expanded CAG repeats are translated to an extended stretch of glutamines commonly called polyQ tract [90, 91]. Htt is an unusually large protein, constituted by 3144 amino acids (approximately 350 kDa). However, the N-terminal portion of mutant Htt (exon 1) harboring the polyQ tract (Fig. 1.11) is sufficient to produce HD phenotypes *in vivo* [92-97]. For this reason, most of the model systems established to study HD *in vitro* and *in vivo* are based on the expression of mutant versions of the exon 1 of Htt gene (Httex1).

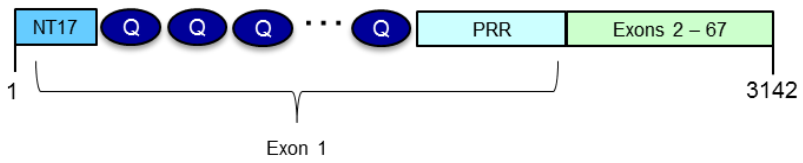

Figure 1.11. Human huntingtin (Htt) is a large protein constituted by 3142 amino acids. The N-terminal domain of this protein, encoded by the exon 1 (Httex1), is highly enriched in the protein inclusions from post-mortem analysis of HD brains. The N-terminal domain of Htt is constituted by the first 17 amino acids (NT17), the polyQ tract (Q-Q-Q…Q) and the proline-rich region (PRR).

The polyQ tract of wild-type Htt contains between 6 and 29 glutamines, while mutant alleles associated to HD contain over 36 glutamines. The longest polyQ tract ever detected in an HD patient was constituted by 130 glutamines [98]. Individuals carrying intermediate alleles containing a range of 29-35 glutamines are healthy and totally asymptomatic. However, due to the meiotic instability of the CAG repeats, these individuals have a very high probability to transmit a pathological polyQ expansion over 36 glutamines to their offspring, especially from the paternal side [99, 100].

The number of glutamines, which is responsible for approximately 70% of the variance, is inversely correlated with the age of onset of the disease, with longer polyQ tracts inducing an earlier and more severe onset of the pathology [101]. The mean age of HD onset is 38 years, although it may vary between the ages of 25 and 70 years. PolyQ tracts containing over 55 glutamines (5% of all cases) produce Juvenile HD, where the onset can start before the age of 20 years [102]. The mean duration of the disease is 17-20 years and patients usually die from pneumonia or suicide [103].

Despite the efforts made to date, there is still no cure for HD and the drugs available can only treat the symptoms. For the development of effective treatments for HD, it is essential to understand the cellular and molecular mechanisms underlying this pathology.

The exact biological function of Htt is unknown, but it was shown to possess an indispensable anti-apoptotic role [104, 105]. There is also evidence that Htt is essential for normal development, as *Htt*-null mutant mice die as embryos at day 7.5 [104, 106, 107]. Surprisingly, Htt is dispensable for *Drosophila* development, but it is crucial for normal long-term mobility and survival in adult flies [108]. Htt interacts with a high number of neuronal proteins involved in a great diversity of cellular

functions, such as endocytosis, neurotransmission, transcriptional regulation, axonal transport and apoptosis [109-111]. Htt could act as scaffold, responsible for bringing together its protein partners and for coordinating the transfer of information among different subcellular compartments, namely between the nucleus and cytoplasm [111]. Htt could also act as a scaffold protein in selective autophagy by promoting cargo recognition and autophagy initiation [112].

The expansion of the polyQ tract promotes conformational changes in Htt that dramatically increase its propensity to misfold and aggregate. Htt aggregation could affect the interaction with its neuronal partners and disturb the normal function of Htt and Htt-interacting proteins. This suggests the involvement of both toxic gain-of-function and loss-of-function mechanisms in the development of HD, by disrupting these protein networks.

1.3.3. Medium spiny neurons vulnerability in Huntington's disease

Although Htt is ubiquitously expressed throughout nervous system and other peripheral tissues (namely, testes, liver, heart and lungs) the pathological effects are predominantly induced in specific neuronal populations of the brain, especially the MSN neurons from the striatum [113-118]. The fact that mutant Htt affects this particular neuronal population points to the possible relevance of cell- or tissue-specific factors in HD pathogenesis, beyond the expanded polyQ tract.

Brain-derived neurotrophic factor (BDNF) is a possible determinant of the increased susceptibility of MSN neurons to neurodegeneration in HD. BDNF is a neurotrophin necessary for the development, survival and proper function of the striatal neurons. Deficient BDNF signaling in the striatum, presumably caused by mutant Htt, has been pointed as strong candidate to be a molecular determinant and modulator in HD pathogenesis (Fig. 1.12) [119].

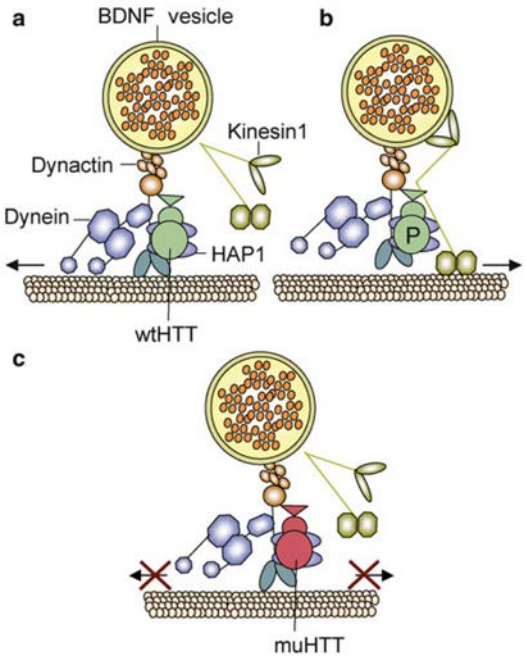

Figure 1.12. The dysregulation of the intracellular transport of brain-derived neurotrophic factor (BDNF), induced by mutant Htt (muHtt) has been pointed as one of the determinants of the increased vulnerability of the striatum neurons in Huntington's disease (HD). (A and B) Wild-type Htt (wtHtt) is involved in the vesicular transport of BDNF along microtubules. Depending on the phosphorylation state of wtHtt the vesicles undergo either retrograde transport (left arrow), mediated by dynein and dynactin, or anterograde transport (right arrow), mediated by kinesin 1. (B) The muHtt binds more tightly to huntington-associated protein 1 (HAP1), inducing an inefficient transport of the vesicles containing BDNF. Adapted from [120]

1.4. Modeling Parkinson's and Huntington's diseases in *Drosophila*

The establishment of animal models is one of the most useful approaches to study the pathogenic mechanisms of human diseases at the molecular, cellular, organic and functional level. *Drosophila melanogaster*, commonly known as fruit fly, is a powerful genetic model organism that has been used to study complex biological phenomena for more than a century, including human neurodegenerative diseases [121].

The identification of genes associated to the familial forms of PD and HD in the last decade allowed the establishment of animal models for these pathologies, which are essential to investigate the early pre-symptomatic stages of pathogenesis and to test new drug candidates.

One of the key factors that contributed to the great success of *Drosophila* as a model organism to study human pathologies is the very high degree of conservation with mammals, since approximately 75% of disease-related loci in humans have at least one *Drosophila* homologue [122]. *Drosophila* also offers a great number of potent genetic tools, it has a very well-known anatomy and has short life cycle and life-span. Finally, the central nervous system of invertebrates and vertebrates shares a common evolutionary origin. Flies have a complex nervous system capable of learning and coordination of intricate behaviors, and there is a significant degree of genetic and functional conservation between the fly central complex and the human basal ganglia, which is the region primarily affected in PD and HD [123]. Such homology constitutes an undeniable advantage to model and study these and other human neurodegenerative diseases.

In order to model a human neurodegenerative disease in flies, it is necessary to express in this organism the human genes associated with this pathology. The most common way of expressing human genes in

Drosophila is by using the binary GAL4-dependent upstream activating sequence (GAL4/UAS) system [124] (Fig. 1.13).

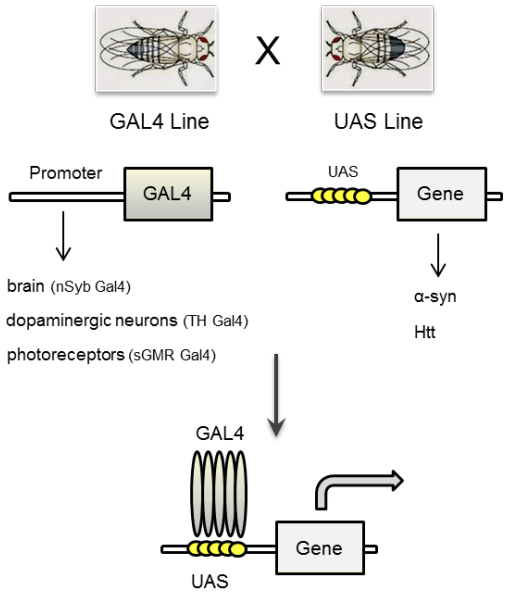

Figure 1.13. The GAL4/UAS system, used for overexpression of proteins in *Drosophila*, is a binary system which allows for the ectopic expression of genes of interest in a specific tissue or cell type. Two transgenic fly lines are created: the UAS line, in which the gene of interest is placed downstream of a UAS (Upstream Activating Sequence) domain, where the yeast transcriptional activator GAL4 binds; and the GAL4 line (driver), which expresses Gal4 under the control of a tissue specific promoter. The gene encoded in the UAS line is only activated when this line is crossed with the GAL4 line. In our study we generated UAS lines encoding for α-synuclein (α-syn) and huntingtin (Htt) and we used pan-neuronal, dopaminergic and photoreceptor drivers.

The gene of interest is subcloned into an UAS expression construct, which is microinjected into fly embryos to establish transgenic lines. The protein of interest is expressed in a targeted way by performing the genetic cross of the UAS line with a Gal4 line that expresses the yeast transcriptional co-activator GAL4 in a specific tissue or cell type. Expression is therefore controlled both in time and space, depending on

the presence of GAL4 in cells and tissues. Many cell-type and developmentally regulated GAL4 lines, commonly called “drivers”, are readily available from *Drosophila* public stock centers (*e.g.* Bloomington Drosophila Stock Center at Indiana University). So, the effect of expressing a human transgene in many different tissues and at various developmental stages can be assayed without creating many independent transgenic lines. The GAL4/UAS system is especially useful when one aims to study the mechanisms of toxicity of human genes linked to the disease which are absent in the *Drosophila* genome, as is the case of α-syn.

In the first *Drosophila* model of PD, transgenic flies expressing wild-type or two familial mutant forms (A30P and A53T) of human α-syn in the brain reproduced key features of PD, including LB-like inclusions (Fig. 1.14), selective degeneration of DA neurons, and abnormalities in the locomotor behavior [125]. Actually, *Drosophila* reproduced PD phenotypes better than mice models of the disease.

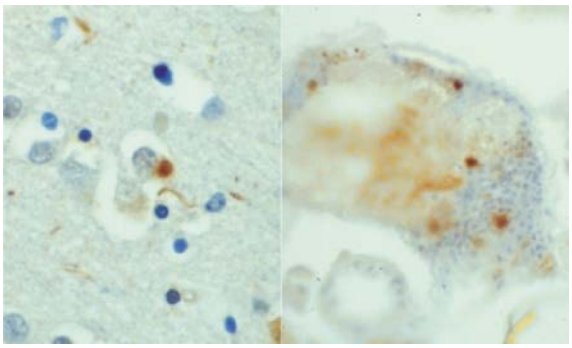

Figure 1.14. In Parkinson’s disease (PD), α-synuclein (α-syn) accumulates in cytoplasmic inclusions (Lewy bodies), as it is shown in a brain section from a patient (left). These protein aggregates, which constitute a hallmark of PD, are also present in a *Drosophila* model for this pathology (right). Adapted from [126].

However, in another report, missexpression of α-syn in the *Drosophila* CNS did not cause death of the DA neurons [127]. The inconsistency of the results from these independent studies may result from the use of different technical approaches. Therefore, there is the need for more independent studies in order to clarify some of these inconsistencies and to generate *Drosophila* models that consistently reproduce the key phenotypes resembling PD conditions.

Concerning HD, *Drosophila* models show the essential features associated to the pathology, such as progressive neurodegeneration [128], motor deficits, protein inclusions in cytoplasm and nucleus (Figure 1.15) and a correlation between polyglutamine repeat length, age of onset and severity of the phenotypes [129].

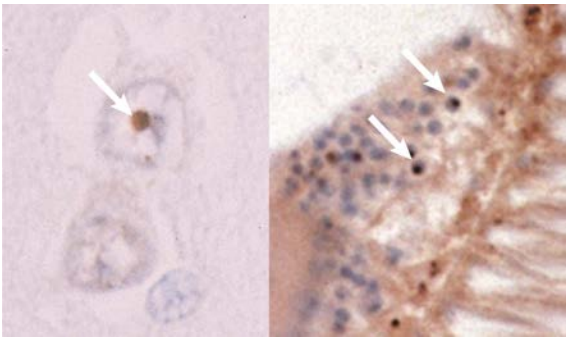

Figure 1.15. In Huntington's disease (HD), mutant huntingtin (Htt) typically accumulates in cytoplasmic and/or nuclear inclusions (arrows) in the brain. These inclusions are revealed by immunohistochemistry in post-mortem analyses of both a brain section from a patient (left) or a *Drosophila* model of HD (right). Adapted from [126].

In this work we have established new transgenic *Drosophila* models for PD and HD, based on the overexpression of wild-type and mutant versions of α-syn and Htt (Fig. 1.16).

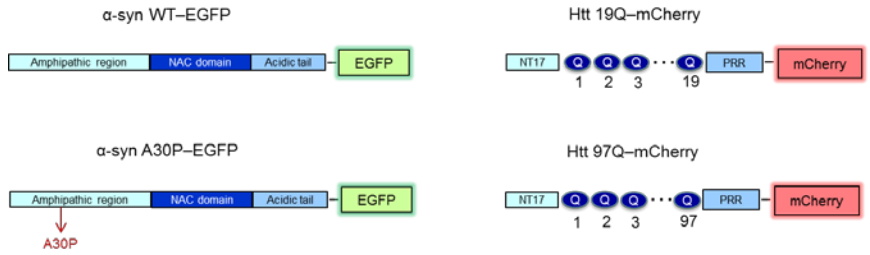

Figure 1.16. We generated UAS transgenic lines encoding fluorescent-tagged versions of two human proteins associated with Parkinson's (PD) and Huntington's diseases (HD). For PD we generated constructs of human α-synuclein (α-syn) fused to EGFP and we used a wild-type (WT) and a familiar mutant form (the missense mutation A30P) of this protein. For HD we generated mCherry-tagged versions of a wild-type form with 19 glutamines (19Q) and a mutant form containing 97 glutamines (97Q) of human huntingtin (Htt).

For the PD model, we used the missense mutation A30P, associated to familial cases of the disease; and for the HD model, we used wild-type and mutant forms of Htt, with 19Q and 97Q in the polyQ tract, respectively. These proteins were fused to fluorescent tags (EGFP for α-syn and mCherry for Htt), allowing microscopy and co-localization studies in either "live" or fixed biological materials.

Taking advantage of the Gal4/UAS system, we were able to induce targeted expression of these proteins in different neuronal tissues of interest, such as in the whole nervous system, using the pan-neuronal driver Elav-Gal4, in the eye retina, using the sGMR-Gal4 driver and in the dopaminergic neurons, using the TH-Gal4 driver (Fig. 1.17).

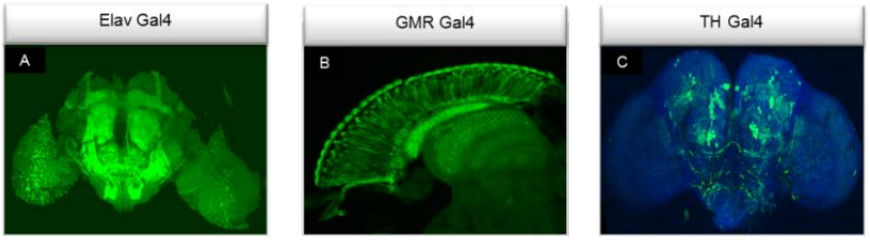

Figure 1.17. Targeted expression of EGFP-tagged α-synuclein using the Gal4/UAS system. Confocal microscopy images of adult flies expressing α-synuclein-EGFP in different tissues: (A) in the whole-brain, using the pan-neuronal driver Elav-Gal4; (B) in the photoreceptors, using the GMR-Gal4 driver; (C) in the dopaminergic (DA) neurons, using the TH-Gal4 driver.

Throughout our study, depending on the specific questions and on the particular experiments to be done, we induced the targeted expression of the proteins of interest in different tissues, such as the whole brain, the eye photoreceptors or the DA neurons. The DA neurons constituted one of our favorite neuronal populations to study PD and HD in our *Drosophila* models, being the TH-Gal4 driver extensively used in our study. This driver expresses Gal4 under the control of the promotor region of tyrosine hydroxylase (TH) gene. TH is the enzyme that catalyzes the rate-limiting step of dopamine biosynthesis and is specifically expressed in all DA cells.

The DA neurons, besides being the neuronal cell type directly affected in PD, the axons of the DA neurons constitute the main input to the MSN from the striatum, affected in HD. The DA system in mammals is involved in the control of locomotor behavior, motivational states and cognitive function, all of them impaired to different degrees in PD and HD. Furthermore, the impairment of particular behaviors, such as the initiation of voluntary actions in mammals has been correlated with the malfunction of specific subpopulations of DA neurons, namely the ones involved in the nigrostriatal pathway [130, 131].

Drosophila DA system is well characterized by means of dopamine and anti-Tyrosine Hydroxylase (TH) immunoreactivity, enabling the characterization of several DA clusters which were named according to their anatomical localization in the brain: paired posterior lateral 1 and 2 (PPL1 and PPL2); paired posterior medial 1 and 2 (PPM1/2); paired posterior medial 3 (PPM3); paired anterior lateral (PAL), and paired anterior medial (PAM). (Fig. 1.18) [132-134]. Similarly to mammals, *Drosophila* DA system is also involved in the modulation and control of locomotor behavior. Furthermore, specific subset of DA neurons are especially vulnerable to neurodegeneration and to induce motor deficits in the context of PD, which is equivalent to the situation observed in humans [135, 136].

For these reasons, we consider *Drosophila* DA neurons a very useful and adequate system to model and study human neurodegenerative diseases affecting motor function, as is the case of PD and HD.

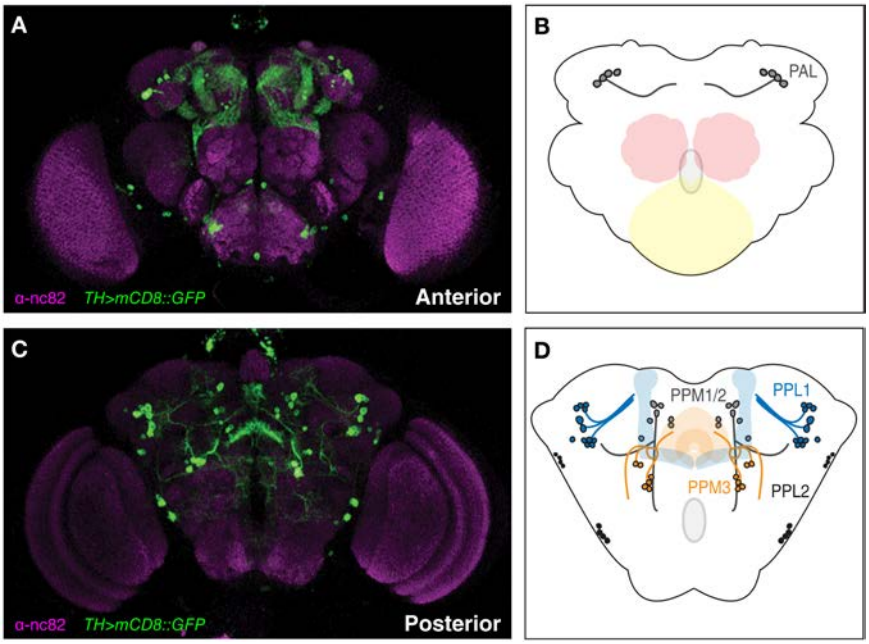

Figure 1.18. The dopaminergic (DA) system in *Drosophila*. The DA neurons are grouped in several clusters in the *Drosophila* adult brain. In (A) and (C) are shown confocal pictures of adult brains expressing GFP-tagged mCD8 under the control of TH-Gal4 driver to label the DA neurons and immunostained with anti-nc82 to label the generic anterior and posterior neuropil structures. In (B) and (D) are shown schematic representations of the cell bodies and axonal projections from DA neurons, which are grouped in 6 distinct clusters: paired posterior lateral 1 and 2 (PPL1 and PPL2); paired posterior medial 1 and 2 (PPM1/2); paired posterior medial 3 (PPM3); paired anterior lateral (PAL), and paired anterior medial (PAM). Adapted from [135].

1.5. Main goals

Using our newly established *Drosophila* models, we were interested in the study of three different particular aspects that we believe to be relevant to the molecular pathogenesis of PD and HD:

- the molecular determinants of the subcellular localization of α-syn in PD (Chapter II)
- the effect of N-terminal phosphorylation in the aggregation and toxicity of Htt *in vitro* and *in vivo* (Chapter III)
- the possible crosstalk between PD and HD molecular mechanisms, by studying the genetic and functional interaction between α-syn and Htt (Chapter IV)

Additionally, we tried to identify new potential therapeutic compounds for PD and HD, being particularly interested in the putative therapeutic effect of mannosylglycerate (MG) in our *Drosophila* models of neurodegeneration (Chapter V). MG is a compatible solute, i.e. a substance compatible with the cellular metabolism that accumulates in the cytoplasm to balance external osmotic pressure. These properties confer potential neuroprotective effects to this compound in the context human neurodegenerative diseases, as previously shown by our collaborators using a yeast model for PD [137].

We believe this work will contribute to a better understanding of the molecular and cellular pathophysiology mechanisms underlying PD and HD.

1.6. References

1. Perry, R.J. and J.R. Hodges, *Spectrum of memory dysfunction in degenerative disease.* Curr Opin Neurol, 1996. **9**(4): p. 281-5.
2. Tsolaki, M., et al., *Extrapyramidal symptoms and signs in Alzheimer's disease: prevalence and correlation with the first symptom.* Am J Alzheimers Dis Other Demen, 2001. **16**(5): p. 268-78.
3. Soto, C., *Unfolding the role of protein misfolding in neurodegenerative diseases.* Nat Rev Neurosci, 2003. **4**(1): p. 49-60.
4. Nussbaum, R.L. and C.E. Ellis, *Alzheimer's disease and Parkinson's disease.* N Engl J Med, 2003. **348**(14): p. 1356-64.
5. van der Vegt, J.P., et al., *Imaging the impact of genes on Parkinson's disease.* Neuroscience, 2009. **164**(1): p. 191-204.
6. Hughes, A.J., et al., *The accuracy of diagnosis of parkinsonian syndromes in a specialist movement disorder service.* Brain, 2002. **125**(Pt 4): p. 861-70.
7. Goedert, M., et al., *100 years of Lewy pathology.* Nat Rev Neurol, 2013. **9**(1): p. 13-24.
8. Jarrett, J.T., E.P. Berger, and P.T. Lansbury, Jr., *The C-terminus of the beta protein is critical in amyloidogenesis.* Ann N Y Acad Sci, 1993. **695**: p. 144-8.
9. Scherzinger, E., et al., *Self-assembly of polyglutamine-containing huntingtin fragments into amyloid-like fibrils: implications for Huntington's disease pathology.* Proc Natl Acad Sci U S A, 1999. **96**(8): p. 4604-9.
10. Wood, S.J., et al., *alpha-synuclein fibrillogenesis is nucleation-dependent. Implications for the pathogenesis of Parkinson's disease.* J Biol Chem, 1999. **274**(28): p. 19509-12.
11. Lorenzo, A. and B.A. Yankner, *Beta-amyloid neurotoxicity requires fibril formation and is inhibited by congo red.* Proc Natl Acad Sci U S A, 1994. **91**(25): p. 12243-7.
12. Pike, C.J., et al., *Neurodegeneration induced by beta-amyloid peptides in vitro: the role of peptide assembly state.* J Neurosci, 1993. **13**(4): p. 1676-87.
13. Pike, C.J., et al., *In vitro aging of beta-amyloid protein causes peptide aggregation and neurotoxicity.* Brain Res, 1991. **563**(1-2): p. 311-4.

14. Kayed, R., et al., *Conformation dependent monoclonal antibodies distinguish different replicating strains or conformers of prefibrillar Abeta oligomers.* Mol Neurodegener, 2010. **5**: p. 57.
15. Okada, T., et al., *Formation of toxic fibrils of Alzheimer's amyloid beta-protein-(1-40) by monosialoganglioside GM1, a neuronal membrane component.* J Mol Biol, 2007. **371**(2): p. 481-9.
16. Novitskaya, V., et al., *Amyloid fibrils of mammalian prion protein are highly toxic to cultured cells and primary neurons.* J Biol Chem, 2006. **281**(19): p. 13828-36.
17. Lotz, G.P. and J. Legleiter, *The role of amyloidogenic protein oligomerization in neurodegenerative disease.* J Mol Med (Berl), 2013. **91**(6): p. 653-64.
18. Terry, R.D., et al., *Some morphometric aspects of the brain in senile dementia of the Alzheimer type.* Ann Neurol, 1981. **10**(2): p. 184-92.
19. Hashimura, T., T. Kimura, and T. Miyakawa, *Morphological changes of blood vessels in the brain with Alzheimer's disease.* Jpn J Psychiatry Neurol, 1991. **45**(3): p. 661-5.
20. Lue, L.F., et al., *Soluble amyloid beta peptide concentration as a predictor of synaptic change in Alzheimer's disease.* Am J Pathol, 1999. **155**(3): p. 853-62.
21. McLean, C.A., et al., *Soluble pool of Abeta amyloid as a determinant of severity of neurodegeneration in Alzheimer's disease.* Ann Neurol, 1999. **46**(6): p. 860-6.
22. Naslund, J., et al., *Correlation between elevated levels of amyloid beta-peptide in the brain and cognitive decline.* JAMA, 2000. **283**(12): p. 1571-7.
23. Tompkins, M.M. and W.D. Hill, *Contribution of somal Lewy bodies to neuronal death.* Brain Res, 1997. **775**(1-2): p. 24-9.
24. Agorogiannis, E.I., et al., *Protein misfolding in neurodegenerative diseases.* Neuropathol Appl Neurobiol, 2004. **30**(3): p. 215-24.
25. Taylor, J.P., J. Hardy, and K.H. Fischbeck, *Toxic proteins in neurodegenerative disease.* Science, 2002. **296**(5575): p. 1991-5.
26. Kowal, S.L., et al., *The current and projected economic burden of Parkinson's disease in the United States.* Mov Disord, 2013. **28**(3): p. 311-8.
27. Dorsey, E.R., et al., *Projected number of people with Parkinson disease in the most populous nations, 2005 through 2030.* Neurology, 2007. **68**(5): p. 384-6.

28. Ross, C.A. and M.A. Poirier, *Opinion: What is the role of protein aggregation in neurodegeneration?* Nat Rev Mol Cell Biol, 2005. **6**(11): p. 891-8.
29. Spatola, M. and C. Wider, *Genetics of Parkinson's disease: the yield.* Parkinsonism Relat Disord, 2014. **20 Suppl 1**: p. S35-8.
30. Winner, B., et al., *Adult neurogenesis and neurite outgrowth are impaired in LRRK2 G2019S mice.* Neurobiol Dis, 2011. **41**(3): p. 706-16.
31. Dachsel, J.C., et al., *A comparative study of Lrrk2 function in primary neuronal cultures.* Parkinsonism Relat Disord, 2010. **16**(10): p. 650-5.
32. Tong, Y., et al., *Loss of leucine-rich repeat kinase 2 causes age-dependent bi-phasic alterations of the autophagy pathway.* Mol Neurodegener, 2012. **7**: p. 2.
33. Ren, Y., et al., *Selective vulnerability of dopaminergic neurons to microtubule depolymerization.* J Biol Chem, 2005. **280**(40): p. 34105-12.
34. Piccoli, G., et al., *LRRK2 controls synaptic vesicle storage and mobilization within the recycling pool.* J Neurosci, 2011. **31**(6): p. 2225-37.
35. Castelo-Branco, G., et al., *Differential regulation of midbrain dopaminergic neuron development by Wnt-1, Wnt-3a, and Wnt-5a.* Proc Natl Acad Sci U S A, 2003. **100**(22): p. 12747-52.
36. Port, F., et al., *Wingless secretion promotes and requires retromer-dependent cycling of Wntless.* Nat Cell Biol, 2008. **10**(2): p. 178-85.
37. Deng, H., K. Gao, and J. Jankovic, *The VPS35 gene and Parkinson's disease.* Mov Disord, 2013. **28**(5): p. 569-75.
38. Tabuchi, M., et al., *Retromer-mediated direct sorting is required for proper endosomal recycling of the mammalian iron transporter DMT1.* J Cell Sci, 2010. **123**(Pt 5): p. 756-66.
39. Schulte, E.C., et al., *Variants in eukaryotic translation initiation factor 4G1 in sporadic Parkinson's disease.* Neurogenetics, 2012. **13**(3): p. 281-5.
40. Kane, L.A., et al., *PINK1 phosphorylates ubiquitin to activate Parkin E3 ubiquitin ligase activity.* J Cell Biol, 2014. **205**(2): p. 143-53.
41. Kazlauskaite, A., et al., *Parkin is activated by PINK1-dependent phosphorylation of ubiquitin at Ser65.* Biochem J, 2014. **460**(1): p. 127-39.

42. Koyano, F., et al., *Ubiquitin is phosphorylated by PINK1 to activate parkin.* Nature, 2014. **510**(7503): p. 162-6.
43. Lazarou, M., et al., *The ubiquitin kinase PINK1 recruits autophagy receptors to induce mitophagy.* Nature, 2015. **524**(7565): p. 309-14.
44. Orenstein, S.J., et al., *Interplay of LRRK2 with chaperone-mediated autophagy.* Nat Neurosci, 2013. **16**(4): p. 394-406.
45. Manzoni, C., et al., *Inhibition of LRRK2 kinase activity stimulates macroautophagy.* Biochim Biophys Acta, 2013. **1833**(12): p. 2900-10.
46. Alegre-Abarrategui, J., et al., *LRRK2 regulates autophagic activity and localizes to specific membrane microdomains in a novel human genomic reporter cellular model.* Hum Mol Genet, 2009. **18**(21): p. 4022-34.
47. Beilina, A., et al., *Unbiased screen for interactors of leucine-rich repeat kinase 2 supports a common pathway for sporadic and familial Parkinson disease.* Proc Natl Acad Sci U S A, 2014. **111**(7): p. 2626-31.
48. Bras, J., R. Guerreiro, and J. Hardy, *SnapShot: Genetics of Parkinson's disease.* Cell, 2015. **160**(3): p. 570-570 e1.
49. Venda, L.L., et al., *alpha-Synuclein and dopamine at the crossroads of Parkinson's disease.* Trends Neurosci, 2010. **33**(12): p. 559-68.
50. Polymeropoulos, M.H., et al., *Mutation in the alpha-synuclein gene identified in families with Parkinson's disease.* Science, 1997. **276**(5321): p. 2045-7.
51. Kruger, R., et al., *Ala30Pro mutation in the gene encoding alpha-synuclein in Parkinson's disease.* Nat Genet, 1998. **18**(2): p. 106-8.
52. Zarranz, J.J., et al., *The new mutation, E46K, of alpha-synuclein causes Parkinson and Lewy body dementia.* Ann Neurol, 2004. **55**(2): p. 164-73.
53. Coskuner, O. and O. Wise-Scira, *Structures and free energy landscapes of the A53T mutant-type alpha-synuclein protein and impact of A53T mutation on the structures of the wild-type alpha-synuclein protein with dynamics.* ACS Chem Neurosci, 2013. **4**(7): p. 1101-13.
54. Choi, J.M., et al., *Analysis of PARK genes in a Korean cohort of early-onset Parkinson disease.* Neurogenetics, 2008. **9**(4): p. 263-9.

55. Lemkau, L.R., et al., *Mutant protein A30P alpha-synuclein adopts wild-type fibril structure, despite slower fibrillation kinetics.* J Biol Chem, 2012. **287**(14): p. 11526-32.
56. Appel-Cresswell, S., et al., *Alpha-synuclein p.H50Q, a novel pathogenic mutation for Parkinson's disease.* Mov Disord, 2013. **28**(6): p. 811-3.
57. Kiely, A.P., et al., *alpha-Synucleinopathy associated with G51D SNCA mutation: a link between Parkinson's disease and multiple system atrophy?* Acta Neuropathol, 2013. **125**(5): p. 753-69.
58. Rutherford, N.J., et al., *Divergent effects of the H50Q and G51D SNCA mutations on the aggregation of alpha-synuclein.* J Neurochem, 2014. **131**(6): p. 859-67.
59. Porcari, R., et al., *The H50Q mutation induces a 10-fold decrease in the solubility of alpha-synuclein.* J Biol Chem, 2015. **290**(4): p. 2395-404.
60. Lesage, S., et al., *G51D alpha-synuclein mutation causes a novel parkinsonian-pyramidal syndrome.* Ann Neurol, 2013. **73**(4): p. 459-71.
61. Fares, M.B., et al., *The novel Parkinson's disease linked mutation G51D attenuates in vitro aggregation and membrane binding of alpha-synuclein, and enhances its secretion and nuclear localization in cells.* Hum Mol Genet, 2014. **23**(17): p. 4491-509.
62. Singleton, A.B., et al., *alpha-Synuclein locus triplication causes Parkinson's disease.* Science, 2003. **302**(5646): p. 841.
63. Muenter, M.D., et al., *Hereditary form of parkinsonism--dementia.* Ann Neurol, 1998. **43**(6): p. 768-81.
64. Konno, T., et al., *Autosomal dominant Parkinson's disease caused by SNCA duplications.* Parkinsonism Relat Disord, 2015.
65. Miller, D.W., et al., *Alpha-synuclein in blood and brain from familial Parkinson disease with SNCA locus triplication.* Neurology, 2004. **62**(10): p. 1835-8.
66. Ibanez, P., et al., *Causal relation between alpha-synuclein gene duplication and familial Parkinson's disease.* Lancet, 2004. **364**(9440): p. 1169-71.
67. Chartier-Harlin, M.C., et al., *Alpha-synuclein locus duplication as a cause of familial Parkinson's disease.* Lancet, 2004. **364**(9440): p. 1167-9.
68. Chiba-Falek, O., G.J. Lopez, and R.L. Nussbaum, *Levels of alpha-synuclein mRNA in sporadic Parkinson disease patients.* Mov Disord, 2006. **21**(10): p. 1703-8.

69. Pihlstrom, L. and M. Toft, *Genetic variability in SNCA and Parkinson's disease.* Neurogenetics, 2011. **12**(4): p. 283-93.
70. Goldman, S.M., et al., *Head injury, alpha-synuclein Rep1 and Parkinson's disease: a meta-analytic view of gene-environment interaction.* Eur J Neurol, 2015. **22**(7): p. e75.
71. Janeczek, P., et al., *Reduced expression of alpha-synuclein in alcoholic brain: influence of SNCA-Rep1 genotype.* Addict Biol, 2014. **19**(3): p. 509-15.
72. Kalivendi, S.V., et al., *Oxidants induce alternative splicing of alpha-synuclein: Implications for Parkinson's disease.* Free Radic Biol Med, 2010. **48**(3): p. 377-83.
73. Cookson, M.R., *Parkinsonism due to mutations in PINK1, parkin, and DJ-1 and oxidative stress and mitochondrial pathways.* Cold Spring Harb Perspect Med, 2012. **2**(9): p. a009415.
74. Lee, F.J. and F. Liu, *Genetic factors involved in the pathogenesis of Parkinson's disease.* Brain Res Rev, 2008. **58**(2): p. 354-64.
75. Shen, J. and M.R. Cookson, *Mitochondria and dopamine: new insights into recessive parkinsonism.* Neuron, 2004. **43**(3): p. 301-4.
76. Ltic, S., et al., *Alpha-synuclein is expressed in different tissues during human fetal development.* J Mol Neurosci, 2004. **22**(3): p. 199-204.
77. Lammel, S., et al., *Unique properties of mesoprefrontal neurons within a dual mesocorticolimbic dopamine system.* Neuron, 2008. **57**(5): p. 760-73.
78. Bolam, J.P. and E.K. Pissadaki, *Living on the edge with too many mouths to feed: why dopamine neurons die.* Mov Disord, 2012. **27**(12): p. 1478-83.
79. Brichta, L. and P. Greengard, *Molecular determinants of selective dopaminergic vulnerability in Parkinson's disease: an update.* Front Neuroanat, 2014. **8**: p. 152.
80. Matsuda, W., et al., *Single nigrostriatal dopaminergic neurons form widely spread and highly dense axonal arborizations in the neostriatum.* J Neurosci, 2009. **29**(2): p. 444-53.
81. Oorschot, D.E., *Total number of neurons in the neostriatal, pallidal, subthalamic, and substantia nigral nuclei of the rat basal ganglia: a stereological study using the cavalieri and optical disector methods.* J Comp Neurol, 1996. **366**(4): p. 580-99.
82. Arbuthnott, G.W. and J. Wickens, *Space, time and dopamine.* Trends Neurosci, 2007. **30**(2): p. 62-9.

83. Attwell, D. and S.B. Laughlin, *An energy budget for signaling in the grey matter of the brain.* J Cereb Blood Flow Metab, 2001. **21**(10): p. 1133-45.
84. Hastings, T.G. and M.J. Zigmond, *Loss of dopaminergic neurons in parkinsonism: possible role of reactive dopamine metabolites.* J Neural Transm Suppl, 1997. **49**: p. 103-10.
85. Cooper, A.A., et al., *Alpha-synuclein blocks ER-Golgi traffic and Rab1 rescues neuron loss in Parkinson's models.* Science, 2006. **313**(5785): p. 324-8.
86. Bisaglia, M., et al., *Are dopamine derivatives implicated in the pathogenesis of Parkinson's disease?* Ageing Res Rev, 2014. **13**: p. 107-14.
87. Roos, R.A., *Huntington's disease: a clinical review.* Orphanet J Rare Dis, 2010. **5**: p. 40.
88. Imarisio, S., et al., *Huntington's disease: from pathology and genetics to potential therapies.* Biochem J, 2008. **412**(2): p. 191-209.
89. Landles, C. and G.P. Bates, *Huntingtin and the molecular pathogenesis of Huntington's disease. Fourth in molecular medicine review series.* EMBO Rep, 2004. **5**(10): p. 958-63.
90. *A novel gene containing a trinucleotide repeat that is expanded and unstable on Huntington's disease chromosomes. The Huntington's Disease Collaborative Research Group.* Cell, 1993. **72**(6): p. 971-83.
91. Ambrose, C.M., et al., *Structure and expression of the Huntington's disease gene: evidence against simple inactivation due to an expanded CAG repeat.* Somat Cell Mol Genet, 1994. **20**(1): p. 27-38.
92. Kim, Y.J., et al., *Caspase 3-cleaved N-terminal fragments of wild-type and mutant huntingtin are present in normal and Huntington's disease brains, associate with membranes, and undergo calpain-dependent proteolysis.* Proc Natl Acad Sci U S A, 2001. **98**(22): p. 12784-9.
93. Cooper, J.K., et al., *Truncated N-terminal fragments of huntingtin with expanded glutamine repeats form nuclear and cytoplasmic aggregates in cell culture.* Hum Mol Genet, 1998. **7**(5): p. 783-90.
94. Hoffner, G., M.L. Island, and P. Djian, *Purification of neuronal inclusions of patients with Huntington's disease reveals a broad range of N-terminal fragments of expanded huntingtin and insoluble polymers.* J Neurochem, 2005. **95**(1): p. 125-36.

95. Davies, S.W., et al., *Formation of neuronal intranuclear inclusions underlies the neurological dysfunction in mice transgenic for the HD mutation.* Cell, 1997. **90**(3): p. 537-48.
96. Landles, C., et al., *Proteolysis of mutant huntingtin produces an exon 1 fragment that accumulates as an aggregated protein in neuronal nuclei in Huntington disease.* J Biol Chem, 2010. **285**(12): p. 8808-23.
97. Sathasivam, K., et al., *Aberrant splicing of HTT generates the pathogenic exon 1 protein in Huntington disease.* Proc Natl Acad Sci U S A, 2013. **110**(6): p. 2366-70.
98. Nahhas, F.A., et al., *Juvenile onset Huntington disease resulting from a very large maternal expansion.* Am J Med Genet A, 2005. **137A**(3): p. 328-31.
99. Duyao, M., et al., *Trinucleotide repeat length instability and age of onset in Huntington's disease.* Nat Genet, 1993. **4**(4): p. 387-92.
100. Trottier, Y., V. Biancalana, and J.L. Mandel, *Instability of CAG repeats in Huntington's disease: relation to parental transmission and age of onset.* J Med Genet, 1994. **31**(5): p. 377-82.
101. Lutz, R.E., *Trinucleotide repeat disorders.* Semin Pediatr Neurol, 2007. **14**(1): p. 26-33.
102. Quarrell, O., et al., *The Prevalence of Juvenile Huntington's Disease: A Review of the Literature and Meta-Analysis.* PLoS Curr, 2012. **4**: p. e4f8606b742ef3.
103. Sorensen, S.A. and K. Fenger, *Causes of death in patients with Huntington's disease and in unaffected first degree relatives.* J Med Genet, 1992. **29**(12): p. 911-4.
104. Zeitlin, S., et al., *Increased apoptosis and early embryonic lethality in mice nullizygous for the Huntington's disease gene homologue.* Nat Genet, 1995. **11**(2): p. 155-63.
105. Rigamonti, D., et al., *Huntingtin's neuroprotective activity occurs via inhibition of procaspase-9 processing.* J Biol Chem, 2001. **276**(18): p. 14545-8.
106. Duyao, M.P., et al., *Inactivation of the mouse Huntington's disease gene homolog Hdh.* Science, 1995. **269**(5222): p. 407-10.
107. Nasir, J., et al., *Targeted disruption of the Huntington's disease gene results in embryonic lethality and behavioral and morphological changes in heterozygotes.* Cell, 1995. **81**(5): p. 811-23.
108. Zhang, S., et al., *Inactivation of Drosophila Huntingtin affects long-term adult functioning and the pathogenesis of a*

Huntington's disease model. Dis Model Mech, 2009. **2**(5-6): p. 247-66.
109. Cattaneo, E., et al., *Loss of normal huntingtin function: new developments in Huntington's disease research.* Trends Neurosci, 2001. **24**(3): p. 182-8.
110. Cattaneo, E., C. Zuccato, and M. Tartari, *Normal huntingtin function: an alternative approach to Huntington's disease.* Nat Rev Neurosci, 2005. **6**(12): p. 919-30.
111. Harjes, P. and E.E. Wanker, *The hunt for huntingtin function: interaction partners tell many different stories.* Trends Biochem Sci, 2003. **28**(8): p. 425-33.
112. Ruzo, A., et al., *Discovery of novel isoforms of huntingtin reveals a new hominid-specific exon.* PLoS One, 2015. **10**(5): p. e0127687.
113. Gutekunst, C.A., et al., *Identification and localization of huntingtin in brain and human lymphoblastoid cell lines with anti-fusion protein antibodies.* Proc Natl Acad Sci U S A, 1995. **92**(19): p. 8710-4.
114. Sharp, A.H., et al., *Widespread expression of Huntington's disease gene (IT15) protein product.* Neuron, 1995. **14**(5): p. 1065-74.
115. Landwehrmeyer, G.B., et al., *Huntington's disease gene: regional and cellular expression in brain of normal and affected individuals.* Ann Neurol, 1995. **37**(2): p. 218-30.
116. Li, S.H., et al., *Huntington's disease gene (IT15) is widely expressed in human and rat tissues.* Neuron, 1993. **11**(5): p. 985-93.
117. Shin, J.Y., et al., *Expression of mutant huntingtin in glial cells contributes to neuronal excitotoxicity.* J Cell Biol, 2005. **171**(6): p. 1001-12.
118. Strong, T.V., et al., *Widespread expression of the human and rat Huntington's disease gene in brain and nonneural tissues.* Nat Genet, 1993. **5**(3): p. 259-65.
119. Baydyuk, M. and B. Xu, *BDNF signaling and survival of striatal neurons.* Front Cell Neurosci, 2014. **8**: p. 254.
120. Zuccato, C. and E. Cattaneo, *Huntington's disease.* Handb Exp Pharmacol, 2014. **220**: p. 357-409.
121. Lu, B. and H. Vogel, *Drosophila models of neurodegenerative diseases.* Annu Rev Pathol, 2009. **4**: p. 315-42.
122. Reiter, L.T., et al., *A systematic analysis of human disease-associated gene sequences in Drosophila melanogaster.* Genome Res, 2001. **11**(6): p. 1114-25.

123. Strausfeld, N.J. and F. Hirth, *Deep homology of arthropod central complex and vertebrate basal ganglia.* Science, 2013. **340**(6129): p. 157-61.
124. Brand, A.H. and N. Perrimon, *Targeted gene expression as a means of altering cell fates and generating dominant phenotypes.* Development, 1993. **118**(2): p. 401-15.
125. Feany, M.B. and W.W. Bender, *A Drosophila model of Parkinson's disease.* Nature, 2000. **404**(6776): p. 394-8.
126. Muqit, M.M. and M.B. Feany, *Modelling neurodegenerative diseases in Drosophila: a fruitful approach?* Nat Rev Neurosci, 2002. **3**(3): p. 237-43.
127. Pesah, Y., et al., *Whole-mount analysis reveals normal numbers of dopaminergic neurons following misexpression of alpha-Synuclein in Drosophila.* Genesis, 2005. **41**(4): p. 154-9.
128. Gunawardena, S., et al., *Disruption of axonal transport by loss of huntingtin or expression of pathogenic polyQ proteins in Drosophila.* Neuron, 2003. **40**(1): p. 25-40.
129. Warrick, J.M., et al., *Expanded polyglutamine protein forms nuclear inclusions and causes neural degeneration in Drosophila.* Cell, 1998. **93**(6): p. 939-49.
130. Costa, R.M., *Plastic corticostriatal circuits for action learning: what's dopamine got to do with it?* Ann N Y Acad Sci, 2007. **1104**: p. 172-91.
131. Palmiter, R.D., *Dopamine signaling in the dorsal striatum is essential for motivated behaviors: lessons from dopamine-deficient mice.* Ann N Y Acad Sci, 2008. **1129**: p. 35-46.
132. Budnik, V. and K. White, *Catecholamine-containing neurons in Drosophila melanogaster: distribution and development.* J Comp Neurol, 1988. **268**(3): p. 400-13.
133. Nassel, D.R. and K. Elekes, *Aminergic neurons in the brain of blowflies and Drosophila: dopamine- and tyrosine hydroxylase-immunoreactive neurons and their relationship with putative histaminergic neurons.* Cell Tissue Res, 1992. **267**(1): p. 147-67.
134. Monastirioti, M., *Biogenic amine systems in the fruit fly Drosophila melanogaster.* Microsc Res Tech, 1999. **45**(2): p. 106-21.
135. White, K.E., D.M. Humphrey, and F. Hirth, *The dopaminergic system in the aging brain of Drosophila.* Front Neurosci, 2010. **4**: p. 205.

136. Riemensperger, T., et al., *A Single Dopamine Pathway Underlies Progressive Locomotor Deficits in a Drosophila Model of Parkinson Disease.* Cell Rep, 2013.
137. Faria, C., et al., *Inhibition of formation of alpha-synuclein inclusions by mannosylglycerate in a yeast model of Parkinson's disease.* Biochim Biophys Acta, 2013. **1830**(8): p. 4065-72.

Chapter II

The subcellular localization and axonal transport of α-synuclein in a *Drosophila* model for Parkinson's disease

Contribution

This chapter contains unpublished data:

Poças, G.M.; Afonso, Y.; Gomes, C.M.; Outeiro, T.F. and Domingos, P.M. Axonal transport and subcellular location of α-synuclein in the Drosophila photoreceptors. manuscript in preparation.

G.M. Poças declares to have actively contributed for the experimental design, data analyses and manuscript writing**.** G.M. Poças performed the Drosophila genetic crosses, retinal cryosections, confocal microscopy, immunoprecipitations and proteomic data analyzes.

2.1. Abstract

α-Synuclein (α-syn) is a neuronal protein highly enriched in the pre-synaptic nerve terminals, which has been extensively associated to a group of neurodegenerative diseases called synucleinopathies, being Parkinson's disease (PD) the most common pathology from this group. Despite all the efforts, the biological function of α-syn remains unclear. However, accumulating evidences support an important role for α-syn in neurotransmission, being the dysregulation of α-syn normal function at the synapses one of the possible causes for neurodegeneration. PD is mostly sporadic, but the existence of familial forms of the disease, namely the ones caused by mutations in the α-syn's locus, has enabled *in vivo* studies by the generation of animal models for this pathology. In this work, we established a new *Drosophila* model for PD, based on the expression of EGFP-tagged versions of the wild-type and the A30P mutant form of α-syn in the photoreceptors. We observed mislocalization of α-syn A30P mutant form in the photoreceptors, comparing to the wild-type form. In order to investigate the molecular mechanisms relevant for the synaptic localization of α-syn we identified, by co-immunoprecipitation (Co-IP) and mass spectrometry, specific protein interactors for the wild-type and A30P mutant forms of α-syn. Subsequently, using the identified protein interactors, we performed an RNAi reverse genetic screen which enabled us to identify three candidate proteins (Tomosyn, Spaghetti Squash, and Synaptotagmin 4) as specific modulators of α-syn's axonal transport and subcellular localization.

2.2. Introduction

α-Synuclein (α-syn) is a small (140 aa) neuronal protein expressed in several regions of the vertebrates' brain and highly enriched in the presynaptic nerve terminals.

During the last two decades, several studies have demonstrated the involvement of α-syn in synucleinopathies, a group of neurodegenerative diseases in which α-syn aggregation and accumulation constitutes a common pathological hallmark. The three most common pathologies belonging to this group are: Parkinson's disease (PD), dementia with Lewy bodies and multiple system atrophy.

Specifically for PD, several mutations in the α-syn locus have been identified, constituting the second most common cause of familial dominant PD. These mutations include genomic duplications and triplications [1, 2] and the point mutations A30P, E46K, H50K, G51D, A53E and A53T [3-8]. Additionally, genome-wide association studies (GWAS) revealed that polymorphisms in the α-syn gene are also associated to the sporadic forms of PD, increasing the susceptibility to develop the disease [9].

The identification of α-syn as one of the major players in PD generated great interest in the scientific community to unveil the biological role of this protein in neuronal cells. Despite all the efforts, the exact biological function of this protein in neuronal cells as well as its relevance for the molecular mechanisms associated with neurodegeneration are still very unclear.

Nevertheless, several studies suggest an important role of α-syn in the maintenance and normal function of synaptic membrane processes and in promoting the assembling of the presynaptic Soluble N-ethylmaleimide-sensitive factor Attachment protein Receptor (SNARE) complex involved in the release of neurotransmitters [10]. The highly acidic C-terminal

domain of α-syn directly binds to the N-terminal sequence of synaptobrevin-2, one of the proteins of the SNARE complex, promoting the SNARE complex assembling (Fig. 2.1) [11].

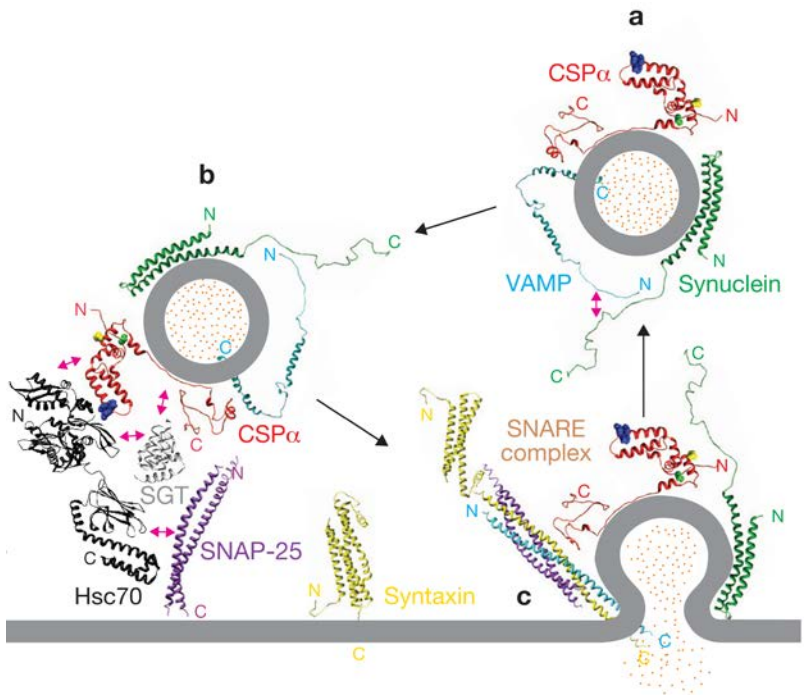

Figure 2.1. The role of α-synuclein (α-syn) in neurotransmission by promoting the SNARE complex assembly. (A) The C-terminal domain of α-syn interacts with the N-terminal domain of synaptobrevin (VAMP) priming the assembling of the SNARE complex. (B) The assembling of the SNARE complex proceeds with the interaction of several other proteins, such as Hsc70, SNAP-25, SGT and CSPα. (C) The assembly of the SNARE complex promotes the fusion of the synaptic vesicles with the pre-synaptic membrane and the release of the neurotransmitters to the synaptic cleft. Adapted from [12]

α-Syn is involved in the SNARE complex assembly and has a protective effect in the massive neurodegeneration and synaptic dysfunction induced by a deficiency in CSPα, a synaptic protein with co-chaperone activity [13-15]. Additional works have been pointing to the importance of α-syn in the synapses, namely those showing a role for α-syn in the regulation of the synaptic vesicle pool size and neurotransmitter release [16-18].

Although these studies point to an important and beneficial function of α-syn, missense mutations or the long-term overexpression of α-syn may impair its function and render misfolded and/or toxic forms of α-syn, typically associated with PD and other synucleinopathies. All the familial point mutations associated to PD have been mapped in the N-terminal portion of α-syn and it has been demonstrated that these mutations affect the ability of α-syn to bind to biological membranes. In the specific case of the A30P mutation, several works have demonstrated less binding of α-syn to membranes [19-21]. A previous study showed that the A30P mutation changes the subcellular localization of α-syn [22]. This abnormal localization may be caused by the effect this mutation has in the fast component of α-syn's axonal transport [20]. Another possibility, which we took in account in our study, is that some gain of toxicity of mutant α-syn is due to spurious binding to biomolecules, namely protein partners, which may sequester α-syn and hinder its normal axonal transport and subcellular localization at the synapses.

In this work, we established a new *Drosophila* model for PD, based on the expression of EGFP-tagged versions of wild-type and A30P mutant α-syn in the photoreceptors, using the Gal4/UAS system. We observed mislocalization of α-syn A30P mutant in the *Drosophila* photoreceptors, comparing to the wild-type form. In order to clarify the molecular mechanisms responsible for the axonal transport and synaptic localization

of α-syn, we performed proteomic analysis by co-IP and mass spectrometry identification of the specific protein interactors for α-syn wild-type and A30P mutant. Subsequently, we performed an RNAi genetic screen, using the identified protein interactors, aiming to discover possible modulators for α-syn's axonal transport and subcellular localization.

2.3. Results

2.3.1. The wild-type form of α-syn accumulates in the synaptic terminals of *Drosophila* photoreceptors

Using the sGMR Gal4 driver, we induced the expression of the wild-type version of α-syn in the *Drosophila* eye, generating a consistent phenotype where α-syn was found to be localized in the terminal portion of the photoreceptors' axons (Fig. 2.2). This observation is consistent with the fact that α-syn is a neuronal protein highly enriched in the synaptic terminals of vertebrate's nervous system.

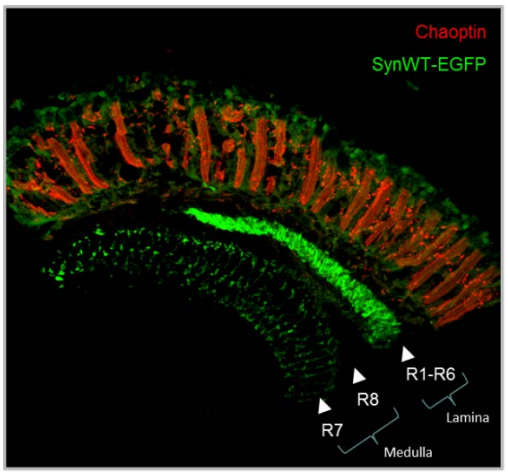

Figure 2.2. The wild-type version of α-syn accumulates in the terminal portion of *Drosophila* photoreceptor's axons. Horizontal retinal cryosection, in which the photoreceptors were marked by anti-chaoptin. The triangles point to the layers where the photoreceptors's axons project into the brain. The photoreceptors 1-6 (R1-R6) project into the lamina, while the photoreceptors 7 (R7) and 8 (R8) project into the medulla. Genotype: sGMR-GAL4, UAS-α-synWT-EGFP

2.3.2. The A30P mutant version of α-syn is mislocalized in the *Drosophila* photoreceptors

The expression of α-syn A30P mutant form, under the control of the sGMR Gal4 driver, led to a strikingly different phenotype comparing to the one characterized for the wild-type form (Fig. 2.3). The A30P mutant version of α-syn lost the specific synaptic enrichment and was found mislocalized throughout the entire cell bodies and axons of the photoreceptors.

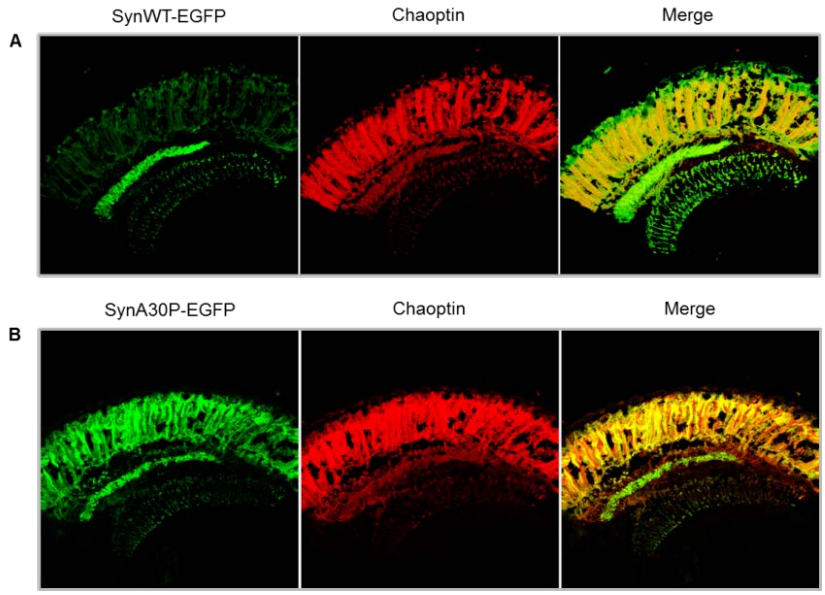

Figure 2.3. The A30P mutant version of α-syn is mislocalized in the *Drosophila* photoreceptors. (A) The subcellular localization of the wild-type form of α-syn is mainly synaptic, accumulating in the axon terminals of photoreceptors. Genotype: sGMR-GAL4, UAS-α-synWT-EGFP. (B) The A30P mutant form of α-syn is detected throughout the cell bodies of the photoreceptors, losing its synaptic enrichment. Genotype: sGMR-GAL4, UAS-α-synA30P-EGFP.

In order to ensure that the eye phenotypes observed were not a simple consequence of different levels of transgene expression in the two independent UAS lines, rendering different protein levels for the wild-type and A30P mutant versions of α-syn, we performed an immunoblot using cellular extracts from these two UAS lines (Fig. 2.4). We found that the levels of protein expression of both UAS lines are equivalent.

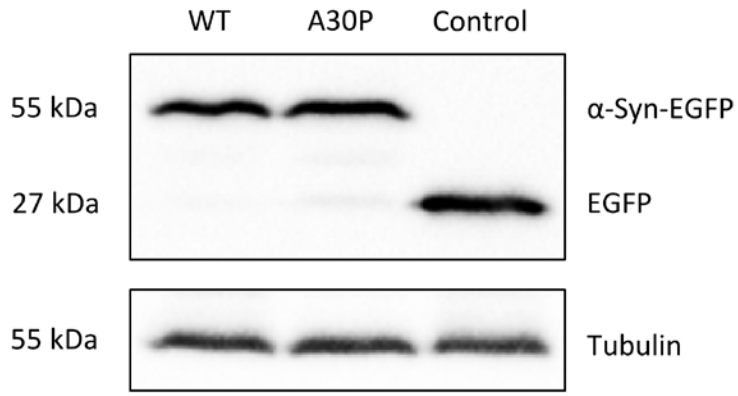

Figure 2.4. The two independent UAS transgenic lines encoding for the wild-type and the A30P mutant versions of α-syn, show similar levels of transgene expression, at the protein level. Immunoblotting (anti-EGFP) of total protein extracts from flies expressing the transgenes (α-synWT-EGFP, α-synA30P-EGFP or EGFP), under the control of sGMR-Gal4 driver. Genotypes: (WT) Genotype: sGMR-GAL4, UAS-α-synWT-EGFP. (A30P) sGMR-GAL4, UAS-α-synA30P-EGFP, (Control) Genotype: sGMR-GAL4, UAS-EGFP.

2.3.3. No differences were detected in the aggregation state of the wild-type and the A30P mutant version of α-syn

In order to explain the difference in phenotypes observed for the wild-type and mutant (A30P) forms of α-syn, in terms of α-syn's sub-cellular localization in the photoreceptors, we tried to characterize the state of α-syn aggregation in our PD model, using the conformational antibodies OC and A11 in dot blot analysis. The conformational antibodies A11 and OC recognize, respectively, generic epitopes of soluble oligomers and fibrils within amyloid proteins [23, 24]. The OC antibody is specific for the fibrillar state recognizing fibrils, being not reactive to prefibrillar oligomers or monomers, while A11 antibody is specific for the prefibrillar state, not recognizing the fibrillar state. In the dot blots analysis of fly head extracts, we could not observe affinity differences between the wild-type and the mutant A30P form of α-syn, for the conformational antibodies OC and A11 (Fig. 2.5). Furthermore, all samples, including controls without α-syn, reacted to the conformational antibodies, thus suggesting a high level of amyloidogenic proteins in the *Drosophila* brains. As expected, in our controls, α-syn aggregates made from purified α-syn bound both OC and A11. Therefore this method was not suitable to probe for the differences observed for the wild-type and mutant forms of α-syn in our model.

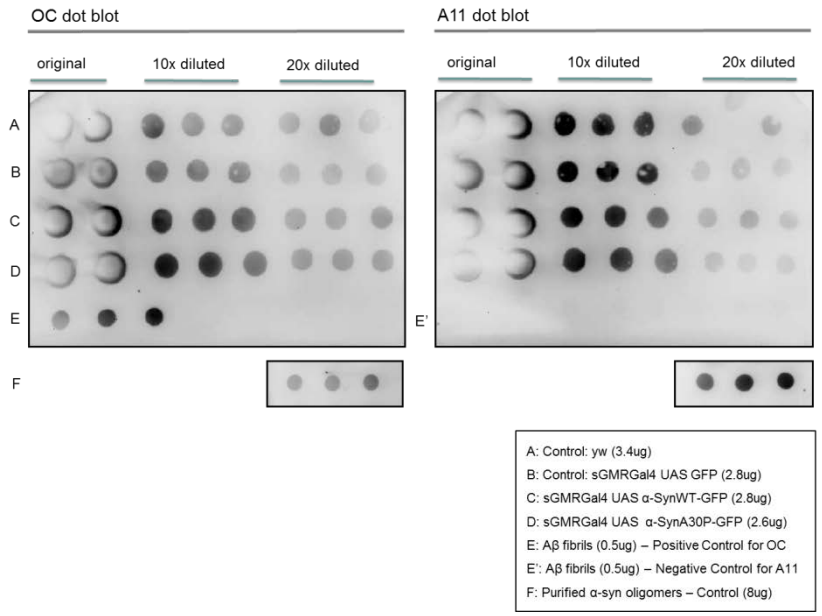

Figure 2.5. Characterization of the aggregation state of the wild-type and the A30P mutant form of α-syn by dot blot analysis, using the conformational antibodies OC and A11. No differences were detected in the aggregation state of these two versions of α-syn for both conformational antibodies tested, being both samples equally reactive (C and D). Samples from control genotypes (A and B) were also reactive to the antibodies. In the box, are indicated the genotypes and the type of aggregates (generated *in vitro*) tested, as well as the total protein quantities (µg) used in this assay.

In another attempt to characterize the aggregation state of α-syn in our *Drosophila* model, we performed immunohistochemistry staining of retinal cryosections with Congo Red and Thioflavin S dyes, two major histological stains used to detect any form of amyloid. These dyes bind to the characteristic β-pleated sheet conformation of amyloid fibrils, not binding to non-fibrillar diffuse aggregates [25]. Once again, we could not find any difference concerning the aggregation state of the two versions α-syn tested. We obtained the same staining profile for both genotypes tested separately for Congo Red and Thioflavin S (Fig. 2.6).

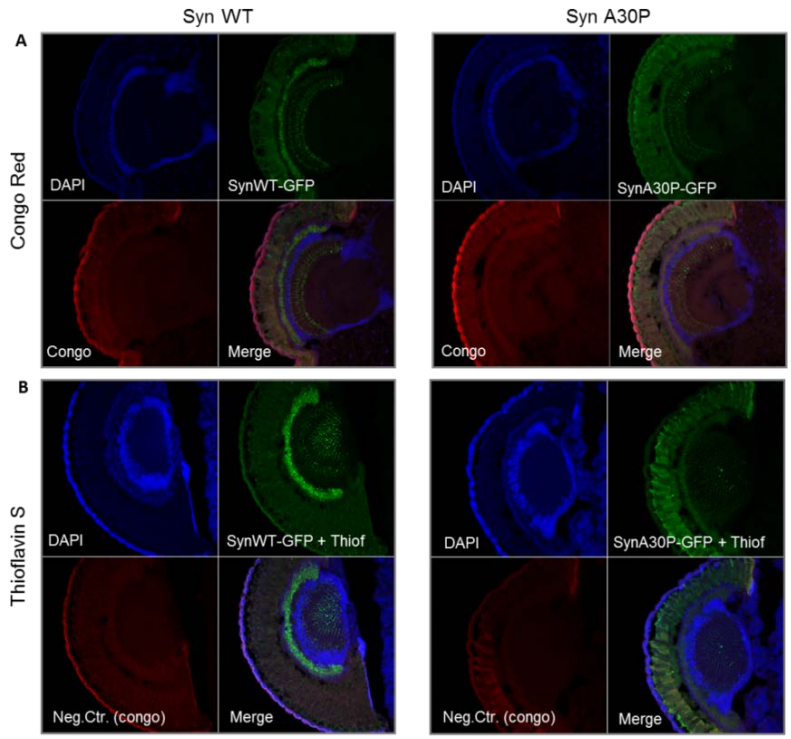

Figure 2.6. Characterization of the aggregation state of the wild-type and the A30P mutant form of α-syn, using Congo Red and Thioflavin S. No difference was detected in the aggregation state of these two versions of α-syn, when tested by staining of retinal cryosections with Congo Red and Thioflavin S (A and B). DAPI indicates the position of cell nuclei in the retina. Genotypes – Syn WT: sGMR-GAL4, UAS-α-synWT-EGFP; Syn A30P: sGMR-GAL4, UAS-α synA30P-EGFP.

2.3.4. Identification of α-syn WT and A30P protein interactors by co-immunoprecipitation and mass spectrometry analysis

As described in the section 2.3.3, the analysis of α-syn's aggregation state in our model did not explain the striking difference in the phenotypes observed for the subcellular localization of the wild-type and the A30P mutant forms of α-syn in the *Drosophila* photoreceptors.

Therefore, we decided to identify specific protein interactors for the two versions of α-syn in our model, by performing Co-IP and mass spectrometry (Fig.2.7).

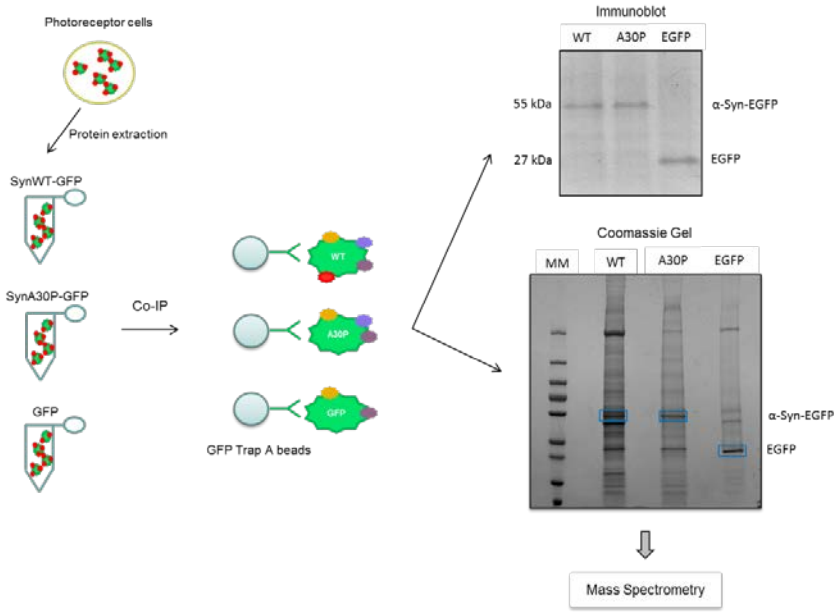

Figure 2.7. The specific protein interactors for the wild-type and the A30P mutant forms of α-syn were identified by Co-IP and mass spectrometry. Protein extracts from each genotype were prepared and incubated with agarose beads coupled to anti-GFP (GFP Trap A), which specifically bind to the EGFP tagged versions of α-syn, promoting their pulldown. The efficiency of the pulldown was evaluated by immunoblot, using an antibody against the EGFP tag. The specific protein interactors were identified by mass spectrometry of the co-immunoprecipitated proteins, which were loaded in a Coomassie gel.

The identification of the specific protein binding partners for the wild-type and A30P α-syn, especially the ones that uniquely interact with one of these versions (and not with the EGFP tag alone, which acts as a negative control), may constitute an opportunity for elaborating hypotheses of the biological processes (and plan further experiments that could corroborate these hypotheses) that may be behind the phenotypic differences observed in our model. By performing the Co-IP of our samples (SynWT-EGFP, SynA30P-EGFP and EGFP alone) and posterior identification of the protein interactors by mass spectrometry, we obtained a list containing a total of 2488 proteins. From these total number of proteins, we subtracted the ones that interacted with the GFP tag alone (1496), obtaining a list of 992 specific protein interactors. From the 992 specific protein interactors, 304 were specific for the wild-type form, while 303 were specific for the A30P mutant form of α-syn. The remaining 384 proteins were identified as being protein partners of both versions of α-syn.

Taking advantage of the DAVID software, we performed a gene ontology (GO) analysis which allowed us to identify the most enriched biological themes in our list of specific protein interactors, generating a general profile of the protein interactors for the two version of α-syn used in our study (Table 2.1). Interestingly, the results of this analysis were very consistent with the phenotypes observed in our model, since for the wild-type form of α-syn the highest scores corresponded to GO terms mostly related to the synaptic vesicle transport, synapse and neurotransmission, while for the A30P mutant form of α-syn this enrichment was lost and the highest scores obtained corresponded to GO terms mostly related with mitochondria and ribosome.

Importantly, some proteins identified as being specific interactors of α-syn in previous studies were also detected in our study, namely:

synaptobrevin, syntaxin, cysteine string protein and synapse protein 25 [11, 26].

In order to validate and further characterize the interactome described in our study in the context of PD, the interaction of α-syn with the specific proteins identified by mass spectrometry should be validated by immunoblot analysis using specific antibodies for these proteins. We successfully validated the interaction of the wild-type version of α-syn with Ferritin 1 heavy chain homologue, one of the specific protein interactors identified by mass spectrometry (Fig. 2.8).

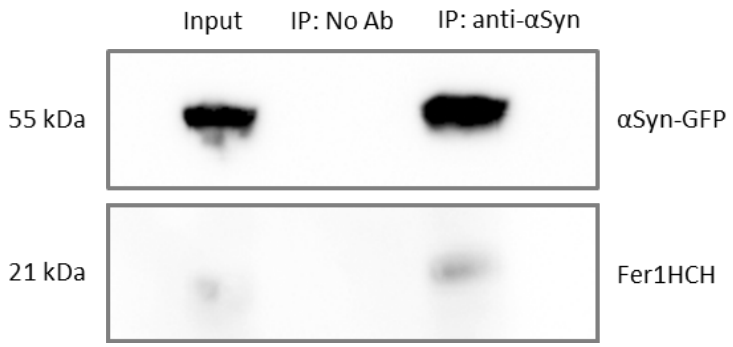

Figure 2.8. The interaction between wild-type α-syn and Ferritin 1 heavy chain homologue (Fer1HCH) was demonstrated by Co-IP and immunoblot analysis. Immunoprecipitation of α-syn-EGFP with an antibody against the EGFP tag pulled down Fer1HCH from photoreceptors. Genotype: sGMR-GAL4, UAS-α-synWT-EGFP

Table 2.1. Gene ontology (GO) analysis of the specific interactors for the wild-type and the A30P mutant forms of α-syn. The annotation clusters shown in the table are the ones found with the highest enrichment scores.

Gene ontology enrichment for α-SynWT interactors				
Annotation Cluster 1	**Enrichment Score: 1.01**	**Count**	**P_Value**	**Benjamini**
GOTERM_CC_FAT	cell junction	5	4.1E-2	9.5E-1
GOTERM_CC_FAT	plasma membrane part	8	9.8E-2	9.5E-1
GOTERM_CC_FAT	plasma membrane	11	2.3E-1	9.9E-1
Annotation Cluster 2	**Enrichment Score: 0.91**	**Count**	**P_Value**	**Benjamini**
GOTERM_BP_FAT	exocytosis	4	1.9E-2	1.0E0
GOTERM_BP_FAT	synaptic transmission	5	7.5E-2	1.0E0
GOTERM_BP_FAT	synaptic vesicle exocytosis	3	7.6E-2	1.0E0
GOTERM_BP_FAT	secretion by cell	4	7.7E-2	1.0E0
GOTERM_BP_FAT	transmission of nerve impulse	5	8.3E-2	9.9E-1
GOTERM_BP_FAT	secretion	4	8.8E-2	9.9E-1
GOTERM_BP_FAT	cell-cell signaling	5	1.0E-1	9.9E-1
GOTERM_BP_FAT	vesicle-mediated transport	7	1.1E-1	9.9E-1
GOTERM_BP_FAT	neurological system process	8	1.8E-1	9.9E-1
GOTERM_BP_FAT	synaptic vesicle transport	3	1.8E-1	9.9E-1
GOTERM_BP_FAT	neurotransmitter secretion	3	2.1E-1	9.9E-1
GOTERM_BP_FAT	generation of a signal involved in cell-cell signaling	3	2.2E-1	9.9E-1
GOTERM_BP_FAT	regulation of neurotransmitter levels	3	2.4E-1	9.9E-1
GOTERM_BP_FAT	neurotransmitter transport	3	2.9E-1	1.0E0
GOTERM_CC_FAT	synapse	3	3.5E-1	9.9E-1

Gene ontology enrichment for α-SynA30P interactors				
Annotation Cluster 1	**Enrichment Score: 4.4**	**Count**	**P_Value**	**Benjamini**
GOTERM_CC_FAT	mitochondrial ribosome	11	3.8E-8	5.5E-6
GOTERM_CC_FAT	organellar ribosome	11	3.8E-8	5.5E-6
GOTERM_CC_FAT	mitochondrion	25	1.5E-7	1.1E-5
GOTERM_CC_FAT	mitochondrial matrix	13	9.1E-7	4.4E-5
GOTERM_CC_FAT	mitochondrial lumen	13	9.1E-7	4.4E-5
GOTERM_CC_FAT	mitochondrial part	20	1.1E-6	4.0E-5
GOTERM_MF_FAT	structural constituent of ribosome	13	1.1E-6	2.5E-4
GOTERM_CC_FAT	ribosomal subunit	13	1.5E-6	4.3E-5
GOTERM_CC_FAT	ribosome	13	5.5E-6	1.3E-4
GOTERM_CC_FAT	mitochondrial large ribosomal subunit	7	3.4E-5	7.2E-4
GOTERM_CC_FAT	organellar large ribosomal subunit	7	3.4E-5	7.2E-4
GOTERM_CC_FAT	large ribosomal subunit	9	6.0E-5	1.1E-3
GOTERM_CC_FAT	membrane-enclosed lumen	18	1.2E-3	1.9E-2
GOTERM_CC_FAT	intracellular organelle lumen	17	2.5E-3	3.5E-2
GOTERM_CC_FAT	organelle lumen	17	2.5E-3	3.5E-2
GOTERM_MF_FAT	structural molecule activity	14	2.7E-3	2.7E-1
GOTERM_CC_FAT	ribonucleoprotein complex	13	4.4E-3	5.6E-2
GOTERM_BP_FAT	translation	14	4.5E-3	7.8E-1
GOTERM_CC_FAT	intracellular non-membrane-bounded organelle	20	4.2E-2	3.8E-1
GOTERM_CC_FAT	non-membrane-bounded organelle	20	4.2E-2	3.8E-1

2.3.5. Tomosyn, Spaghetti Squash, and Synaptotagmin 4 are modulators α-syn axonal transport and subcellular localization

Aiming to explain the differences observed in the axonal transport and subcellular localization for the wild-type and the A30P mutant forms of α-syn, we decided to perform a reverse RNAi screen to knock down the genes encoding specific protein interactors for these two versions of α-syn. For this genetic screen we used the RNAi lines from TRiP (Harvard Medical School) which were crossed with our line expressing the A30P mutant form of α-syn in the *Drosophila* eye. The aim was to identify modulator genes, which upon knock down, could promote the synaptic localization of A30P. From the 100 RNAi lines tested (Supplementary Table 2.1), we could identify 3 genes, enconding the proteins Tomosyn, Spaghetti Squash and Synaptotagmin 4, whose knock down promoted the synaptic localization of the A30P mutant form of α-syn (Figure 2.9).

Tomosyn is a 120-130 kDa protein, firstly identified as a Syntaxin1a-binding protein [27], with a negative regulator effect on the SNARE-dependent exocytosis, resulting from the inhibition to the priming step involved in the fusion of the vesicles with the plasma membrane [28-41]. Spaghetti Squash belongs to the group of myosin light chain proteins and is required for cytokinesis in *Drosophila* [42]. Synaptotagmin 4 is one of the members of the family of membrane-trafficking proteins, with the ability to bind calcium and to control neurotransmission by promoting the fusion of the vesicles containing neurotransmitters with plasma membranes [43]. Interestingly, the three candidate molecular modulators were closely related to neurotransmission and to the SNARE complex functioning. One may speculate that part of the toxicity of the A30P mutant version of α-syn could be caused by the abnormal interaction with other neuronal proteins, namely molecular players involved in the control of the neurotransmitters' release into the synaptic cleft.

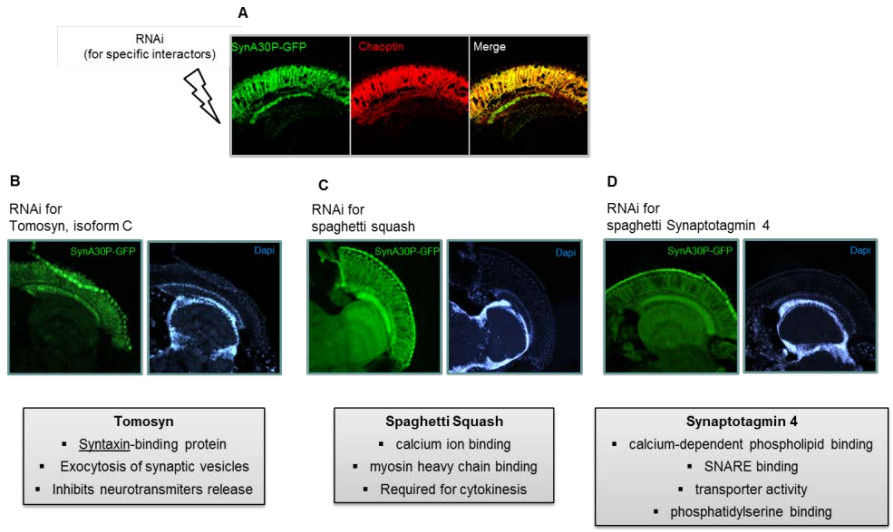

Figure 2.9. Tomosyn, Spaghetti Squash and Synaptotagmin 4, were identified in a RNAi screen, as modulators of α-syn's axonal transport in *Drosophila* photoreceptors. (A) The genetic screen consisted in performing the knocking-down of the genes encoding the specific proteins identified by immunoprecipitation and mass spectrometry as specific interactors of the mutant A30P form of α-syn, in the genetic background of flies expressing this mutant form of α-syn in the photoreceptors. (B, C, D) Tomosyn, Spaghetti Squash and Synaptotagmin 4 are 3 genes identified as being able to rescue the phenotype characterized for the wild-type form of α-syn (when genetically knocked down), thus being candidate modulator genes for the axonal transport and subcellular location of α-syn. The main biological functions of these genes (by UniProt) are indicated in the boxes.

2.4. Discussion

In our study we used a newly established *Drosophila* model for PD, expressing the wild-type and the mutant A30P versions of α-syn fused with EGFP.

Taking advantage of the Gal4/UAS system, we induced the expression of these proteins in the eye, using the sGMRGal4 driver. We observed a consistent phenotype with our model for the subcellular localization of the two versions of α-syn in the photoreceptors: the wild-type version was mainly detected in the photoreceptors' synapses, while the mutant A30P form was detected throughout the whole photoreceptors cytoplasm.

The synaptic enrichment of the wild-type version of α-syn in our model is consistent with the normal localization of this protein in the vertebrate nervous system. We believe this observation may constitute a good indication that *Drosophila* nervous system and, in this particular case, our PD model based on the expression of α-syn in the photoreceptors, may be a useful tool to study α-syn's biology at the molecular and cellular level and the relevance of this protein in the neurodegenerative context of PD.

The loss of the normal synaptic enrichment by the A30P mutant form of α-syn may be associated with the deleterious effect of this mutant form of the protein, responsible for a familial form of PD. The negative effects of this mislocalization could be caused by the loss of function of α-syn in the synaptic processes and/or by gain of toxicity by increasing the propensity of this protein to interact, co-aggregate and accumulate with other neuronal proteins in the typical protein aggregates, commonly known as Lewy Bodies, found in post-mortem analysis of PD patients' brains. It is still unclear if the mislocalization of α-syn is an early cause or a consequence of the neurodegenerative events occurring in the context of

PD and more studies, carefully designed with proper controls, are needed to clarify this issue.

In order to characterize the aggregation state of the two versions of α-syn (wild-type and A30P) used in our study, we performed two different experiments. In one of these experiments, we used the conformational antibodies OC and A11 in dot blot analysis, in the other we used the Congo Red and Thioflavin S dies for immunohistochemistry of retinal cryosections. These experiments did not contribute for the explanation of the phenotypic differences observed in our model, since the results obtained were similar for all the samples tested, with no differences being detected between the lines expressing the wild-type or the A30P mutant version of α-syn. The differential phenotypes found were not the simple consequence of different states and/or levels of aggregation of the two versions of α-syn tested.

A simple and plausible explanation for the phenotype observed in our model for the A30P mutant form of α-syn is the loss of ability to bind to the vesicles moved by the fast component of axonal transport, being the transport of this mutant version of α-syn to the synapses less efficient, when compared to the wild-type version, and consequently a bigger quantity of this mutant version of α-syn can be detected throughout the cytoplasm of the photoreceptors.

An alternative hypothesis that we took into account in our study, is a change in the affinity and propensity to interact with other biomolecules, namely the neuronal protein partners, by the A30P mutant form of α-syn. The experimental approach we chose to test this last hypothesis consisted in the identification of the specific protein partners for the wild-type and A30P mutant versions of α-syn, by Co-IP and mass spectrometry. We could identify 304 protein partners specific for the wild-type form of α-syn and 303 for the A30P mutant form. The profiles of protein interactors

found for each of these versions of α-syn were quite consistent with the phenotypes observed. For the wild-type version of α-syn, detected as being highly enriched in the synaptic terminals of the photoreceptors, the protein partners with highest scores were related to neurotransmission at the synapses, while for the A30P mutant form the majority of protein partners were associated to mitochondria or ribosome. The protein interactors selected in our study are indicated in Supplementary Table 2.1

The identification of the specific protein interactors for the A30P mutant form of α-syn, allowed us to perform a reverse genetic RNAi screen aiming to identify protein modulators that could reverse or ameliorate de subcellular mislocalization of this α-syn version. From the total number of 303 specific partners identified, we tested 100, the ones having a correspondent RNAi line available at TRiP stock center (Harvard Medical School) (Supplementary Table 2.2). From these 100 genes tested, we found 3 (Tomosyn, Spaghetti Squash and Synaptotagmin 4) that could rescue/ameliorate the phenotype, increasing the amount of α-syn A30P at the synapse.

2.5. Material and Methods

Drosophila stocks

We generated two different UAS-α-Syn-EGFP lines, one encoding a wild-type version of α-syn (UAS-α-synWT-EGFP) and the other encoding a familial mutant version of α-syn (UAS-α-synA30P-EGFP). To generate and subclone these constructs from the original plasmids, we fused α-syn cDNAs with EGFP and cloned into pUAST using the BglII and Acc65I restriction sites. The transgenic flies were generated by BestGene, USA. Four different drivers were obtained from the Bloomington Stock Center (Indiana University, Bloomington, IN, USA): nSyb-GAL4 (active in the entire nervous system, under the control of the Synaptobrevin promoter), TH-GAL4 (active in dopaminergic neurons, under the control of the tyrosine hydroxylase promoter), GMR-GAL4 (active in the eye, under the control of the glass multiple reporter) and Rh1-GAL4 (active in the photoreceptors R1–R6, under the control of the rhodopsin1 promoter).

The RNAi lines were obtained from TRiP at Harvard Medical School (NIH/NIGMS R01-GM084947). *Drosophila* stocks were maintained at 25°C on standard cornmeal media in an incubator with a 12 h light/dark cycle.

Immunohistochemistry and microscopy

Retinal cryosections of adult flies were done for confocal microscopy imaging. Briefly, adult heads were embedded in OCT (Optimal Cutting Temperature, Tissue-Tek) and frozen at -20ºC. Subsequently, 10 µm sections were cut in a cryostat (Microm HM 550). The samples were fixed during 20 min in PBS 1X + formaldehyde 4%. Finally, we proceeded with the immunostaining of the cryosections, as previously described for adult eyes [44]. The photoreceptors were stained

by incubation for 24 h at 4°C, in a humid Tupperware box, with mouse 24B10 anti-chaoptin antibody (Developmental Studies Hybridoma Bank – IA, USA) diluted 1:150 in PBST (1× PBS + 0.3% Triton X-100) containing 5% (v/v) normal goat serum. Three 10-min washes with PBST were done before incubation with a secondary anti-mouse Cy3 (Jackson ImmunoResearch), also diluted in PBST-containing 5% (v/v) normal goat serum. The retinal cryosections were analyzed and images were collected using a LSM 710 Meta Zeiss confocal microscope. Images were acquired with a resolution of 1024 × 1024, with a slice thickness of 1 µm and a line-average of 4. Z-projections were generated using ImageJ and the images were processed using Adobe Photoshop. For the Congo Red and Thioflavin S (Sigma) stainings we performed the protocol previously described, with small adaptions [45].

Dot blotting using amyloid conformational antibodies

10µl of of each sample was dotted in triplicates onto PVDF membranes and probed with a 1:500 dilution of the anti-amyloid oligomer A11 antibody (AB9234 Merck Millipore) and 1:1000 for the anti-amyloid fibrils OC antibody (AB2286 Merck Millipore) according to manufacturer instructions. Dots were visualized using an IgG HRP conjugate secondary antibody with a chemiluminescence detection system (GE Healthcare). Images were recorded and analyzed using the quantity one analysis software from Bio-Rad.

Immunoprecipitation

Flies were transferred to 50-ml tubes, frozen in liquid nitrogen and immediately decapitated by vigorous vortexing. Isolated heads were collected to 1.5-ml tubes and maintained in dry ice. Proteins were extracted in lysis buffer supplemented with Complete Protease Inhibitor Cocktail tablets from Roche (Basel, Switzerland). Total protein was quantified using the DC Protein Assay, from Bio-Rad (CA, USA). In the immunoprecipitation experiments, α-syn-EGFP, α-synA30P-EGFP and EGFP alone were pulled down from 2 mg of total protein extract, using GFP-Trap_A beads, following manufacturer's instructions (Chromotek, Munich, Germany). The pull-down of the proteins of interest was analyzed by immunoblotting using anti-GFP (3H9) antibody from Chromotek, diluted 1:1000 in PBS. Input lane corresponds to 30 µg of total protein extract and co-IP lane corresponds to one-fifth of the immunoprecipitated material.

Mass spectrometry analysis

After protein separation on a SDS–PAGE (4-12% NuPAGE Bis-Tris Gel, Invitrogen), the entire lanes of the Coomassie blue-stained gel were cut into 23 slices. All slices were reduced with 10 mM DTT for 55 min at 56°C, alkylated with 55 mM IAA for 20 min at 26°C and digested with modified trypsin (Serva) overnight at 37°C. Tryptic peptides were injected into a C18 pre-column (25 mm, 360 µm o.d., 150 µm i.d., Reprosil-Pur 120 Å, 5 µm, C18-AQ, Dr Maisch GmbH) at a flow rate of 10 µl/min. Bound peptides were eluted and separated on a C18 capillary column (12 cm, 360 µm o.d., 75 µm i.d., Reprosil-Pur 120 Å, 3 µm, C18-AQ, Dr Maisch GmbH) at a flow rate of 300 nl/min, with a gradient from 5 to 36% ACN in 0.1% formic acid for 50 min using an Agilent 1100 nano-flow LC system (Agilent Technologies) coupled to a LTQ-Orbitrap Velos hybrid

mass spectrometer (Thermo Fisher). The mass spectrometer was operated in the data-dependent mode to automatically switch between MS and MS/MS acquisition. Survey MS spectra were acquired in the Orbitrap (*m/z* 350–1600) with the resolution set to 30,000 at m/z 400 and automatic gain control target at 5 × 10E5 ions. The fifteen most intense ions were sequentially isolated for CID MS/MS fragmentation and detection in the linear ion trap. Ions with single and unrecognized charge states were excluded. Raw data was analyzed with Mascot search engine for peptide and protein identifications. The mass spectrometry analysis was performed in the Bioanalytic mass spectrometry facility at the Max Planck Institute for Biophysical chemistry, Goettingen.

Proteomic data analysis

We used Ingenuity Pathways Analysis (Ingenuity Systems®, www.ingenuity.com, IPA) software to integrate the identified proteins into signaling pathways with biological meaning. Functional analysis identified the most significant molecular and cellular functions and/or disorders to each dataset. For the identification of the enriched biological themes and the Gene Ontology terms, we used DAVID (Database for Annotation, Visualization and Integrated Discovery, (http://david.niaid.nih.gov) software.

Supplementary Table 2.1. Specific protein interactors identified by co-IP and mass spectrometry selected in our study.

				Nº Unique Peptides		
Protein	**CG**	**UniProt**	**MW**	**SynWT**	**SynA30P**	**GFP**
1-cys peroxiredoxin DPx-2540-1	CG12405	Q9GPQ1	25 kDa	3	4	0
1-cys peroxiredoxin DPx-6005	CG3083	Q9GPQ2	25 kDa	2	0	0
Ac3, isoform A	CG1506	Q9V9R3	130 kDa	4	5	0
activating transcription factor-2, isoform A	CG30420	Q9W0Z5	93 kDa	5	2	0
AKAP550	CG6775	Q9W4E2	393 kDa	2	4	0
annexin B11, isoform A	CG9968	Q9VXG4	36 kDa	4	0	0
Arc2	CG13941	Q7JV70	23 kDa	4	0	0
Arpc3A, isoform C	CG4560	Q9VF28	20 kDa	4	2	0
baldspot, isoform A	CG3971	Q9VV87	37 kDa	0	2	0
basigin, isoform A	CG31605	Q8IPG9	29 kDa	0	2	0
beta subunit of type II geranylgeranyl transferase	CG18627	Q9XZ68	39 kDa	2	2	0
brahma protein	CG5942	P25439	185 kDa	2	6	0
bride of sevenless	CG8285	P22815	100 kDa	0	3	0
brown protein	CG17632	P12428	76 kDa	0	2	0
bruce	CG6303	Q9VH01	539 kDa	3	3	0
bunched, isoform F	CG42281	Q24523	113 kDa	2	0	0
c12.2	CG12149	Q9W347	156 kDa	7	4	0
cactus zygotic protein	CG5848	Q03017	52 kDa	3	2	0
calmodulin, isoform A	CG8472	P62152	17 kDa	0	4	0
calmodulin-binding protein	CG18345	P48994	128 kDa	9	13	0
carnation, isoform A	CG12230	Q9Y1I2	69 kDa	4	0	0

Ced-12	CG5336	Q9VKB2	83 kDa	7	4	0
CG10075	CG10075	Q9VRZ7	29 kDa	3	2	0
CG10253, isoform A	CG10253	Q9V778	71 kDa	3	2	0
CG10362	CG10362	Q9VYR9	115 kDa	0	3	0
CG10417, isoform A	CG10417	Q7K4Q5	72 kDa	0	3	0
CG10562	CG10562	Q961Q8	46 kDa	2	0	0
CG10915	CG10915	Q8SX68	65 kDa	3	3	0
CG10973, isoform B	CG10973	Q95RI2	34 kDa	3	2	0
CG10990, isoform A	CG10990	Q9VY91	56 kDa	0	2	0
CG1104, isoform A	CG1104	Q9VI55	87 kDa	5	3	0
CG11055, isoform B	CG11055	Q7JR83	97 kDa	4	0	0
CG11092	CG11092	Q9XZ06	94 kDa	4	3	0
CG1134	CG1134	Q9VZJ9	38 kDa	0	3	0
CG11679	CG11679	Q9VXQ8	48 kDa	4	2	0
CG11875	CG11875	Q9VBU8	35 kDa	2	0	0
CG11943, isoform B	CG11943	Q8IQV9	235 kDa	8	6	0
CG12082	CG12082	Q9VZU7	92 kDa	3	3	0
CG12121	CG12121	Q9W366	84 kDa	2	2	0
CG12355, isoform B	CG12355	A8JNT1	23 kDa	2	0	0
CG12547	CG12547	Q9W5T4	80 kDa	3	0	0
CG13365	CG13365	Q9W5E7	14 kDa	0	2	0
CG13506	CG13506	Q9W259	57 kDa	7	5	0
CG14184, isoform A	CG14184	Q9VW73	21 kDa	4	0	0
CG14591, isoform A	CG14591	Q7JRB2	38 kDa	2	4	0
CG14786	CG14786	Q9W592	120 kDa	4	7	0
CG15118, isoform E	CG15118	A8DYI9	71 kDa	2	4	0

CG15661, isoform B	CG15661	Q9W2J3	61 kDa	7	0	0
CG17493	CG17493	Q8SXJ8	32 kDa	2	2	0
CG17514, isoform A	CG17514	Q7PLL6	294 kDa	2	6	0
CG17528, isoform D	CG17528	Q7PLI7	83 kDa	0	4	0
CG17839, isoform B	CG17839	Q7KUK9	179 kDa	3	2	0
CG18259	CG18259	Q9VWQ6	53 kDa	3	0	0
CG1909, isoform A	CG1909	Q7K4Y8	67 kDa	4	4	0
CG2658, isoform A	CG2658	Q9W4W8	90 kDa	3	3	0
CG30291	CG30291	Q95SK3	58 kDa	3	2	0
CG3036	CG3036	Q9VR44	54 kDa	2	0	0
CG31436	CG31436	Q8IMT3	50 kDa	2	0	0
CG3164, isoform B	CG3164	Q9VPJ9	78 kDa	6	7	0
CG31760, isoform B	CG31760	Q9VKA4	98 kDa	5	4	0
CG32226	CG32226	Q9VWB0	149 kDa	4	2	0
CG3226	CG3226	Q9W3Y3	26 kDa	3	3	0
CG32649	CG32649	Q9VYI6	74 kDa	4	4	0
CG32699, isoform B	CG32699	Q0KHU5	60 kDa	3	0	0
CG34132	CG34132	Q0E8V7	10 kDa	0	3	0
CG34228	CG34228	Q6IGN6	10 kDa	2	2	0
CG34306	CG34306	A8JQT5	406 kDa	3	0	0
CG34310, isoform A	CG34310	A8DYW4	9 kDa	2	2	0
CG3436, isoform A	CG3436	Q9VPL0	39 kDa	2	0	0
CG34417, isoform H	CG34417	A8JV00	558 kDa	6	2	0
CG3532	CG3532	Q9VGE4	130 kDa	2	5	0
CG40042, isoform A	CG40042	Q8MRW1	22 kDa	2	3	0
CG40045	CG40045	Q8SYG3	19 kDa	2	0	0

CG4038	CG4038	Q7KVQ0	23 kDa	4	0	0
CG40451	CG40451	Q7PLT4	18 kDa	4	4	0
CG42354, isoform A	CG42354	Q8IR21	57 kDa	0	3	0
CG4289	CG4289	Q9VPB8	31 kDa	3	2	0
CG4666	CG4666	Q9W440	23 kDa	4	4	0
CG4688	CG4688	Q7JYX0	27 kDa	0	3	0
CG5112	CG5112	Q9VBQ5	58 kDa	5	5	0
CG5154 protein	CG5154	E1UIB8	50 kDa	4	0	0
CG5508, isoform A	CG5508	Q9Y137	95 kDa	4	4	0
CG6123	CG6123	Q9VWW2	64 kDa	6	2	0
CG6364, isoform B	CG6364	B7Z0P8	34 kDa	3	4	0
CG6406, isoform B	CG6406	Q7K1C5	60 kDa	2	2	0
CG6523	CG6523	Q9VJZ6	24 kDa	4	5	0
CG7135	CG7135	Q9VWY5	49 kDa	3	2	0
CG7215, isoform A	CG7215	Q9VEC8	15 kDa	0	3	0
CG7261	CG7261	Q9VQ78	135 kDa	3	2	0
CG7378, isoform B	CG7378	A8JUQ2	26 kDa	3	2	0
CG7770	CG7770	Q9VW56	14 kDa	0	2	0
CG7772	CG7772	Q9VX02	18 kDa	2	2	0
CG7900	CG7900	Q9VHV9	59 kDa	5	0	0
CG7956, isoform B	CG7956	Q59DV6	126 kDa	5	6	0
CG8031	CG8031	Q9VG04	33 kDa	2	3	0
CG8176, isoform C	CG8176	Q6AWD5	130 kDa	4	4	0
CG8298, isoform A	CG8298	Q7JY99	66 kDa	0	4	0
CG8329	CG8329	Q9VT23	28 kDa	8	4	0
CG8858	CG8858	Q9V677	212 kDa	0	9	0

CG9009, isoform A	CG9009	Q9VXZ8	66 kDa	3	3	0
CG9027, isoform D	CG9027	Q0E9C3	23 kDa	2	0	0
CG9339, isoform A	CG9339	Q9VIH7	67 kDa	3	0	0
cGMP-dependent protein kinase	CG10033	Q03043	121 kDa	4	2	0
CHKov2	CG10675	Q9VBS0	48 kDa	2	0	0
complexin, isoform A	CG32490	Q8IPM8	16 kDa	2	0	0
CP60	CG1825	Q24147	48 kDa	0	3	0
Cullin-3, isoform C	CG11861	Q9V475	90 kDa	2	0	0
DCAPL1	CG18408	Q966V1	268 kDa	3	2	0
down syndrome cell adhesion molecule, isoform AK	CG17800	Q0E9K5	224 kDa	0	2	0
Dsrc41	CG7873	Q9V9J3	59 kDa	8	7	0
D-stat protein short form	CG4257	Q24151	86 kDa	3	0	0
dystrophin, isoform H	CG34157	Q9VDW6	410 kDa	2	4	0
fermitin 1, isoform A	CG14991	Q9VZI3	80 kDa	2	5	0
ferritin 1 heavy chain homologue, isoform A	CG2216	Q7KRU8	23 kDa	5	4	0
focal contact protein paxillin	CG31794	Q9GSE0	62 kDa	7	0	0
G protein alpha49B, isoform H	CG17759	P23625	42 kDa	4	4	0
G protein alphai subunit 65A	CG10060	P20353	41 kDa	0	4	0
G protein gamma 1, isoform C	CG8261	P38040	8 kDa	4	3	0
G protein-coupled receptor kinase 2	CG17998	P32866	81 kDa	0	3	0
gamma-syntrophin-like protein SYN2	CG4905	Q9GT68	53 kDa	0	2	0
glutamate-gated chloride channel	CG7535	Q94900	52 kDa	9	0	0
GST-containing FLYWCH zinc-finger protein, isoform D	CG33546	Q8INS9	27 kDa	3	3	0
highwire	CG32592	Q9NB71	566 kDa	2	2	0

histone deacetylase 6 isoform A	CG6170	Q86NK9	125 kDa	0	6	0
hook	CG10473	Q9VJ12	77 kDa	4	3	0
hook-like, isoform A	CG10473	Q9VJ12	84 kDa	4	2	0
junctophilin	CG4405	Q966S5	116 kDa	3	2	0
kismet, isoform A	CG3696	Q9VPL9	574 kDa	0	2	0
krueppel target at 95D, isoform A	CG5405	Q9VCE7	125 kDa	5	2	0
kugelkern, isoform A	CG5175	Q8SX89	60 kDa	2	0	0
laminin B2 chain	CG3322	P15215	182 kDa	7	0	0
lin19 protein	CG1877	Q24311	89 kDa	2	2	0
longitudinals lacking, isoform D	CG12052	Q7KQZ4	79 kDa	2	2	0
MAP kinase activated protein-kinase-2, isoform B	CG3086	P49071	41 kDa	0	3	0
MAP kinase kinase 4, isoform A	CG9738	O61444	48 kDa	3	2	0
Mi-2, isoform A	CG8103	O97159	224 kDa	5	6	0
microtubule associated protein	CG5000	Q9U5W6	227 kDa	4	8	0
mitoferrin	CG4963	Q9VAY3	42 kDa	0	3	0
Myb-interacting protein 40	CG15119	Q7K159	30 kDa	4	4	0
myosin heavy chain-like, isoform G	CG31045	Q0KI67	242 kDa	5	11	0
neural lazarillo	CG33126	Q8SXR1	24 kDa	6	4	0
nitric oxide synthase	CG6713	Q27571	152 kDa	5	5	0
no mitochondrial derivative	CG5395	Q9VL02	42 kDa	3	4	0
p115	CG1422	Q9W3N6	92 kDa	2	6	0
presenilin, isoform A	CG18803	O02194	59 kDa	3	0	0
protein tyrosine phosphatase 61F, isoform A	CG9181	Q9W0G1	62 kDa	3	2	0
pyruvate dehydrogenase kinase, isoform B	CG8808	A8DY78	48 kDa	0	5	0

Rab11 interacting protein, isoform A	CG6606	Q9VWS3	92 kDa	5	0	0
Rab35, isoform A	CG9575	Q9W5X0	23 kDa	7	5	0
rab3-GEF, isoform A	CG5627	A8JUX2	225 kDa	9	12	0
rho-like	CG9366	Q24192	22 kDa	7	5	0
ric8a	CG15797	Q9W358	66 kDa	4	3	0
roadblock	CG10751	Q7KMS3	11 kDa	3	0	0
Roe1	CG6155	P48604	24 kDa	4	3	0
sec10	CG6159	Q9XTM1	82 kDa	0	4	0
slowpoke binding protein, isoform A	CG6772	Q8IPH9	58 kDa	2	2	0
SP2637, isoform C	CG5473	Q7KIS4	35 kDa	0	5	0
spaghetti squash	CG3595	P40423	20 kDa	7	2	0
spenito, isoform B	CG2910	Q7KMJ6	89 kDa	7	0	0
synaptojanin, isoform B	CG6562	Q5U0V7	135 kDa	2	2	0
synaptotagmin 4	CG10047	Q9U6P7	52 kDa	3	0	0
syndecan, isoform A	CG10497	P49415	42 kDa	4	0	0
syntaxin 8	CG4109	Q9VV76	26 kDa	2	2	0
target of rapamycin	CG5092	Q9VK45	281 kDa	2	3	0
tho2, isoform A	CG31671	Q9VQ76	189 kDa	0	3	0
tomosyn, isoform C	CG17762	Q9VYK6	158 kDa	3	5	0
translocation protein 1, isoform A	CG4758	Q9VL50	47 kDa	4	3	0
transport and golgi organization 5, isoform A	CG32675	Q9W2S1	58 kDa	5	5	0
Trs23	CG9298	Q9VLI9	25 kDa	2	2	0
Ucp4A, isoform A	CG6492	Q9VX14	37 kDa	2	4	0
vacuolar protein sorting 45	CG8228	Q9VHB5	65 kDa	4	6	0

Supplementary Table 2.2. RNAi lines from TRiP (Harvard Medical School) tested in the reverse genetic screen for modulators of α-syn sub-cellular localization.

Protein name	**CG**	**Bloomington**	**TRiP**
1-cys peroxiredoxin DPx-2540-1	CG12405	32497	HMS00500
A kinase anchor protein 200, isoform D	CG13388	28532	HM05018
Ac3, isoform A	CG1506	28626	JF03041
acetylcholine esterase, isoform A	CG17907	25958	JF01978
activating transcription factor-2, isoform A	CG30420	26210	JF02108
annexin B11, isoform A	CG9968	38311	HMS01775
Arpc3A, isoform C	CG4560	27044	JF02370
bendless, isoform A	CG18319	28721	JF03148
beta subunit of type II geranylgeranyl transferase	CG18627	34902	HMS01247
beta-coatomer protein	CG6223	33741	HMS01079
brahma protein	CG5942	34520	HMS00050
bruchpilot, isoform H	CG42344	25891	JF01932
bubblegum	CG4501	28639	JF03054
bunched, isoform F	CG42281	28322	JF02954
cactus zygotic protein	CG5848	34775	HMS00084
calcium activated protein for secretion, isoform B	CG33653	31984	JF03418
Calcium/calmodulin-dependent protein kinase, isoform B	CG6703	32857	HMS00644
calcium-independent phospholipase A2 VIA, isoform A	CG6718	36129	HMS01544
calmodulin, isoform A	CG8472	34609	HMS01318
calmodulin-binding protein	CG18345	26722	JF02264
carnation, isoform A	CG12230	34007	HMS00972

Cdk5 gene	CG8203	27517	JF02667
Ced-12	CG5336	28556	HM05042
CG10132	CG10132	31992	JF03427
CG10253, isoform A	CG10253	34350	HMS01339
CG10417, isoform A	CG10417	39051	HMS01971
CG10915	CG10915	34879	HMS00199
CG11092	CG11092	33908	HMS00850
CG12082	CG12082	31886	JF02163
CG17514, isoform A	CG17514	34355	HMS01344
CG17528, isoform D	CG17528	26292	JF02061
CG18259	CG18259	34081	HMS01089
CG1909, isoform A	CG1909	28024	JF02858
CG31103	CG31103	28359	JF02995
CG32226	CG32226	34370	HMS01359
CG3226	CG3226	32875	HMS00662
CG4038	CG4038	34013	HMS00979
CG6364, isoform B	CG6364	35351	GL00263
CG8298, isoform A	CG8298	34524	HMS00813
CG8858	CG8858	34975	HMS01128
complexin, isoform A	CG32490	42017	HMS02442
connector of kinase to AP-1, isoform A	CG7392	34522	HMS00081
CP60	CG1825	32458	HMS00457
Cullin-3, isoform C	CG11861	36684	HMS01572
DCAPL1	CG18408	36663	HMS01551
dj-1beta	CG1349	38999	HMS01915
D-stat protein short form	CG4257	33637	HMS00035
fermitin 1, isoform A	CG14991	25966	JF01986

focal contact protein paxillin	CG31794	28695	JF03111
G protein alpha49B, isoform H	CG17759	36775	JF02390
G protein alphai subunit 65A	CG10060	34924	HMS01273
G protein gamma 1, isoform C	CG8261	34372	HMS01361
G protein-coupled receptor kinase 2	CG17998	34843	HMS00161
gamma-syntrophin-like protein SYN2	CG4905	28363	JF02999
GST-containing FLYWCH zinc-finger protein, isoform D	CG33546	32399	HMS00394
highwire	CG32592	28031	JF02866
histone deacetylase 6 isoform A	CG6170	34072	HMS0007
Hsp70/Hsp90 organizing protein homolog	CG2720	32979	HMS00779
kinesin heavy chain	CG7765	35770	HMS01519
kinesin light chain	CG5433	33934	HMS00883
kismet, isoform A	CG3696	34908	HMS01254
Klp10A, isoform A	CG1453	33963	HMS00920
kugelkern, isoform A	CG5175	28750	JF03178
laminin A chain	CG10236	28071	JF02908
lin19 protein	CG1877	29520	HM05197
longitudinals lacking, isoform D	CG12052	26714	JF02254
megator	CG8274	32941	HMS00735
Mi-2, isoform A	CG8103	33419	HMS00301
microtubule associated protein	CG5000	38990	HMS01906
microtubule-associated protein	CG1483	32939	HMS00733
mitoferrin	CG4963	34038	HMS01013
Myb-interacting protein 40	CG15119	32834	HMS00524
nitric oxide synthase	CG6713	28792	JF03220
Numb-associated kinase, isoform A	CG10637	38326	HMS01793

Phosphatidylinositol 4-kinase III alpha	CG10260	38242	HMS01686
presenilin, isoform A	CG18803	38374	HMS01843
protein tyrosine phosphatase 61F, isoform A	CG9181	32426	HMS00421
pyruvate dehydrogenase kinase, isoform B	CG8808	28635	JF03050
Rab11 interacting protein, isoform A	CG6606	38325	HMS01792
Rab35, isoform A	CG9575	28342	JF02978
rab3-GEF, isoform A	CG5627	28954	HM05165
Rab-protein 4, isoform B	CG4921	33757	HMS01100
rho-like	CG9366	33723	HMS00605
ric8a	CG15797	28910	HM05121
roadblock	CG10751	31977	JF03411
sec10	CG6159	27483	JF02633
slowpoke binding protein, isoform A	CG6772	27492	JF02642
SP2637, isoform C	CG5473	37522	HMS01664
spaghetti squash	CG3595	32439	HMS00437
synaptojanin, isoform B	CG6562	34378	HMS01368
synaptotagmin 4	CG10047	39016	HMS01934
syntaxin 8	CG4109	26013	JF02038
target of rapamycin	CG5092	33951	HMS00904
tho2, isoform A	CG31671	28537	HM05023
tomosyn, isoform C	CG17762	31980	JF03414
Transcription elongation factor SPT5	CG7626	34837	HMS00153
transportin, isoform A CG7398	CG7398	27546	JF02697
Trs23	CG9298	38303	HMS01765
vacuolar protein sorting 45	CG8228	38944	HMS01858
zormin, isoform D	CG33484	34039	HMS01014

2.6. References

1. Singleton, A.B., et al., *alpha-Synuclein locus triplication causes Parkinson's disease.* Science, 2003. **302**(5646): p. 841.
2. Chartier-Harlin, M.C., et al., *Alpha-synuclein locus duplication as a cause of familial Parkinson's disease.* Lancet, 2004. **364**(9440): p. 1167-9.
3. Polymeropoulos, M.H., et al., *Mutation in the alpha-synuclein gene identified in families with Parkinson's disease.* Science, 1997. **276**(5321): p. 2045-7.
4. Kruger, R., et al., *Ala30Pro mutation in the gene encoding alpha-synuclein in Parkinson's disease.* Nat Genet, 1998. **18**(2): p. 106-8.
5. Zarranz, J.J., et al., *The new mutation, E46K, of alpha-synuclein causes Parkinson and Lewy body dementia.* Ann Neurol, 2004. **55**(2): p. 164-73.
6. Lesage, S., et al., *G51D alpha-synuclein mutation causes a novel parkinsonian-pyramidal syndrome.* Ann Neurol, 2013. **73**(4): p. 459-71.
7. Pasanen, P., et al., *Novel alpha-synuclein mutation A53E associated with atypical multiple system atrophy and Parkinson's disease-type pathology.* Neurobiol Aging, 2014. **35**(9): p. 2180 e1-5.
8. Proukakis, C., et al., *A novel alpha-synuclein missense mutation in Parkinson disease.* Neurology, 2013. **80**(11): p. 1062-4.
9. Marques, O. and T.F. Outeiro, *Alpha-synuclein: from secretion to dysfunction and death.* Cell Death Dis, 2012. **3**: p. e350.
10. Bellucci, A., et al., *From alpha-synuclein to synaptic dysfunctions: new insights into the pathophysiology of Parkinson's disease.* Brain Res, 2012. **1476**: p. 183-202.
11. Burre, J., et al., *Alpha-synuclein promotes SNARE-complex assembly in vivo and in vitro.* Science, 2010. **329**(5999): p. 1663-7.
12. Burgoyne, R.D. and A. Morgan, *Chaperoning the SNAREs: a role in preventing neurodegeneration?* Nat Cell Biol, 2011. **13**(1): p. 8-9.
13. Fernandez-Chacon, R., et al., *The synaptic vesicle protein CSP alpha prevents presynaptic degeneration.* Neuron, 2004. **42**(2): p. 237-51.
14. Umbach, J.A., et al., *Presynaptic dysfunction in Drosophila csp mutants.* Neuron, 1994. **13**(4): p. 899-907.
15. Zinsmaier, K.E., et al., *Paralysis and early death in cysteine string protein mutants of Drosophila.* Science, 1994. **263**(5149): p. 977-80.

16. Murphy, D.D., et al., *Synucleins are developmentally expressed, and alpha-synuclein regulates the size of the presynaptic vesicular pool in primary hippocampal neurons.* J Neurosci, 2000. **20**(9): p. 3214-20.
17. Cabin, D.E., et al., *Synaptic vesicle depletion correlates with attenuated synaptic responses to prolonged repetitive stimulation in mice lacking alpha-synuclein.* J Neurosci, 2002. **22**(20): p. 8797-807.
18. Nemani, V.M., et al., *Increased expression of alpha-synuclein reduces neurotransmitter release by inhibiting synaptic vesicle reclustering after endocytosis.* Neuron, 2010. **65**(1): p. 66-79.
19. Bodner, C.R., et al., *Differential phospholipid binding of alpha-synuclein variants implicated in Parkinson's disease revealed by solution NMR spectroscopy.* Biochemistry, 2010. **49**(5): p. 862-71.
20. Jensen, P.H., et al., *Binding of alpha-synuclein to brain vesicles is abolished by familial Parkinson's disease mutation.* J Biol Chem, 1998. **273**(41): p. 26292-4.
21. Vamvaca, K., M.J. Volles, and P.T. Lansbury, Jr., *The first N-terminal amino acids of alpha-synuclein are essential for alpha-helical structure formation in vitro and membrane binding in yeast.* J Mol Biol, 2009. **389**(2): p. 413-24.
22. Fortin, D.L., et al., *Lipid rafts mediate the synaptic localization of alpha-synuclein.* J Neurosci, 2004. **24**(30): p. 6715-23.
23. Kayed, R., et al., *Common structure of soluble amyloid oligomers implies common mechanism of pathogenesis.* Science, 2003. **300**(5618): p. 486-9.
24. Kayed, R., et al., *Fibril specific, conformation dependent antibodies recognize a generic epitope common to amyloid fibrils and fibrillar oligomers that is absent in prefibrillar oligomers.* Mol Neurodegener, 2007. **2**: p. 18.
25. Dickson, D.W., *The pathogenesis of senile plaques.* J Neuropathol Exp Neurol, 1997. **56**(4): p. 321-39.
26. Sharma, M., J. Burre, and T.C. Sudhof, *CSPalpha promotes SNARE-complex assembly by chaperoning SNAP-25 during synaptic activity.* Nat Cell Biol, 2011. **13**(1): p. 30-9.
27. Fujita, Y., et al., *Tomosyn: a syntaxin-1-binding protein that forms a novel complex in the neurotransmitter release process.* Neuron, 1998. **20**(5): p. 905-15.
28. Widberg, C.H., et al., *Tomosyn interacts with the t-SNAREs syntaxin4 and SNAP23 and plays a role in insulin-stimulated GLUT4 translocation.* J Biol Chem, 2003. **278**(37): p. 35093-101.

29. Cheviet, S., et al., *Tomosyn-1 is involved in a post-docking event required for pancreatic beta-cell exocytosis.* J Cell Sci, 2006. **119**(Pt 14): p. 2912-20.
30. Zhang, W., et al., *Tomosyn is expressed in beta-cells and negatively regulates insulin exocytosis.* Diabetes, 2006. **55**(3): p. 574-81.
31. Yamamoto, Y., et al., *The tail domain of tomosyn controls membrane fusion through tomosyn displacement by VAMP2.* Biochem Biophys Res Commun, 2010. **399**(1): p. 24-30.
32. Williams, A.L., et al., *Structural and functional analysis of tomosyn identifies domains important in exocytotic regulation.* J Biol Chem, 2011. **286**(16): p. 14542-53.
33. Gladycheva, S.E., et al., *Receptor-mediated regulation of tomosyn-syntaxin 1A interactions in bovine adrenal chromaffin cells.* J Biol Chem, 2007. **282**(31): p. 22887-99.
34. Ashery, U., et al., *Friends and foes in synaptic transmission: the role of tomosyn in vesicle priming.* Trends Neurosci, 2009. **32**(5): p. 275-82.
35. Chen, K., et al., *Tomosyn-dependent regulation of synaptic transmission is required for a late phase of associative odor memory.* Proc Natl Acad Sci U S A, 2011. **108**(45): p. 18482-7.
36. Gracheva, E.O., et al., *Tomosyn inhibits synaptic vesicle priming in Caenorhabditis elegans.* PLoS Biol, 2006. **4**(8): p. e261.
37. Gracheva, E.O., et al., *Tomosyn negatively regulates both synaptic transmitter and neuropeptide release at the C. elegans neuromuscular junction.* J Physiol, 2007. **585**(Pt 3): p. 705-9.
38. Hu, Z., X.J. Tong, and J.M. Kaplan, *UNC-13L, UNC-13S, and Tomosyn form a protein code for fast and slow neurotransmitter release in Caenorhabditis elegans.* Elife, 2013. **2**: p. e00967.
39. Gracheva, E.O., et al., *Tomosyn negatively regulates CAPS-dependent peptide release at Caenorhabditis elegans synapses.* J Neurosci, 2007. **27**(38): p. 10176-84.
40. Dybbs, M., J. Ngai, and J.M. Kaplan, *Using microarrays to facilitate positional cloning: identification of tomosyn as an inhibitor of neurosecretion.* PLoS Genet, 2005. **1**(1): p. 6-16.
41. Gracheva, E.O., et al., *Differential Regulation of Synaptic Vesicle Tethering and Docking by UNC-18 and TOM-1.* Front Synaptic Neurosci, 2010. **2**: p. 141.
42. Karess, R.E., et al., *The regulatory light chain of nonmuscle myosin is encoded by spaghetti-squash, a gene required for cytokinesis in Drosophila.* Cell, 1991. **65**(7): p. 1177-89.

43. Wang, Z. and E.R. Chapman, *Rat and Drosophila synaptotagmin 4 have opposite effects during SNARE-catalyzed membrane fusion.* J Biol Chem, 2010. **285**(40): p. 30759-66.
44. Walther, R.F. and F. Pichaud, *Immunofluorescent staining and imaging of the pupal and adult Drosophila visual system.* Nat Protoc, 2006. **1**(6): p. 2635-42.
45. Iijima, K., et al., *Abeta42 mutants with different aggregation profiles induce distinct pathologies in Drosophila.* PLoS One, 2008. **3**(2): p. e1703.

Chapter III

The role of huntingtin N-terminal phosphorylation on its aggregation and toxicity in a *Drosophila* model for Huntington's disease

Contribution

This chapter contains unpublished data:

Branco-Santos, J*, **Poças, GM*,** Herrera, F*, Domingos, PM, Giorgini, F and Outeiro, TF, N-terminal phosphorylation modulates mutant huntingtin aggregation and toxicity. Manuscript in preparation. * equal contribution.

G.M. Poças declares to have actively contributed for the experimental design, data analyses and manuscript writing**.** G.M. Poças performed the *Drosophila* genetic crosses, confocal microscopy of *Drosophila* samples and the climbing and survival assays. J. Branco-Santos and F. Herrera carried out the experiments in mammalian cell cultures.

3.1. Abstract

Huntington's disease (HD) is an autosomal dominant neurodegenerative disorder caused by a mutation in the first exon of the *IT-15* gene. This mutation encodes for an abnormally elongated polyglutamine (polyQ) amino acid sequence within the N-terminal region of huntingtin protein (Htt), leading to conformational changes of the protein, which dramatically increase its propensity to misfold and aggregate. N-terminal Htt fragments harboring the expanded polyQ tract are directly involved in HD pathogenesis. Our model for HD is based on the overexpression of an N-terminal truncated form of mutant human Htt, encoded by Htt exon 1 (Httex1). Among the first 17 amino acid residues in the N-terminal (NT17) domain of Htt protein there are three that are susceptible to be post-translationally modified by the action of kinases and phosphatases: threonine 3 (T3), serine 13 (S13) and serine 16 (S16). We analyzed the relative contribution of the phosphorylation state of each one of these amino acid residues to Httex1 oligomerization, aggregation and toxicity in mammalian cells and *Drosophila*. Single mutations mimicking the phosphorylation state of mutant Htt (phosphomimic mutants) at any of the three residues completely abolished Htt aggregation in cultured cells but enhanced aggregation in *Drosophila*. Biochemical inhibition or genetic knockdown of specific protein phosphatases also modulated Htt aggregation and toxicity. Our results indicate that single phosphorylation events in Httex1 are sufficient to modulate Htt aggregation and toxicity depending on the biological context. These findings suggest that modulation of Httex1 phosphorylation at specific sites might be a target for therapeutic interventions against HD.

3.2. Introduction

Huntington's disease (HD) is a polyQ disease pathology caused by a mutation in the first exon of the *IT-15* gene, which encodes for an expanded polyQ tract (with more than 36 glutamines) in the huntingtin protein (Htt), as previously explained in chapter I.

N-terminal Htt fragments harboring the polyQ tract are directly involved in HD pathogenesis [1-6]. Neuronal aggregates enriched in this truncated forms of mutant Htt constitute an HD hallmark observed both in mouse models and in post-mortem analysis of patients' brains [7]. Htt contains several proteolytic cleavage sites for different proteases, namely from the caspase family [8]. The cleavage of mutant Htt at the position 586 by caspase-6 constitutes a prerequisite for neuronal dysfunction and death in HD [9]. For this reason, caspase-6 is currently considered one of the most attractive therapeutic targets for HD [10]. The relevance of Htt cleavage for HD is consistent with the fact that expression of the truncated protein containing Htt exon 1 is enough to produce HD in animal models [1, 5-7, 9].

Our collaborators (Outeiro and Herrera) have recently developed a system for the simultaneous visualization of oligomeric species and inclusion bodies in living cells [11, 12] (Fig. 3.1). In this system, based on the Bimolecular Fluorescence Complementation (BiFC) assay, wild type (19Q) or disease-causing (97Q) Httex1 (the truncated form of Htt encoded by exon 1) are fused to two non-fluorescent halves of Venus, a bright yellow variant of the Green fluorescent protein. When Htt fragments dimerize, the Venus halves are brought together and reconstitute the functional fluorophore. Fluorescence is therefore proportional to the extent of Httex1 dimerization/oligomerization. Mutant versions of BiFC constructs were made for each of the phosphorylatable residues in NT17, changing these amino acids to either alanine (phosphoresistant) or to

aspartic acid (phosphomimic). Importantly, these phosphomutants behave like phosphorylated peptides in terms of their aggregation *in vitro* [17].

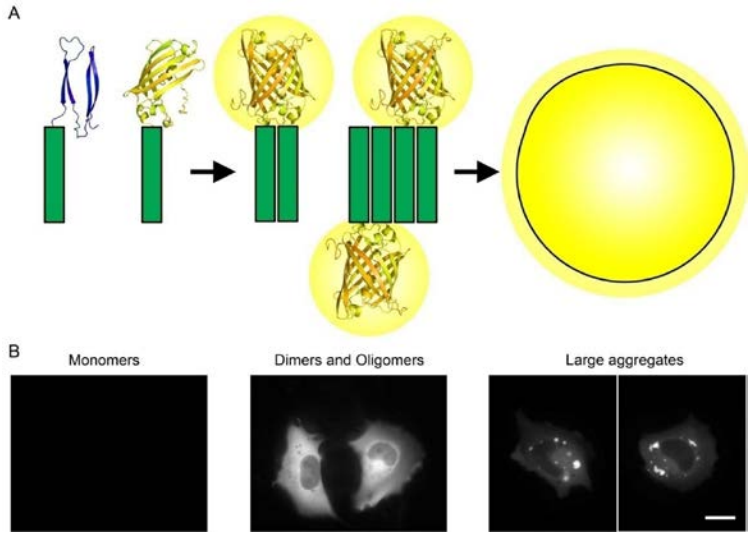

Figure 3.1. Schematic representation of the BiFC cellular model used for the visualization of Htt oligomerization and aggregation in living mammalian cells. (A) Httex1 is fused to two non-fluorescent halves of the Venus fluorescent protein. When Htt dimerizes, the Venus halves are brought together, reconstituting the functional fluorophore and emitting fluorescence. (B) Using this BiFC system the monomeric species do not show fluorescence; dimers and oligomers show a homogeneously distributed fluorescence in the subcellular compartment where they are formed; large aggregates are observed as bright fluorescent regions, "scavenging" the fluorescence from the rest of the cell. Scale bar, 20 µm. Adapted from [13].

Our *Drosophila* model for HD is also based on the transgenic expression of the N-terminal truncated form of mutant human Httex1, which is constituted by three domains: the first 17 amino acids at the N-terminus (NT17), the polyQ tract and the proline-rich region (PRR) (Fig.3.2).

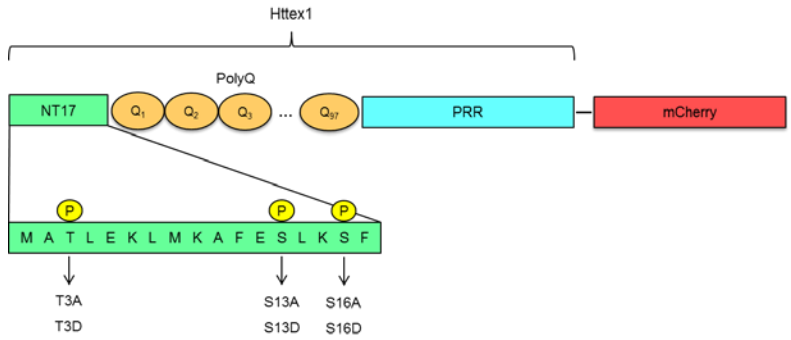

Figure 3.2. Schematic representation of the exon-1 truncated form of mutant Htt (Httex1) generated in our study. Httex1 is constituted by 3 domains: the first 17 amino acids at the N-terminal domain (NT17), the polyQ tract and the proline-rich region (PRR). The amino acid sequence of NT17 is shown and its phosphorylatable sites (P) are indicated in yellow. The Phosphomutations generated in our study for the residues T3, S13 and S16 are also indicated. In the phosphomimetic mutants these residues were substituted for aspartate (D) while in the phosphoresistant mutants the substitutions were for an alanine (A). The fluorescent protein tag mCherry was fused to the C-terminal portion of Httex1.

We generated an Httex1 construct containing an expanded polyQ tract of 97 glutamines and fused to the mCherry fluorescent tag in the c-terminal domain (97QHttex1-mCherry). A wild-type form of this construct, with a polyQ tract containing 19 glutamines (19QHttex1-mCherry), was also generated.

Post-translational modifications (PTMs) have a critical role in the structure and function of proteins and several studies have suggested a major role for PTMs in HD pathogenesis (reviewed in [14]). Htt contains several residues susceptible to be post-translationally modified in the NT17 domain. The most common PTMs in the NT17 are phosphorylation, ubiquitination, SUMOylation and acetylation [15]. Concerning the phosphorylation in NT17, there are 3 amino acid residues susceptible to the action of kinases and phosphatases: threonine 3 (T3), serine 13 (S13) and serine 16 (S16). Phosphorylation is one of the most prevalent and studied PTM in the context of HD, and previous studies have shown that

phosphorylation of mutant Htt has a protective role in HD, affecting the aggregation and toxicity levels of this protein [16-19]. Presently, IKK is the only kinase identified as being directly involved in the phosphorylation of NT17 [20], although CK-2 inhibitors can also modulate its phosphorylation at Ser13/Ser16 [21]. To the best of our knowledge, no phosphatase has been identified to date as being responsible for the dephosphorylation of NT17.

In this work, we generated transgenic flies expressing different mutant forms of Httex1 with the T3, S13 and S16 residues being either mutated to aspartate (D), mimicking the phosphorylated state (phosphomimetic), or to alanine (A), rendering them non-phosphorylatable (phosphoresistant) (Fig.3.1). With our new *Drosophila* tools, we intended to study the effects of the phosphorylation/dephosphorylation of T3, S13 and S16 residues on the aggregation and toxicity of mutant Htt *in vivo*. Furthermore, we aimed to identify some of the phosphatases involved in the dephosphorylation of these residues, which may constitute a promising therapeutic target in HD.

3.3. Results

3.3.1. Cdc25 inhibitors prevent mutant huntingtin aggregation and regulate its phosphorylation

The inhibition of certain kinases can modulate Htt N-terminal phosphorylation. For example, Casein kinase-2 inhibitors reduce N-terminal phosphorylation at S13 and S16, increasing the toxicity caused by mutant Htt and suggesting that phosphorylation of these residues has a protective role for cells [21]. IKK, a kinase involved in inflammatory response, directly phosphorylates Htt at S13 and S16, and it activates Htt clearance through the activation of proteasomal and lysosomal degradation mechanisms [20].

However, nothing is still known about protein phosphatases modulating Htt N-terminal dephosphorylation and its effects in terms of mutant Htt oligomerization, aggregation and toxicity. Therefore, we intended to identify relevant phosphatases in the context of HD.

Our collaborators used a library of pharmacological inhibitors (Enzo Life Sciences) to test the effect of 33 phosphatase inhibitors on mutant Htt aggregation (Fig. 3.3).

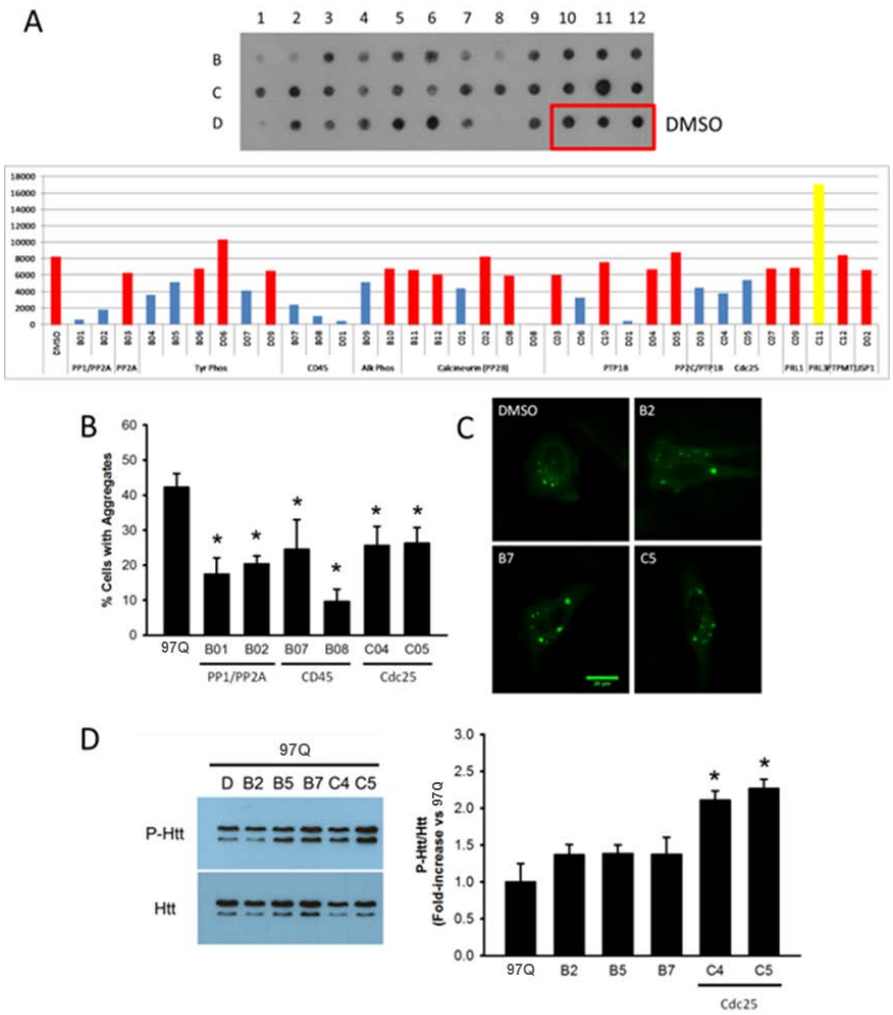

Figure 3.3. Cdc25 inhibitors prevent mutant huntingtin aggregation and regulate its phosphorylation in Human H4 glioma cells. (A) The effect of 33 phosphatase inhibitors (Enzo Life Sciences) on the aggregation mutant Htt, was tested by filter trap assays. Normal Htt does not produce aggregates (Not shown). Graph shows optic density readings from the immunoblot. PP1/PP2A, CD45 and Cdc25 inhibitors showed the most consistent results, and were therefore selected for further analyses (B-D). (B) PP1/PP2A, CD45 and Cdc25 inhibitors reduced significantly the percentage of cells with aggregates. (C) However, no differences in the average number and size of aggregates were detected upon treatment with phosphatase inhibitors. (D) Western blot for total levels of Htt and phosphorylated Htt (anti phosho-Htt, Ambion), that recognizes phosphorylation at serines 13 and 16). Only Cdc25 inhibitors produced an increase in Htt phosphorylation. Graphs

show the average ± standard deviation of three independent experiments. *, significant versus 97Q plus DMSO, $p<0.05$*. Scale bar, 20 μm. AU, arbitrary units.

This approach led to the identification of inhibitors for 3 phosphatases (Cdc25, PP1/PP2A and CD45) that decreased mutant Htt aggregation in mammalian cells. Inhibition of these phosphatases significantly reduced the percentage of cells with aggregates (Fig. 3.3B). However, in cells with Htt aggregates, no significant differences in the average number and size of aggregates were detected upon treatment with inhibitors for these phosphatases (Fig. 3.3C). Concerning the effect of the inhibitors in the phosphorylation of NT17 residues, only Cdc25 inhibitors produced an increase in Htt phosphorylation at S13 and S16 (Fig. 3.3D). For this reason, we decided to further characterize the effect of the Cdc25 phosphatase in our *Drosophila* model for HD.

3.3.2. Genetic knockdown of Cdc25 in *Drosophila* dopaminergic neurons reduced the aggregation of mutant Htt

We decided to validate the results obtained in cell culture for Cdc25, by doing genetic knockdown experiments in *Drosophila*. We knocked down *string*, the *Drosophila* homologue for Cdc25, in the dopaminergic (DA) neurons (Fig. 3.4).

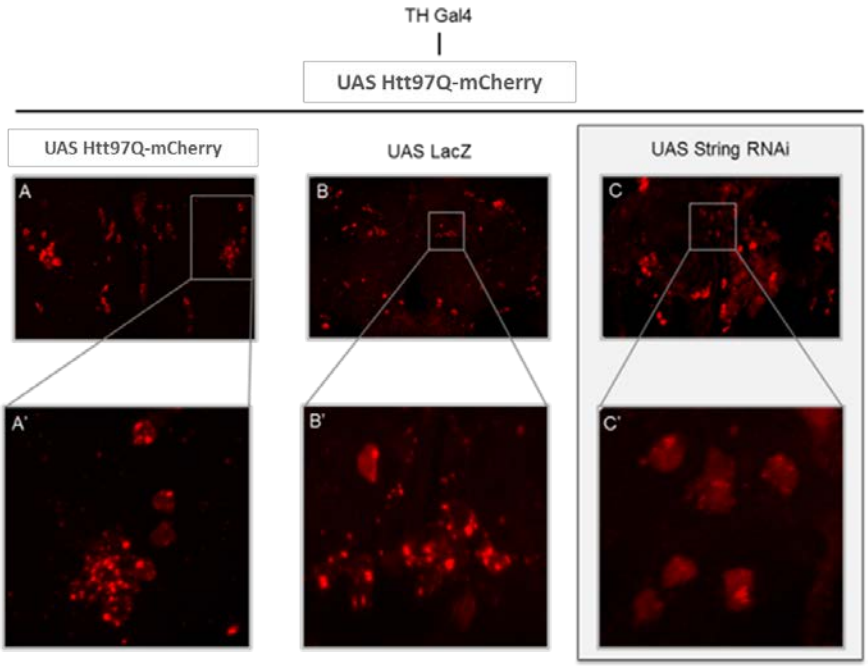

Figure 3.4. The genetic knockdown of *string*, *Drosophila* homologue for Cdc25, reduced the aggregation of mutant Htt in *Drosophila* dopaminergic (DA) neurons. (A) Protein aggregates generated by the expression of mutant Htt. Genotype: TH-GAL4, UAS-Htt97Q-mCherry. (B) The co-expression of the inert LacZ had no effect on Htt aggregation. Genotype: TH-GAL4, UAS-Htt97Q-mCherry/UAS-LacZ. (C) The genetic knocking down of String promoted a significant reduction of Htt aggregation. Genotype: TH-GAL4, UAS-Htt97Q-mCherry/UAS-StringRNAi.

Expression of mutant Htt in DA neurons induced the accumulation of protein aggregates, as expected (Fig. 3.4A). Co-expressing mutant Htt with the *string* RNAi reduced Htt aggregation, validating the results obtained in mammalian cells (Fig. 3.4C). To exclude a non-specific effect of the *string* RNAi line, we induced the co-expression of mutant Htt with LacZ. The Htt/LacZ cross showed a phenotype similar to mutant Htt alone. This strongly indicates that the reduction in the aggregation of mutant Htt was specifically induced by specific inhibition of Cdc25 (Fig. 3.4B).

Cdc25 is involved in the control of the cell-division cycle, by activating cyclin-dependent protein kinases (Cdks), through dephosphorylation events [22]. Therefore, Cdc25 induces the entry and the progression of the different phases of the cell cycle, including mitosis. Although Cdks are absent in post-mitotic differentiated adult neurons, it was previously demonstrated an increased activity of Cdc25 in brain samples from AD patients, suggesting a possible association between cell cycle misregulation and neurodegeneration [23]. Taking into account our results in living human cells and *Drosophila*, we think it would be relevant to further investigate the role of Cdc25 in the context of HD."

3.3.3. The phosphorylation of NT17 residues modulates the oligomerization and aggregation of mutant Htt in human H4 glioma cells and in *Drosophila* dopaminergic neurons

Using human H4 glioma cells, we found by fluorescence microscopy that 97QHttex1-Venus BiFC pairs promptly oligomerized and generated inclusion bodies (Fig. 3.5A). By performing filter-trap assays and Native-PAGE, it was confirmed that the wild-type 19QHttex1-Venus BiFC pairs, when compared to the mutant (97Q) pairs, generated significantly less oligomeric species and did not accumulated as SDS-insoluble aggregates (Fig. 3.6). Remarkably, all single mutations mimicking the phosphorylated state of 97QHttex1 (T3D, S13D or S16D) completely inhibited the formation of large insoluble inclusion bodies in living cells (Fig. 3.5A and 3.6FT). This inhibitory effect in the aggregation of mutant Htt was not observed with phosphoresistant mutations (T3A, S13A and S16A), being the pattern of aggregation similar to non-mutated 97QHttex1 pairs (Fig. 3.5 and 3.6). Native-PAGE analyses confirmed that all phosphomutants formed oligomeric species (Fig. 3.6). In order to test the effect of the phosphomutations in the neurotoxicity of mutant Htt, we performed a toxicity assay based on the levels of LDH release. We found that the T3D phosphomimic significantly reduced the neurotoxicity of mutant Htt, to equivalent levels of the wild-type (19Q) Htt (Fig. 3.5C). For the rest of the phosphomutants, we could not detect any significant difference in terms of toxicity, in comparison to the normal mutant (97Q) Htt.

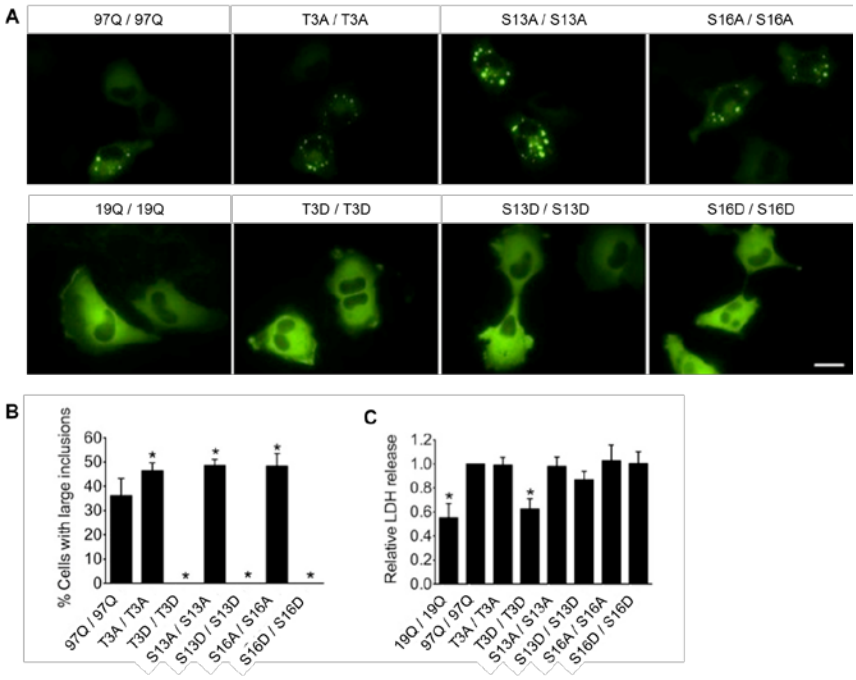

Figure 3.5. Phosphorylation of NT17 residues abolishes the accumulation of large Htt aggregates in H4 cells. (A) Cells were transfected with the indicated pairs of BiFC constructs and Htt aggregation was evaluated by fluorescence microscopy. The 97QHtt pair typically shows large aggregates in the cytosol. While the phenotype of phosphoresistant mutants resembles the 97QHtt wt phenotype, the phosphomimic mutants showed homogeneous fluorescence in the cytosol, with a total absence of aggregates. Scale bar, 20 μm. (B) Quantitative analyses of microscopy pictures showed that the phosphoresistant mutations increase the percentage of cells with aggregates (C) The toxicity assay analyzed by LDH release, revealed that only the phosphomimic T3D mutation induced a significant reduction in the toxicity levels. *, Significant versus non-mutated 97QHtt BiFC constructs, $p<0.05$.

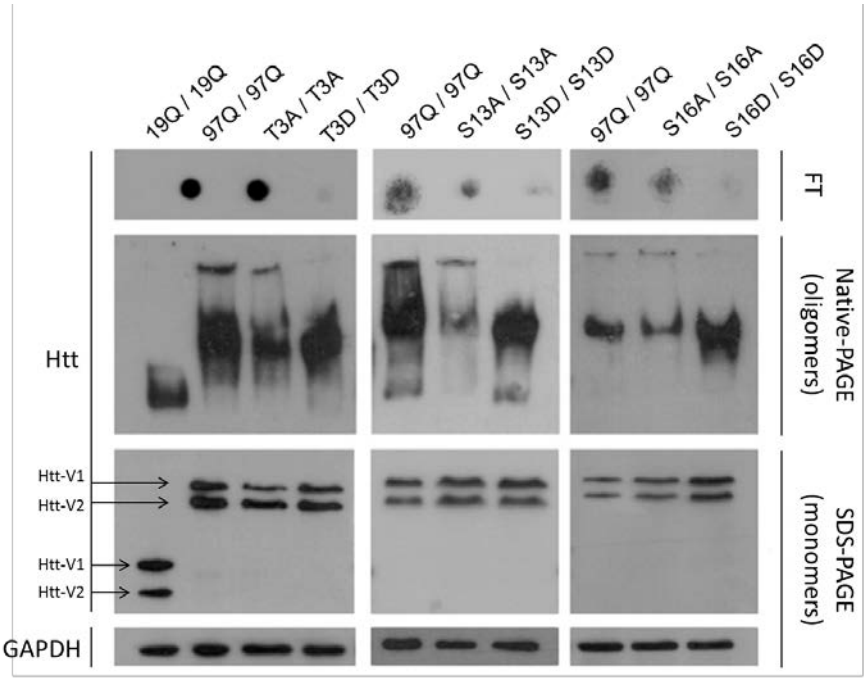

Figure 3.6. Phosphorylation of NT17 residues affects Htt oligomerization and the formation of large aggregates in H4 cells. Filter trap (FT) assays were consistent with microscopy results, showing that phosphomimic mutants do not produce SDS-insoluble aggregates. In the case of the S16D mutant, there is also a striking increase in the production of oligomeric species, as can be observed in native-PAGE conditions. Htt wt (19Q) did not produce SDS-insoluble aggregates or large amounts of oligomeric species. When transfected together phosphomimic 97QHtt-V1 BiFC mutant and non-mutated 97QHtt-V2 BiFC constructs showed similar levels of SDS-insoluble aggregates but a mixed pattern in terms of oligomerization.

We expanded these human cell studies by testing the effect of each single-residue phosphoresistant and phosphomimic versions of Htt in the levels of mutant Htt aggregation and neurotoxicity in *Drosophila*. Phosphoresistant mutants showed a slight tendency to generate a higher number of aggregates of smaller sizes, but the patterns of aggregation were very similar to non-mutated 97QHtt-mCherry, with protein aggregates present in the cytoplasm (Fig. 3.7 C,E,G). Phosphomimic mutants showed visibly larger aggregates inside and outside cells (Fig. 3.7 D,F,H).

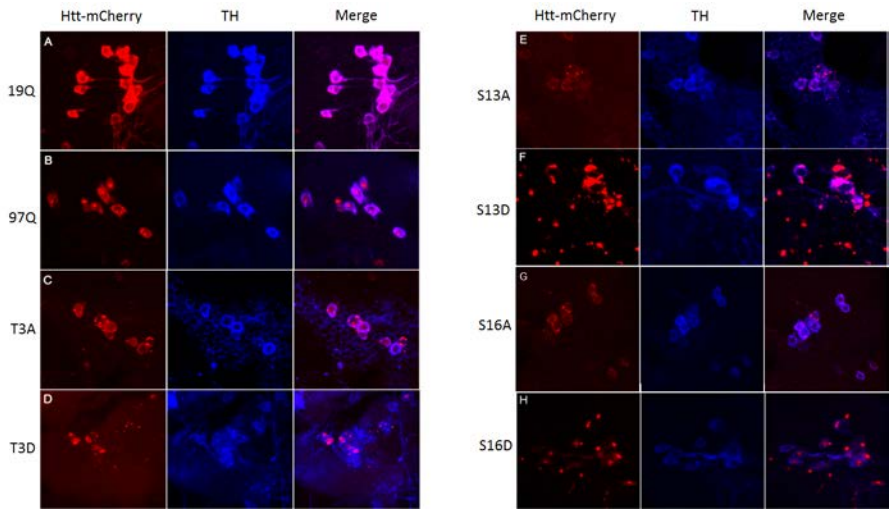

Figure 3.7. Phosphorylation of NT17 residues affects Htt aggregation in *Drosophila* dopaminergic (DA) neurons. (A) The wild-type version 19Htt-mCherry did not generate inclusions. (B) The normal mutant 97QHtt-mCherry accumulated as protein aggregates. (C, E, G) The phosphoresistant mutations T3A, S13A and S16A in the mutant Htt promoted the formation protein aggregates morphologically similar to the normal mutant version of Htt, although with a tendency to form smaller and a higher number of aggregates. (D, F, H) The phosphomimic mutations T3D, S13D and S16D promoted the formation of significantly larger aggregates when compared to the normal or to the phosphoresistant versions of mutant Htt. All the different versions of Htt fused to mCherry tag were expressed in the DA neurons using the TH Gal4 driver.

Therefore, we demonstrated that single NT17 phosphorylation events affect the state of aggregation of muntant Htt. The next step consisted in evaluating the effect of these phosphorylation events in the motor abilities and survival of the flies, by performing climbing and survival assays.

3.3.4. The dephosphorylation of NT17 residues induces motor dysfunction and life span decrease in *Drosophila*

We evaluated the motor function and life span of flies expressing the different phosphomutant versions of mutant Htt in the central nervous system under the control of the nSyb-GAL4 driver (Fig. 3.8).

Flies expressing mutant Htt containing the phosphoresistant mutations T3A, S13A and S13A showed a stronger and faster deterioration of their motor function when compared to the ones expressing the phosphomimic versions T3D, S13D and S16D or the normal version (non-phosphomutant) of mutant Htt (Htt97Q-mcherry) (Fig. 3.8A). Remarkably, flies expressing the T3D phosphomutant completely lost the geotactic response on the third week of the assay (approximately 26 days-old flies).

The expression of T3A, S13A and S16A mutant forms of Htt also induced a significant decrease in flies' life span when compared to the rest of the genotypes tested (Fig. 3.8B).

Interestingly, the decline of the motor functions and the increase of mortality both started at the same age (around the beginning of the third week), suggesting that these phenotypes are both consequence of the same factor, presumably an increase in the neurotoxicity of dephosphorylated Htt.

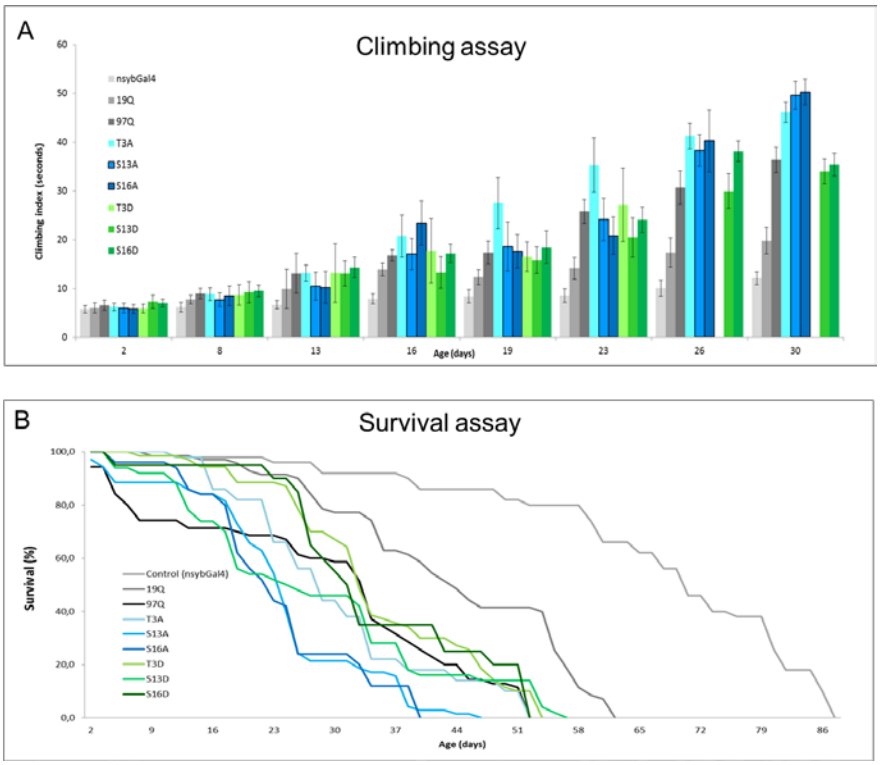

Figure 3.8. The dephosphorylation of NT17 residues induced a strong impairment of flies' motor abilities and an increase in the mortality. (A) The expression of mutant Htt (driven by nSyb-GAL4) containing the phosphoresistant mutations T3A, S13A and S16A induced a strong impairment of flies' motor abilities compared to all the other genotypes tested, including the phosphomimic mutations T3D, S13D and S16D. The Y-axis represents the time (in seconds), it took for five males to climb 15 cm (mean ± SEM). Statistically significant values, comparing each of genotypes, were calculated by doing two-way ANOVA with Bonferroni post-test. (B) The expression of mutant Htt (driven by nSyb-GAL4) containing the phosphoresistant mutations T3A, S13A and S16A promoted a significant reduction of flies' life span in comparison with the rest of the genotypes tested. The phosphomimic mutations T3D, S13D and S16D promoted a significant increase of flies' longevity comparing to the normal (non-phosphomutant) mutant Htt (Htt97Q-mCherry). Values on the Y-axis represent the percentage of flies alive at each time point analyzed.

However, our results clearly suggest a deleterious effect of NT17 dephosphorylation since flies expressing the phosphoresistant mutant versions of Htt showed a faster and stronger progression of HD-like phenotypes, comparing to the rest of the genotypes tested. It seems that the dephosphorylation of mutant Htt may contribute for an enhancement of its toxicity, inducing an earlier onset and faster progression of HD. Therefore, phosphatases involved in the dephosphorylation of NT17 residues may constitute a very interesting therapeutic target in HD.

3.4. Discussion

The results obtained in this study suggest an important role of NT17 phosphorylation in HD. We presented evidence that single NT17 phosphorylation events can modulate mutant Htt aggregation and that the final outcome of this modulation depends on the biological context.

Previous studies demonstrated a protective effect of double phosphorylation events at S13 and S16 in the context of HD [18, 24]. Actually, despite single phosphorylation events are more common than double phosphorylation events [25], the majority of the works developed with the aim of investigating the effect of the NT17 phosphorylation on mutant Htt aggregation and neurotoxicity have focused on double phosphorylation events at S13 and S16. The occurrence of these double phosphorylation events would implicate high levels of specific kinases, only possible by their overexpression [20]. Additionally, previous studies also demonstrated that both single and double S13 and S16 phosphorylation similarly inhibit mutant Htt aggregation in vitro [24]. Therefore, we decided to direct our efforts to investigate the therapeutical potential of single NT17 phosphorylation events in cells and in vivo, and to identify phosphatases involved in this process, which we believe to be a more promising approach.

Although our study is not the first one to specifically focus on single phosphorylation events at T3, S13 and S16 residues [21, 26], it is the only one to address the effect of these events on the aggregation and neurotoxicity of mutant Htt. We developed our study in two different systems, one using human cells in culture, and other using a new *Drosophila* model for HD. In living cells, we found that all the phosphomimic mutations (T3D, S13D and S16D) abolished the aggregation of mutant Htt, which is consistent with previous works demonstrating an inhibitory effect of NT17 phosphorylation in mutant Htt

aggregation [24]. In contrast, in our *Drosophila* model for HD, these phosphomimic mutations had the opposite effect in terms of mutant Htt aggregation, enhancing it, which is partially coherent with a previous study in *Drosophila* where it was also observed that the phosphomimic mutation T3D enhanced aggregation of mutant Htt, while the T3A mutation slightly reduced it [19]. Interestingly, in our fly model, we found that higher levels of mutant Htt aggregation and the formation of bigger aggregates were correlated with a reduction in the neurotoxicity.

With our work we also found that the inhibition of specific protein phosphatases resulted in lower aggregation of mutant Htt. Specifically, the inhibition of Cdc25 promoted a reduction of mutant Htt aggregation, both in human H4 cells and in *Drosophila* DA neurons. We are currently interested in identifying the specific residues in the NT17 which are substrate to the action of the phosphatases identified in our study as being modulators of mutant Htt aggregation.

Despite the contradictory observations in our study, concerning mutant Htt aggregation and toxicity, depending on the model used, we demonstrated that single NT17 phosphorylations are sufficient to modulate mutant Htt aggregation and neurotoxicity. Moreover, our work suggests that the neurotoxicity of mutant Htt could be efficiently modified by NT17 phosphorylation independently of its effect on protein aggregation. We hope that the continuation of this study could consistently establish NT17 as a promising target in the search for new drugs for HD.

3.5. Material and Methods

Cell culture and BiFC plasmids

Human H4 glioma cells (ATCC HTB-148, LGC Standards, Barcelona, Spain) were maintained in OPTI-MEM I medium supplemented with 10% fetal bovine serum and penicillin/streptomycin (1%), under controlled conditions of temperature and CO2 (37oC, 5% CO2). All reagents were purchased from Gibco (Invitrogen, Barcelona, Spain). For all the experiments, cells were seeded at a density of 10.000 cells/cm^2. Depending on the analytical method, cells were seeded on different types of plates. The density was maintained among the different sizes of plates in order to obtain comparable results with different techniques. For flow cytometry and toxicity assays, cells were grown on 6-well plates (Techno Plastic Cultures AG, Switzerland) and seeded in duplicate for each experimental group (2 wells per group). For microscopy, cells were seeded on glass- bottom 35 mm dishes (MatTek Corporation, Ashland, MA, USA). For protein extraction (PAGE and filter trap assays) cells were seeded in 100 mm dishes (Techno Plastic Cultures AG, Switzerland). Twenty-four hours later, X-tremeGene 9 DNA transfection reagent (Roche diagnostics, Mannheim, Germany) was used to transiently transfect cells with the different combinations of plasmids, according to the manufacturer's instructions. We and others have observed that 97QHtt expression is much less efficient than 19QHtt expression, resulting in impaired protein levels when cells are transfected with the same amount of plasmid. Such expression differences cause biased experimental results, 19QHtt being more toxic and producing more aggregates than 97QHtt. In order to correct this, 97QHtt-Venus (phosphomutants and nonmutated plasmids) and 19QHtt-Venus BiFC plasmids were used in an approximate proportion of 1:6, as previously

described (Herrera et al., 2011). Twenty-four hours after transfection, cells were handled according to the requirements of each analytical method.

Drosophila stocks

We generated eight constructs each encoding different versions of UAS-Htt-mCherry lines: one encoding a wild-type version of Htt with a 19 polyQ tail, another encoding a mutant version of Htt with a 97 polyQ tail, and the other six encoding phosphomutant versions (T3A/D, S13A/D and S16A/D) of Htt also containing a polyQ tract with 97 glutamines. We cloned these constructs into pWalium10-roe, using the Gateway cloning technology (Thermo Fisher Scientific, USA). The transgenic lines were generated using phiC31 integrase-mediated DNA integration (BestGene Strain #9723, attP acceptor site in 28E7). Two different drivers were obtained from the Bloomington Stock Center (Indiana University, Bloomington, IN, USA): TH-GAL4 (active in DA neurons, under the control of the tyrosine hydroxylase promoter) and nSyb-GAL4 (active in the entire nervous system, under the control of the Synaptobrevin promoter). *Drosophila* stocks were maintained at 19°C on standard cornmeal media in an incubator with a 12 h light/dark cycle.

Immunohistochemistry and microscopy

Brain preparations for confocal microscopy imaging were done as previously described [27]. Briefly, adult flies were anesthetized with CO_2 and the brains were isolated from the head cuticles and fixed in phosphate buffered saline (PBS) containing 4% paraformaldehyde.

DA neurons were stained by incubation for 48 h at 4°C with mouse anti-TH antibody (Immunostar, Hudson, WI, USA) diluted 1:50 in PBST (1× PBS + 0.3% Triton X-100) containing 5% (v/v) normal goat serum. Three 10-min washes with PBST were done before incubation with a

secondary anti-mouse Cy5 (Jackson ImmunoResearch), also diluted in PBST-containing 5% (v/v) normal goat serum. Brain samples were analyzed and images were collected using a LSM 710 Meta Zeiss confocal microscope. Images were acquired with a resolution of 1024 × 1024, with a slice thickness of 1 µm and a line-average of 4. Z-projections were generated using ImageJ and the images were processed using Adobe Photoshop.

Immunoblotting analysis

Western blotting analyses were performed using equivalent amounts of protein (15 µg) from the different extracts tested. Protein extraction was done under denaturing or native conditions for western blots and filter traps, respectively. For denaturing conditions, the samples were boiled for 5 min at 95 ºC in a denaturing loading buffer (200 mM Tris-HCl pH 6.8; 8% SDS; 40% glycerol; 6.3% β-mercaptoethanol; 0.4% bromophenol blue). Subsequently, the samples were resolved on a 12% SDS-polyacrylamide gel by electrophoresis. For native conditions, the samples were resuspended and lysed in SDS- and mercaptoethanol-free loading buffer (200 mM Tris-HCl pH 6.8; 40% glycerol; 0.4% bromophenol blue) and they were not boiled. Then the samples were directly loaded and run on 5% Native (SDS-free)-polyacrylamide gels. After electrophoresis, the proteins were transferred onto PVDF membranes using the Trans-Blot TurboTM Transfer Starter System (Bio-rad, Hercules, CA, USA). Posteriorly to the transfer, in order to confirm the efficiency of the protein transfer and the equal loading of the samples, a Ponceau S staining was performed on membranes. The membranes were incubated on blocking solution [5% non-fat dry milk in Tris-HCl buffer saline-Tween with a (TBS-T) (150 mM NaCl, 50 mM Tris pH 7.4, 0.5% Tween-20)] for 1 hour at room temperature and with agitation. Membranes were then incubated

with the appropriate dilution of primary antibodies in a solution of 5% bovine serum albumin (BSA) in TBS 1X (150 mM NaCl, 50 mM Tris pH 7.4) and 0.05% of sodium azide. The mouse monoclonal Htt antibody (Millipore, Billerica, MA, USA) was incubated in a 1:500 dilution overnight at 4 ºC and with agitation. The mouse monoclonal GAPDH antibody (Ambion, Austin, TX, USA) was incubated for 1 hour at room temperature with agitation in a dilution of 1:30000. Membranes were then washed 3 times in TBS-T and incubated with a secondary mouse IgG Horseradish Peroxidase-linked antibody (GE Healthcare Life Sciences, Uppsala, Sweden), diluted in 5% non-fat dry milk in TBS-T, under the following conditions: 1:5000 for 2-3 hours (for Htt) or 1:40000 for 30 min (for GAPDH) at room temperature and with agitation. Membranes were washed 3 times in TBS-T and the immunoblot signal was revealed using enhanced chemiluminescence reagents (Millipore, Billerica, MA, USA) and visualized after exposition to autoradiographic films.

Filter trap assay

Protein extracts were obtained in native conditions, as described above, and SDS was added to 100 μg of each extract to a final SDS concentration of 0.4% (w/v). The samples were passed through cellulose acetate membranes (0.22 μm pore; GE Water & Process Technologies, Fairfield, CT, USA) by vacuum, using a dot blot device. Cellulose acetate membranes were previously incubated with PBS 1X and 1% (w/v) SDS solution. Posteriorly to the filtration step, 2 washing steps were carried out, using a PBS 1X and 1% (w/v) SDS solution to clean the wells; and membranes were treated with the blocking solution, and incubated with antibodies as described above. The chemiluminescence detection was done as previously described.

Climbing assays and survival assays

Motor function was analyzed by startle-induced locomotion and negative geotaxis response assays, commonly called climbing assays, as previously described [28]. Briefly, groups of 10 males of the same age of each genotype of interest were placed into 18-cm-long vials, at room temperature for environmental acclimatization, and 30 min later they were gently tapped to the bottom of the vial (a minimum number of 30 males per genotype was tested). We recorded the climbing time when five flies crossed the 15-cm finish line. For each genotype we tested three independent groups of males and performed five trials for each time point. Results are the average climbing time ± SEM of these independent experiments.

For survival assays, flies were maintained in a humid incubator at 19°C under a 12 h light/dark cycle. Thirty adult females of the same age were placed in three vials (10 flies per vial) containing fresh food. Each 3 days the flies were transferred into vials with fresh food and the number of living flies was registered.

Statistical analysis

Statistical analyses were done using GraphPad Prism software version 5 (San Diego, CA, USA). For BiFC, we performed a One-way ANOVA followed by a post-hoc Tukey test for average comparison. For climbing assays, we performed a Two-way ANOVA followed by a Bonferroni post-test. For the survival assays, we performed a Log-rank (Mantel-Cox) test.

3.6. References

1. Kim, Y.J., et al., *Caspase 3-cleaved N-terminal fragments of wild-type and mutant huntingtin are present in normal and Huntington's disease brains, associate with membranes, and undergo calpain-dependent proteolysis.* Proc Natl Acad Sci U S A, 2001. **98**(22): p. 12784-9.
2. Cooper, J.K., et al., *Truncated N-terminal fragments of huntingtin with expanded glutamine repeats form nuclear and cytoplasmic aggregates in cell culture.* Hum Mol Genet, 1998. **7**(5): p. 783-90.
3. Hoffner, G., M.L. Island, and P. Djian, *Purification of neuronal inclusions of patients with Huntington's disease reveals a broad range of N-terminal fragments of expanded huntingtin and insoluble polymers.* J Neurochem, 2005. **95**(1): p. 125-36.
4. Davies, S.W., et al., *Formation of neuronal intranuclear inclusions underlies the neurological dysfunction in mice transgenic for the HD mutation.* Cell, 1997. **90**(3): p. 537-48.
5. Landles, C., et al., *Proteolysis of mutant huntingtin produces an exon 1 fragment that accumulates as an aggregated protein in neuronal nuclei in Huntington disease.* J Biol Chem, 2010. **285**(12): p. 8808-23.
6. Sathasivam, K., et al., *Aberrant splicing of HTT generates the pathogenic exon 1 protein in Huntington disease.* Proc Natl Acad Sci U S A, 2013. **110**(6): p. 2366-70.
7. Wellington, C.L., et al., *Caspase cleavage of mutant huntingtin precedes neurodegeneration in Huntington's disease.* J Neurosci, 2002. **22**(18): p. 7862-72.
8. Qin, Z.H. and Z.L. Gu, *Huntingtin processing in pathogenesis of Huntington disease.* Acta Pharmacol Sin, 2004. **25**(10): p. 1243-9.
9. Graham, R.K., et al., *Cleavage at the caspase-6 site is required for neuronal dysfunction and degeneration due to mutant huntingtin.* Cell, 2006. **125**(6): p. 1179-91.
10. Wang, X.J., et al., *Activation and regulation of caspase-6 and its role in neurodegenerative diseases.* Annu Rev Pharmacol Toxicol, 2015. **55**: p. 553-72.
11. Herrera, F., et al., *Visualization of cell-to-cell transmission of mutant huntingtin oligomers.* PLoS Curr, 2011. **3**: p. RRN1210.
12. Outeiro, T.F., et al., *Formation of toxic oligomeric alpha-synuclein species in living cells.* PLoS One, 2008. **3**(4): p. e1867.

13. Branco-Santos, J., *The role of N-terminal phosphorylation on huntingtin oligomerization, aggregation and toxicity.* Master Thesis, 2012.
14. Ehrnhoefer, D.E., L. Sutton, and M.R. Hayden, *Small changes, big impact: posttranslational modifications and function of huntingtin in Huntington disease.* Neuroscientist, 2011. **17**(5): p. 475-92.
15. Arndt, J.R., M. Chaibva, and J. Legleiter, *The emerging role of the first 17 amino acids of huntingtin in Huntington's disease.* Biomol Concepts, 2015. **6**(1): p. 33-46.
16. Watkin, E.E., et al., *Phosphorylation of mutant huntingtin at serine 116 modulates neuronal toxicity.* PLoS One, 2014. **9**(2): p. e88284.
17. Warby, S.C., et al., *Phosphorylation of huntingtin reduces the accumulation of its nuclear fragments.* Mol Cell Neurosci, 2009. **40**(2): p. 121-7.
18. Gu, X., et al., *Serines 13 and 16 are critical determinants of full-length human mutant huntingtin induced disease pathogenesis in HD mice.* Neuron, 2009. **64**(6): p. 828-40.
19. Aiken, C.T., et al., *Phosphorylation of threonine 3: implications for Huntingtin aggregation and neurotoxicity.* J Biol Chem, 2009. **284**(43): p. 29427-36.
20. Thompson, L.M., et al., *IKK phosphorylates Huntingtin and targets it for degradation by the proteasome and lysosome.* J Cell Biol, 2009. **187**(7): p. 1083-99.
21. Atwal, R.S., et al., *Kinase inhibitors modulate huntingtin cell localization and toxicity.* Nat Chem Biol, 2011. **7**(7): p. 453-60.
22. Pines, J., *Four-dimensional control of the cell cycle.* Nat Cell Biol, 1999. **1**(3): p. E73-9.
23. Ding, X.L., et al., *The cell cycle Cdc25A tyrosine phosphatase is activated in degenerating postmitotic neurons in Alzheimer's disease.* Am J Pathol, 2000. **157**(6): p. 1983-90.
24. Mishra, R., et al., *Serine Phosphorylation Suppresses Huntingtin Amyloid Accumulation by Altering Protein Aggregation Properties.* J Mol Biol, 2012.
25. Bustamante, M.B., et al., *Detection of huntingtin exon 1 phosphorylation by Phos-Tag SDS-PAGE: Predominant phosphorylation on threonine 3 and regulation by IKKbeta.* Biochem Biophys Res Commun, 2015. **463**(4): p. 1317-22.
26. Havel, L.S., et al., *Preferential accumulation of N-terminal mutant huntingtin in the nuclei of striatal neurons is regulated by phosphorylation.* Hum Mol Genet, 2011. **20**(7): p. 1424-37.

27. Wu, J.S. and L. Luo, *A protocol for dissecting Drosophila melanogaster brains for live imaging or immunostaining.* Nat Protoc, 2006. **1**(4): p. 2110-5.
28. Park, J., et al., *Mitochondrial dysfunction in Drosophila PINK1 mutants is complemented by parkin.* Nature, 2006. **441**(7097): p. 1157-61.

Chapter IV

Crosstalk between Parkinson's and Huntington's diseases: α-synuclein modifies mutant huntingtin aggregation and neurotoxicity in *Drosophila*

Contribution

Version of the manuscript entitled:

Poças, G.M.; Branco-Santos, J.; Herrera, F.; Outeiro, T.F. and Domingos, P.M. (2014) α-Synuclein modifies mutant huntingtin aggregation and neurotoxicity in Drosophila. Human Molecular Genetics, 2015. 24(7): p. 1898-907

G.M. Poças declares to have actively contributed for the experimental design, data analyses and manuscript writing. G.M. Poças performed the Drosophila genetic crosses, confocal microscopy, immunoprecipitation, Triton-X solubility, immunoblotting analysis and climbing and survival assays.

4.1. Abstract

Protein misfolding and aggregation is a major hallmark of neurodegenerative disorders such as Alzheimer's disease (AD), Parkinson's disease (PD) and Huntington's disease (HD). Until recently, the consensus was that each aggregation-prone protein was characteristic of each disorder [α-synuclein (α-syn)/PD, mutant huntingtin (Htt)/HD, Tau and amyloid beta peptide/AD]. However, growing evidence indicates that aggregation-prone proteins can actually co-aggregate and modify each other's behavior and toxicity, suggesting that this process may also contribute to the overlap in clinical symptoms across different diseases. Here, we show that α-syn and mutant Htt co-aggregate in vivo when co-expressed in *Drosophila* and produce a synergistic age-dependent increase in neurotoxicity associated to a decline in motor function and life span. Altogether, our results suggest that the co-existence of α-syn and Htt in the same neuronal cells worsens aggregation-related neuropathologies and accelerates disease progression.

4.2. Introduction

The presence of protein aggregates in the brain is a common hallmark for several neurodegenerative diseases, such as Alzheimer's disease (AD), Parkinson's disease (PD) and Huntington's disease (HD). The specific subcellular location and composition of protein aggregates are characteristics for each disorder. PD hallmarks are the formation of Lewy bodies, intracytoplasmic inclusions of misfolded proteins containing mainly α-synuclein (α-syn) and the demise of dopaminergic neurons in the substantia nigra. In AD, deposits of amyloid-beta and tau proteins in the brain lead to hippocampal degeneration, cognitive impairment and dementia. In HD, mutant huntingtin (Htt) with polyglutamine (polyQ) repeat expansion accumulates in cytoplasmic and intranuclear aggregates leading to neurodegeneration in the striatum [1].

Although each neurodegenerative disorder has its characteristic pathophysiology, current evidence indicates that there is also significant overlap between apparently different disorders. For example, α-syn is the protein that characteristically aggregates in PD, but it was originally discovered as a constituent of amyloid plaques in AD [2] and, later on, was found in protein aggregates in diverse pathologies of the central nervous system, such as HD, trisomy of chromosome 21, progressive supranuclear palsy and frontotemporal dementia [3-7]. Tau, an AD-associated protein, was detected in protein aggregates in patients with PD, sporadic dementia with Lewy bodies and multiple system atrophy, as well as in some animal models for synucleinopathies [8-14].

This apparent convergence of the molecular and cellular phenomena is accompanied by an overlap in the symptoms. For instance, patients suffering from diseases that affect movement control and coordination, as is the case of PD and HD, may also exhibit dementia in more advanced

stages of disease [15]. Conversely, patients afflicted by dementia can also show PD- or HD-like motor symptoms [16].

There is growing evidence that co-occurrence of aggregate-prone proteins may decisively influence the pathophysiology and severity of neural disorders. Tau and α-syn interact and co-aggregate, and this is associated with an increase in neurotoxicity in cellular and *Drosophila* models [17, 18]. Htt has been recently shown to co-aggregate with proteins associated with synucleinopathies and tauopathies [19-22]. Mutant Htt induces Tau hyperphosphorylation and aggregation, preventing its association to the microtubular network and producing large ring-like aggregates close to the microtubular network [19, 20]. DJ-1, which is associated with familial PD, interacts and co-aggregates with α-syn and Htt, modulating their toxicity in models of PD and HD [20, 22].

We have previously shown that α-syn modifies the dynamics and aggregation pattern of mutant Htt in cells in culture [23]. Here, we expand those studies and report that co-existence of α-syn and mutant Htt in vivo strongly enhances PD- and HD-related neuropathology in *Drosophila melanogaster*, suggesting that the interplay between the two proteins deserves further investigation in the context of HD and PD.

4.3. Results

4.3.1. Co-expression of mutant Htt and α-syn alters Htt aggregation pattern

Expression of normal (25Q) Htt or α-syn bimolecular fluorescence complementation (BiFC) pairs in human (H4) cells produced mostly homogeneous fluorescence, Htt being more often restricted to the cytosol and α-syn spreading both through nucleus and cytosol (Fig. 4.1A). On the other hand, mutant (103Q) Htt BiFC pairs produced protein aggregates. The combination of mutant Htt/α-syn also produced aggregates, but they seemed fewer and larger than pure 103Q aggregates. This was confirmed quantitatively (Fig. 4.1B–D), as the number of aggregates per cell was reduced 2-fold in mutant Htt/α-syn combinations (Fig. 4.1B), and the number of cells with <10 aggregates grew at the expense of cells with >25 aggregates (Fig. 4.1C). Finally, the percentage of aggregates larger than 3 μm increased in mutant Htt/α-syn combinations at the expense of aggregates smaller than 1 μm (Fig. 4.1D). The proportion of cells with 10–25 aggregates and of aggregates between 1 and 3 μm remained unchanged.

Both mutant Htt and α-syn increased cell death 24 h after transfection of H4 cells with the corresponding combinations of BiFC constructs (Fig. 4.1E). However, and in spite of the clear changes induced by α-syn on mutant Htt aggregation pattern, we did not observe changes at the viability level, even 72 h after transfection (data not shown). Longer experiments are extremely difficult to carry out in this experimental setup.

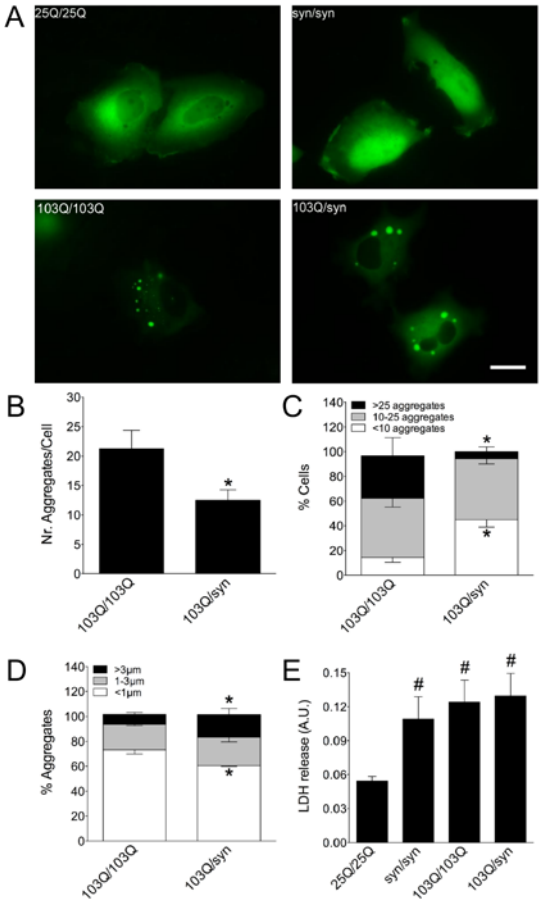

Figure 4.1. Co-expression of mutant Htt and α-syn alters Htt aggregation pattern. (A) H4 cells transfected with different combinations of α-syn- and Htt-Venus BiFC constructs. Cells transfected with a Htt25Q-Venus BiFC pair of plasmids show homogeneous fluorescence indicative of oligomeric species, while a Htt103Q-Venus BiFC pair produces both oligomeric species and large intracellular fluorescent aggregates with variable size and morphology. Htt location is primarily cytosolic. α-Syn-Venus BiFC pair produces homogeneous fluorescence distributed throughout all cellular compartments, including the nucleus. When α-syn and Htt103Q BiFC constructs were combined, there is a change in the aggregation pattern of both proteins, quantified in B–D. Co-transfection of Htt103Q with α-syn BiFC constructs decreases the average number of aggregates per cell (B and C) and increases the average size of aggregates (D). (E) The α-syn pair or the Htt103Q pair are more toxic than the wild-type Htt pair and combining α-syn with Htt103Q does not enhance toxicity in this model. *Significant versus 103Q/103Q, P< 0.01; # Significant versus 25Q/25Q, P< 0.001. Scale bar, 20 µm. AU, arbitrary units.

4.3.2. Htt103Q-mCherry and α-syn-EGFP co-localize and co-aggregate in dopaminergic neurons and in photoreceptors

In order to confirm our results with human cells in culture and to be able to measure neurotoxic effects of Htt/α-syn combinations during longer periods of time, we performed assays using transgenic overexpression in *Drosophila*. Co-expression of a mutant version of Htt containing 103 glutamines (Htt103Q-mCherry) and wild-type α-syn-EGFP in dopaminergic neurons (TH-GAL4) showed co-localization and co-aggregation of these two proteins (Fig. 4.2), confirming our results in cultured human cells. In terms of subcellular location, we found that these α-syn-EGFP/Htt103Q-mCherry aggregates accumulate both in cell bodies (Fig. 4.2A) and neurites (Fig. 4.2B) of dopaminergic neurons. In contrast, flies co-expressing α-syn-EGFP with a wild-type version of Htt (Htt25Q-mCherry) do not show aggregates (Fig. 4.2C), suggesting that only mutant Htt stimulates the deposition of α-syn in these aggregates. Flies expressing α-syn-EGFP or wild-type Htt25Q-mCherry alone did not show aggregates (Fig. 4.2D and E).

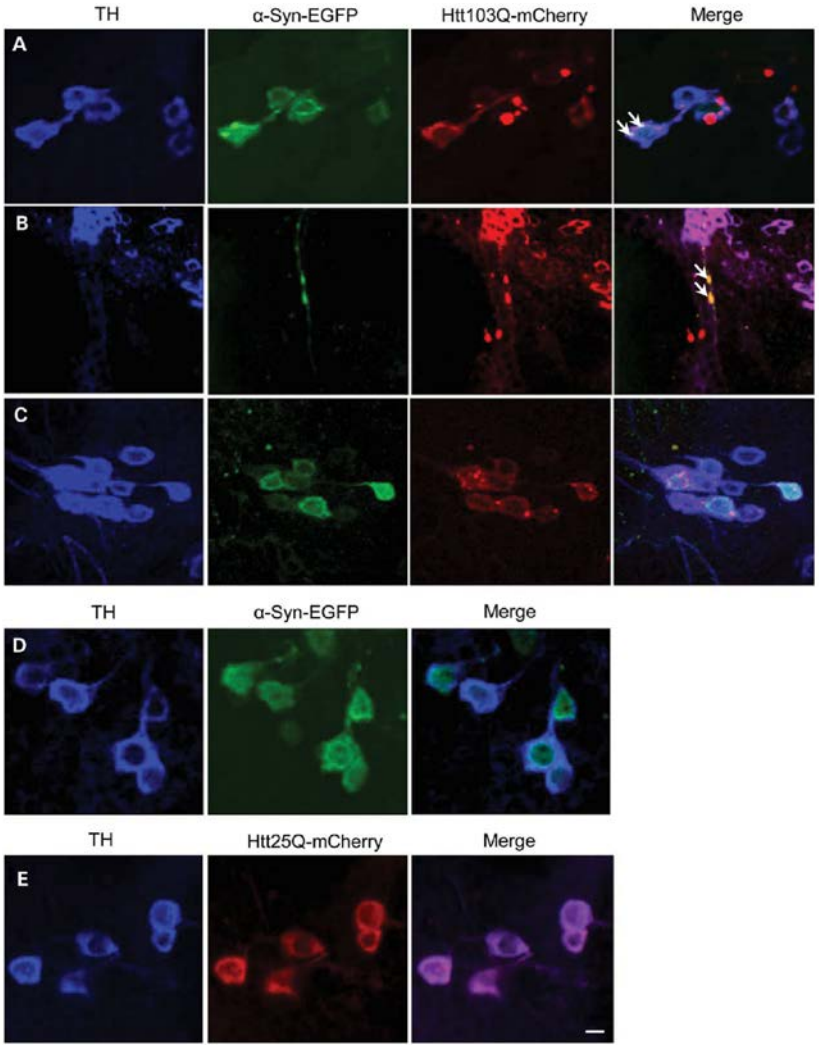

Figure 4.2. Htt103Q-mCherry and α-syn-EGFP co-localize and co-aggregate when expressed in dopaminergic neurons. (A) Co-localization of Htt103Q-mCherry and α-syn-EGFP aggregates in cell bodies of dopaminergic neurons (arrows). (B) Co-localization of Htt103Q-mCherry and α-syn-EGFP aggregates in neurites of dopaminergic neurons (arrows). (C) Wild-type Htt (Htt25Q-mCherry) does not form aggregates with α-syn-EGFP. (D and E) The expression of α-syn-EGFP alone or Htt25Q-mCherry does not induce the formation of aggregates. The images in A–E show dopaminergic neurons in the paired posterior lateral 1 (PPL1) cluster marked by an anti-TH antibody (against tyrosine hydroxylase). Genotypes: (A, B) TH-GAL4, UAS-α-syn-EGFP/UAS-Htt103Q-mCherry, (C) TH-GAL4, UAS-α-syn-EGFP/UAS-Htt25Q-mCherry, (D) TH-GAL4, UAS-α-syn-EGFP and (E) TH-GAL4, UAS-Htt25Q-mCherry. Scale bars represent 10 μm.

Using sGMR-GAL4 we induced the co-expression of Htt103Q-mCherry and α-syn-EGFP in eye imaginal discs of third instar larvae (Fig. 4.3). We observed co-localization and co-aggregation of α-syn and mutant Htt in the cytoplasm of the photoreceptors (Fig. 4.3A and A′), and also in the axonal projections of the photoreceptors in the larval brain (Fig. 4.3B).

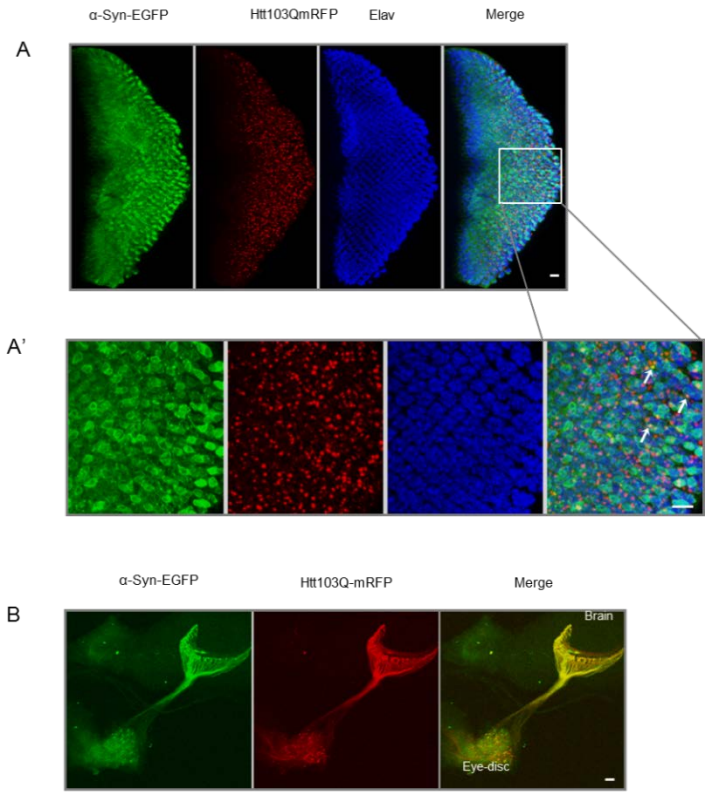

Figure 4.3. Htt103Q-mCherry and α-syn-EGFP co-localize and co-aggregate in the eye discs of third instar larvae. (A) Third instar larval eye disc from double transgenics stained with the pan-neuronal marker anti-elav. α-Syn-EGFP co-localized and co-aggregated with Htt103Q-mCherry aggregates in the cytoplasm of larval photoreceptors. (A′) Magnified area delimited by the box in (A). Arrows indicate foci of co-aggregated proteins. (B) Htt103Q-mCherry and α-syn-EGFP co-localized in the photoreceptors' axonal projections in the larval brain. Genotype: sGMR-GAL4, UAS-α-syn-EGFP/UAS-Htt103Q-mCherry. Scale bars represent 10 µm.

4.3.3. Htt103Q-mCherry and α-syn-EGFP are physically interacting

Mutant Htt103Q-mCherry was co-immunoprecipitated with α-syn-EGFP, using an antibody against the green fluorescent protein (GFP) tag, further demonstrating that mutant Htt103Q-mCherry and α-syn-EGFP interact and co-aggregate in *Drosophila* cells (Fig. 4.4A). In order to analyze the solubility status of these proteins when they are co-expressed, we performed a Triton-X solubility experiment using protein extracts from 8 days old adult heads. We found that the levels of α-syn-EGFP and Htt103Q-mCherry in the Triton insoluble fraction increased when these proteins are co-expressed, in comparison when they are expressed alone (Fig. 4.4B). This result indicates that co-expression of α-syn-EGFP and Htt103Q-mCherry causes an increase in the formation of insoluble aggregates containing these two proteins.

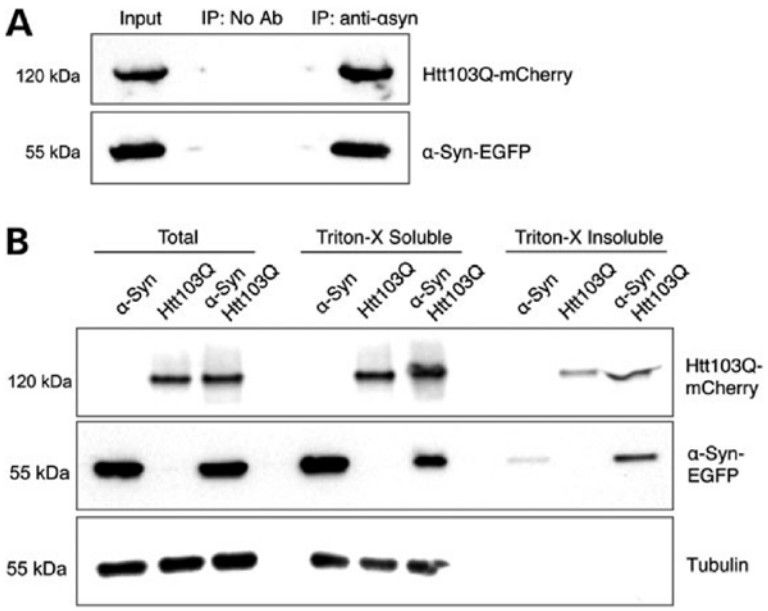

Figure 4.4. Htt103Q-mCherry and α-syn-EGFP are physically interacting. (A) Immunoprecipitation of α-syn-EGFP with an antibody against the EGFP tag pulled down Htt103Q-mCherry from dopaminergic neurons, showed by immunoblotting analysis. (B) Immunoblotting of Total, Triton-X soluble and Triton-X insoluble fractions of α-syn-EGFP and Htt103Q-mCherry from adult heads of flies co-expressing these two proteins. The levels of α-syn-EGFP and Htt103Q-mCherry in the insoluble fraction are higher when these proteins are co-expressed. Genotypes: (A) TH-GAL4, UAS-α-syn-EGFP/UAS-Htt103Q-mCherry. (B) α-Syn: sGMR-GAL4, UAS-α-syn-EGFP. Htt103Q: sGMR-GAL4, UAS-Htt103Q-mCherry. α-Syn/Htt103Q-mCherry: sGMR-GAL4, UAS-α-syn-EGFP/UAS-Htt103Q-mCherry.

4.3.4. Co-expression of Htt103Q-mCherry and α-syn-EGFP produces premature and severe degeneration in the photoreceptors

Next, we expressed Htt103Q-mCherry and α-syn-EGFP in the eye using sGMR-GAL4 and analyzed the external morphology of the adult eye in 8 days old flies (Fig. 4.5A–D). Expression of the GFP tag alone had no effect on eye development or viability as the eyes looked normal (Fig. 4.5A). Flies expressing α-syn-EGFP alone also developed a normal eye, identical to control flies (Fig. 4.5B). On the other hand, flies expressing mutant Htt103Q-mCherry, alone or in combination with α-syn-EGFP, showed striking retinal degeneration, producing a strong rough eye phenotype (Fig. 4.5C and D). Co-expression of mutant Htt103Q-mCherry and α-syn-EGFP did not worsen the rough eye phenotype in comparison with Htt103Q-mCherry alone. However, co-expression of Htt103Q-mCherry and α-syn-EGFP specifically in the photoreceptors R1–R6, using Rh1-GAL4, showed a stronger and premature degeneration phenotype (Fig. 4.5G) in comparison with Htt103Q-mCherry alone (Fig. 4.5H). In this case, control GFP or α-syn-EGFP alone did not show any degeneration phenotype (Fig. 4.5E and F). These results indicate that co-expression of α-syn-EGFP and mutant Htt103Q-mCherry enhances neurodegeneration of the *Drosophila* photoreceptors in vivo.

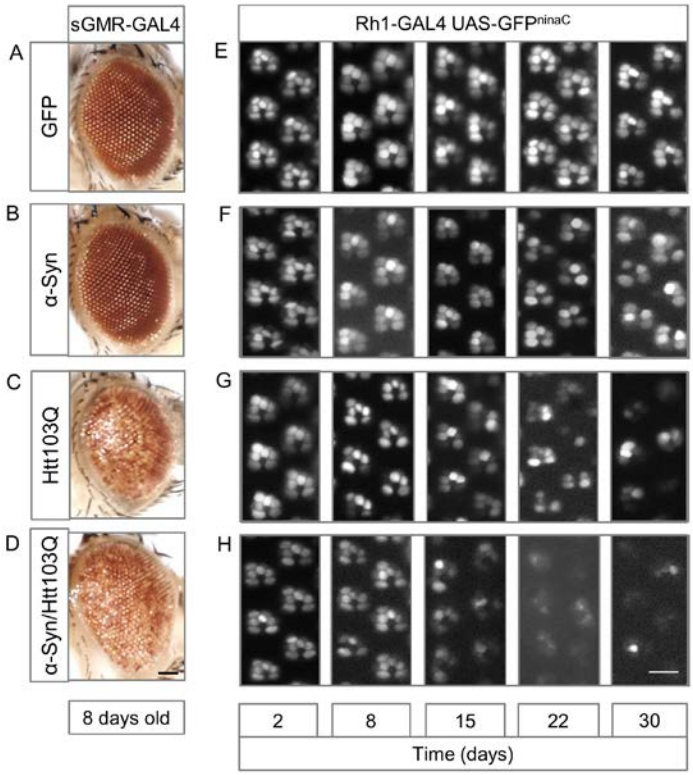

Figure 4.5. Co-expression of Htt103Q-mCherry and α-syn-EGFP produces premature and severe degeneration in the photoreceptors. (A–D) External morphology of the adult eye. (A and B) Expression of GFP or α-syn-EGFP does not affect external eye morphology. (C and D) Co-expression of Htt103Q-mCherry and α-syn-EGFP produces a rough eye phenotype identical to the one induced by the single expression of Htt103Q-mCherry. (E–H) Photoreceptors neurodegeneration in the adult eye, analyzed by water immersion microscopy assay of the retinas. (E) Expression of GFP did not induce degeneration of the photoreceptors, with the six photoreceptors being present in the ommatidial clusters; (F, G) flies expressing α-syn-EGFP or Htt103Q-mCherry showed progressive degeneration of the photoreceptors. (H) Co-expression of Htt103Q-mCherry and α-syn-EGFP induced severe and early degeneration of the photoreceptors. Genotypes are indicated in the boxes on top and lateral of the figures: (A) sGMR-GAL4, UAS-GFP, (B) sGMR-GAL4, UAS-α-syn-EGFP, (C) sGMR-GAL4, UAS-Htt103Q-mCherry, (D) sGMR-GAL4, UAS-α-syn-EGFP/UAS-Htt103Q-mCherry, (E) Rh1-GAL4, UAS-GFP, (F) Rh1-GAL4, UAS-α-syn-EGFP, (G) Rh1-GAL4, UAS-Htt103Q-mCherry and (H) Rh1-GAL4, UAS-α-syn-EGFP/UAS-Htt103Q-mCherry. Scale bars represent 50 μm (A–D) and 10 μm (E–H).

4.3.5. Co-expression of Htt103Q-mCherry and α-syn-EGFP in the nervous system causes severe motor dysfunction and a decrease in life span

We evaluated the motor function and life span of flies co-expressing mutant Htt103Q-mCherry and α-syn-EGFP in the central nervous system, using nSyb-GAL4 (Fig. 4.6). To test motor function we used "climbing assays", where flies of different genotypes were tapped to the bottom of the vial and allowed to climb up the walls (Fig. 4.6A). We recorded the climbing time when 5 flies crossed a 15-cm finish line. Eight days old flies co-expressing Htt103Q-mCherry and α-syn-EGFP took, on average, 4 more seconds to reach the finish line than the other genotypes tested. The motor abilities of Htt103Q-mCherry/α-syn-EGFP co-expressing flies deteriorated more and faster than the other genotypes, with the difference in climbing times reaching 32 seconds by day 30.

Flies co-expressing Htt103Q-mCherry and α-syn-EGFP also showed a dramatic decrease in life span, with 44 days of maximum survival (Fig. 4.6B). Flies co-expressing Htt25Q-mCherry and a-syn-EGFP had a maximum survival of 71 days. Maximum survival of flies expressing GFP, α-syn-EGFP, Htt25Q-mCherry or Htt103Q-mCherry alone ranged from 59 to 83 days. Interestingly, neurotoxicity, motor dysfunction and fly death started around days 8-15 and their increase occurred in parallel, indicating an association between these events. These results suggest that co-expression of α-syn and mutant Htt synergistically enhances each other's toxicity, eventually accelerating the progression of the disorder.

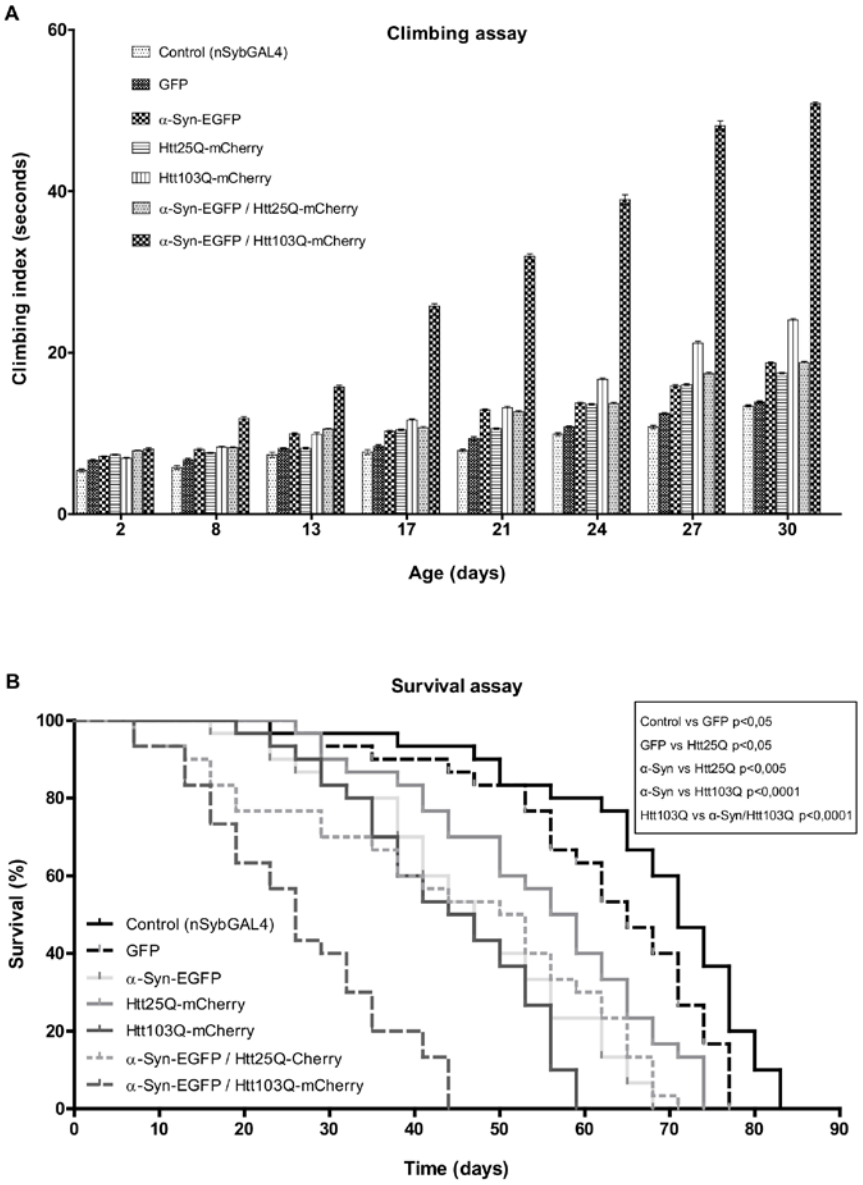

Figure 4.6. Co-expression of Htt103Q-mCherry and α-syn-EGFP in the nervous system causes severe motor dysfunction and a decrease in life span. (A) Flies co-expressing Htt103Q-mCherry and α-syn-EGFP under the control of nSyb-GAL4 show a strong impairment of the motor abilities compared with the rest of the genotypes tested. The Y-axis represents the time (in seconds), it took for five males to climb 15 cm (mean ± SEM). Statistically significant values, comparing each of genotypes, were calculated by doing two-way ANOVA with Bonferroni post-test. With very few exceptions, all the differences detected between the

genotypes tested in this assay were statistically significant with a P< 0.001 (except the difference between the genotypes Htt25Q-mCherry and α-Syn-EGFP/Htt25Q-mCherry which is significant for a P< 0.01). The differences not statistically significant (P> 0.05) were GFP versus Htt25Q-mCherry at day 13; α-Syn-EGFP versus Htt103Q-mCherry at day 13; α-Syn-EGFP versus α-Syn-EGFP/Htt25Q-mCherry at days 24 and 30; Htt103Q-mCherry versus α-Syn-EGFP/Htt25Q-mCherry at day 8. (B) Flies co-expressing Htt103Q-mCherry and α-syn-EGFP under the control of nSyb-GAL4 have a life span significantly shorter in comparison with the rest of the genotypes tested. Values on the Y-axis represent the percentage of flies alive at each time point analyzed. The maximum survival (in days) is indicated for each genotype (the mean values indicate the number of days it took for half of the flies to die): control (nSyb-GAL4) 83 (mean = 70), GFP (nSyb-GAL4, UAS-GFP) 77 (mean = 64), α-syn-EGFP (nSyb-GAL4, UAS-α-syn-EGFP) 68 (mean= 45), Htt25Q-mCherry (nSyb-GAL4, UAS- Htt25Q-mCherry) 74 (mean= 56), Htt103Q-mCherry (nSyb-GAL4, UAS-Htt103Q-mCherry) 59 (mean = 44), α-syn-EGFP/Htt25Q-mCherry (nSyb-GAL4, UAS-α-syn-EGFP/UAS-Htt25Q-mCherry) 71 (mean= 50) and α-syn-EGFP/Htt103Q-mCherry (nSyb-GAL4, UAS-α-syn-EGFP/UAS-Htt103Q-mCherry) 44 (mean= 25). Statistical significance is indicated in the graph (log-rank, Mantel–Cox test).

4.4. Discussion

Here, we show that α-syn and mutant Htt, two proteins associated with PD and HD, respectively, can interact and co-aggregate in vivo. Furthermore, their co-expression produced a synergistic deterioration of neural tissue, motor function and life span in *Drosophila*. The effects of α-syn/Htt co-expression under the different promoters are summarized in Table 1. While co-expression of other proteins associated with human neurodegenerative diseases have also shown deleterious effects in different models [17, 18, 23, 24], this is the first demonstration that co-expression of α-syn and mutant Htt can enhance neurodegeneration in *Drosophila*.

Table 4.1. GAL4 lines used in this study and respective phenotypes.

GAL4 line	Tissue	Phenotype (co-expression of α-syn and mutant Htt)
TH-GAL4	Dopaminergic neurons	Co-localization, interaction and co-aggregation of α-syn and Htt
nSyb-GAL4	Nervous system	Impairment of motor abilities and reduced life span
sGMR-GAL4	Eye	Co-localization, co-aggregation and retinal degeneration
Rh1-GAL4	Photoreceptors R1-R6	Premature degeneration of the photoreceptors

Our results support the idea that the co-occurrence of these two different aggregation-prone proteins in neural cells can produce striking changes in the pathology, symptoms and disease progression. Moreover, our study may give some clues why some patients suffering with a specific neuropathology may show, at the symptomatic level, a significant overlap between different human neurodegenerative diseases. It is possible that a HD patient containing a mutant version of the Htt gene (expansion of the trinucleotide CAG) and thereby suffering from the consequences of mutant Htt aggregation and toxicity, may be also in risk of developing aggregation of α-syn and therefore being affected by some of the symptoms associated

with PD. This could occur as a consequence of the propensity of mutant Htt and α-syn to interact, co-aggregating and interfering with their normal biological roles in cells. In addition, the two most affected brain regions in patients with PD and HD, the substantia nigra and striatum, respectively, are anatomically and functionally interconnected, reinforcing the interest of studying the crosstalk between these two neuropathologies. Finally, the models established in this work may constitute useful tools to screen and discover new candidate drugs against PD and HD.

4.5. Material and Methods

Cell culture and BiFC plasmids

Maintenance of H4 human glioma cells and Htt and α-syn BiFC constructs were previously described in detail [23, 25]. Briefly, in our BiFC systems, Htt and α-syn were fused to two non-fluorescent halves of the Venus protein (Venus 1, amino acids 1–157; and Venus 2, amino acids 158–239). When the Htt and α-syn dimerize, the Venus halves get together and reconstitute a functional fluorophore. Fluorescence is therefore proportional to the amount of Htt/α-syn dimers and oligomers. H4 cells were transfected with the corresponding BiFC pairs and 24 h later pictures were taken on a Zeiss Axiovert200M. A total of 150 cells from three independent experiments were analyzed. Graphs of Figure 1 show mean ± SD of three independent experiments.

Drosophila stocks

To generate UAS-α-Syn-EGFP, we fused α-syn with EGFP and cloned into pUAST using the BglII and Acc65I restriction sites. The transgenic flies were generated by BestGene, USA. We generated two different UAS-Htt-mCherry lines, one encoding a wild-type version of Htt (exon 1) with a 25 polyQ tail and the other encoding a mutant version of Htt with a 103 polyQ tail. These two constructs were cloned into pWalium10-roe and transgenic lines were generated using phiC31 integrase-mediated DNA integration (BestGene Strain #9723, attP acceptor site in 28E7). Four different drivers were obtained from the Bloomington Stock Center (Indiana University, Bloomington, IN, USA): nSyb-GAL4 (active in the entire nervous system, under the control of the Synaptobrevin promoter), TH-GAL4 (active in dopaminergic neurons, under the control of the tyrosine hydroxylase promoter), GMR-GAL4

(active in the eye, under the control of the glass multiple reporter) and Rh1-GAL4 (active in the photoreceptors R1–R6, under the control of the rhodopsin1 promoter). *Drosophila* stocks were maintained at 25°C on standard cornmeal media in an incubator with a 12 h light/dark cycle.

Immunohistochemistry and microscopy

Brain preparations for confocal microscopy imaging were done as previously described [26]. Briefly, adult flies were anesthetized with CO_2 and the brains were isolated from the head cuticles and fixed in phosphate buffered saline (PBS) containing 4% paraformaldehyde.

Dopaminergic neurons were stained by incubation for 48 h at 4°C with mouse anti-TH antibody (Immunostar, Hudson, WI, USA) diluted 1:50 in PBST (1× PBS + 0.3% Triton X-100) containing 5% (v/v) normal goat serum. Three 10-min washes with PBST were done before incubation with a secondary anti-mouse Cy5 (Jackson ImmunoResearch), also diluted in PBST-containing 5% (v/v) normal goat serum. Brain samples were analyzed and images were collected using a LSM 710 Meta Zeiss confocal microscope. Images were acquired with a resolution of 1024 × 1024, with a slice thickness of 1 µm and a line-average of 4. Z-projections were generated using ImageJ and the images were processed using Adobe Photoshop.

The degenerative effects caused by co-expression of α-syn and mutant Htt were assessed in the photoreceptors of adult eyes. To analyze external eye morphology, we used a Leica Z16 APO macroscope and a Leica DFC420C camera. To analyze photoreceptor degeneration, we performed water immersion microscopy as previously described [27]. Images were obtained using a Leica DM5500 B microscope and an Andor LucaR camera.

Immunoprecipitation, Triton-X solubility and immunoblotting analysis

Flies were transferred to 50-ml tubes, frozen in liquid nitrogen and immediately decapitated by vigorous vortexing. Isolated heads were collected to 1.5-ml tubes and maintained in dry ice. Proteins were extracted in lysis buffer supplemented with Complete Protease Inhibitor Cocktail tablets from Roche (Basel, Switzerland). Total protein was quantified using the DC Protein Assay, from Bio-Rad (CA, USA). In the immunoprecipitation experiments, α-syn-EGFP was pulled down from 1 mg of total protein extract, using GFP-Trap_A beads or blocked agarose beads (No Ab, no antibody negative control), following manufacturer's instructions (Chromotek, Munich, Germany). α-syn-EGFP pull-down and Htt103Q-mCherry co-immunoprecipitation were analyzed by immunoblotting using anti-GFP (3H9) and anti-RFP (5F8) antibodies from Chromotek, both diluted 1:1000 in PBS. Input lane corresponds to 30 µg of total protein extract and co-IP lane corresponds to one-fifth of the immunoprecipitated material.

The Triton-X solubility experiment was performed as previously described [28]. Briefly, 200 µg of total protein extract was incubated with 1% Triton X-100 on ice during 30 min. Triton soluble and insoluble proteins fractions were separated by a 60-min centrifugation step at 15000g at 4°C. The supernatant, containing the soluble proteins fraction (Triton-X soluble), was carefully collected and the pellet, containing the insoluble proteins fraction (Triton-X insoluble), was resuspended in 40 µl of 2% sodium dodecyl sulfate Tris–HCl buffer pH 7.4 by pipetting and sonication for 10 s. For the immunoblotting analysis, equal volumes of each fraction were loaded and the presence of α-syn-EGFP and Htt103Q-mCherry in the total, soluble and insoluble fractions was detected using anti-GFP (3H9) and anti-RFP (5F8). Additionally, anti-α-tubulin (AA4.3)

from Developmental Studies Hybridoma Bank (IA, USA), diluted 1:500 in PBS, was used as loading control.

Climbing assays and survival assays

Motor function was analyzed by startle-induced locomotion and negative geotaxis response assays, commonly called climbing assays, as previously described [29]. Briefly, groups of 10 males of the same age of each genotype of interest were placed into 18-cm-long vials, at room temperature for environmental acclimatization, and 30 min later they were gently tapped to the bottom of the vial (a minimum number of 30 males per genotype was tested). We recorded the climbing time when five flies crossed the 15-cm finish line. For each genotype we tested three independent groups of males and performed five trials for each time point.

Results are the average climbing time ± SEM of these independent experiments.

For survival assays, flies were maintained in a humid incubator at 25°C under a 12 h light/dark cycle. Thirty adult females of the same age were placed in three vials (10 flies per vial) containing fresh food. Each 3 days the flies were transferred into vials with fresh food and the number of living flies was registered.

Statistical analysis

Statistical analyses were done using GraphPad Prism software version 5 (San Diego, CA, USA). For BiFC we performed a One-way ANOVA followed by a post-hoc Tukey test for average comparison. For climbing assays, we performed a Two-way ANOVA followed by a Bonferroni post-test. For the survival assays, we performed a Log-rank (Mantel-Cox) test.

4.6. Acknowledgements

We thank Maria Luísa Vasconcelos, Rui Martinho and the Bloomington Stock Centre for *Drosophila* stocks. We thank the TRiP at Harvard Medical School (NIH/NIGMS R01-GM084947) for providing plasmid vectors used in this study. We thank Developmental Studies Hybridoma Bank for antibodies.

Conflict of Interest statement. None declared.

4.7. Funding

This work was supported by grant FCT-ANR/NEU-NMC/0006/ 2013 from Fundação para a Ciência e a Tecnologia, Portugal. G.M.P. was supported by a doctoral fellowship from the Fundação para a Ciência e a Tecnologia (SFRH/BD/61477/2009). J.B.S. and F.H. were supported by fellowships from the Fundação para a Ciência e a Tecnologia (SFRH/BD/85275/2012 and SFRH/BPD/63530/2009, respectively). F.H. and T.F.O. were also supported by seed funds from the European Huntington's Disease Network

(EHDN). T.F.O. is supported by the DFG Center for Nanoscale Microscopy and Molecular Physiology of the Brain.

4.8. References

1. Soto, C. and L.D. Estrada, *Protein misfolding and neurodegeneration.* Arch Neurol, 2008. **65**(2): p. 184-9.
2. Yoshimoto, M., et al., *NACP, the precursor protein of the non-amyloid beta/A4 protein (A beta) component of Alzheimer disease amyloid, binds A beta and stimulates A beta aggregation.* Proc Natl Acad Sci U S A, 1995. **92**(20): p. 9141-5.
3. Wilhelmsen, K.C., et al., *17q-linked frontotemporal dementia-amyotrophic lateral sclerosis without tau mutations with tau and alpha-synuclein inclusions.* Arch Neurol, 2004. **61**(3): p. 398-406.
4. Hamilton, R.L., *Lewy bodies in Alzheimer's disease: a neuropathological review of 145 cases using alpha-synuclein immunohistochemistry.* Brain Pathol, 2000. **10**(3): p. 378-84.
5. Raghavan, R., et al., *Detection of Lewy bodies in Trisomy 21 (Down's syndrome).* Can J Neurol Sci, 1993. **20**(1): p. 48-51.
6. Judkins, A.R., et al., *Co-occurrence of Parkinson's disease with progressive supranuclear palsy.* Acta Neuropathol, 2002. **103**(5): p. 526-30.
7. Charles, V., et al., *Alpha-synuclein immunoreactivity of huntingtin polyglutamine aggregates in striatum and cortex of Huntington's disease patients and transgenic mouse models.* Neurosci Lett, 2000. **289**(1): p. 29-32.
8. Galpern, W.R. and A.E. Lang, *Interface between tauopathies and synucleinopathies: a tale of two proteins.* Ann Neurol, 2006. **59**(3): p. 449-58.
9. Clarimon, J., et al., *Early-onset familial lewy body dementia with extensive tauopathy: a clinical, genetic, and neuropathological study.* J Neuropathol Exp Neurol, 2009. **68**(1): p. 73-82.
10. Galloway, P.G., et al., *Lewy bodies contain epitopes both shared and distinct from Alzheimer neurofibrillary tangles.* J Neuropathol Exp Neurol, 1988. **47**(6): p. 654-63.
11. Giasson, B.I., et al., *Initiation and synergistic fibrillization of tau and alpha-synuclein.* Science, 2003. **300**(5619): p. 636-40.
12. Ishizawa, T., et al., *Colocalization of tau and alpha-synuclein epitopes in Lewy bodies.* J Neuropathol Exp Neurol, 2003. **62**(4): p. 389-97.
13. Wills, J., et al., *Elevated tauopathy and alpha-synuclein pathology in postmortem Parkinson's disease brains with and without dementia.* Exp Neurol, 2010. **225**(1): p. 210-8.
14. Haggerty, T., et al., *Hyperphosphorylated Tau in an alpha-synuclein-overexpressing transgenic model of Parkinson's disease.* Eur J Neurosci, 2011. **33**(9): p. 1598-610.

15. Perry, R.J. and J.R. Hodges, *Spectrum of memory dysfunction in degenerative disease.* Curr Opin Neurol, 1996. **9**(4): p. 281-5.
16. Tsolaki, M., et al., *Extrapyramidal symptoms and signs in Alzheimer's disease: prevalence and correlation with the first symptom.* Am J Alzheimers Dis Other Demen, 2001. **16**(5): p. 268-78.
17. Roy, B. and G.R. Jackson, *Interactions between Tau and alpha-synuclein augment neurotoxicity in a Drosophila model of Parkinson's disease.* Hum Mol Genet, 2014. **23**(11): p. 3008-23.
18. Badiola, N., et al., *Tau Enhances alpha-Synuclein Aggregation and Toxicity in Cellular Models of Synucleinopathy.* PLoS One, 2011. **6**(10): p. e26609.
19. Blum, D., et al., *Mutant huntingtin alters Tau phosphorylation and subcellular distribution.* Hum Mol Genet, 2014.
20. Sajjad, M.U., et al., *DJ-1 modulates aggregation and pathogenesis in models of Huntington's disease.* Hum Mol Genet, 2014. **23**(3): p. 755-66.
21. Gratuze, M., et al., *Tau hyperphosphorylation and deregulation of calcineurin in mouse models of Huntington's disease.* Hum Mol Genet, 2014.
22. Zondler, L., et al., *DJ-1 interactions with alpha-synuclein attenuate aggregation and cellular toxicity in models of Parkinson's disease.* Cell Death Dis, 2014. **5**: p. e1350.
23. Herrera, F. and T.F. Outeiro, *alpha-Synuclein modifies huntingtin aggregation in living cells.* FEBS Lett, 2012. **586**(1): p. 7-12.
24. Corrochano, S., et al., *alpha-Synuclein levels modulate Huntington's disease in mice.* Hum Mol Genet, 2011.
25. Herrera, F., et al., *Visualization of cell-to-cell transmission of mutant huntingtin oligomers.* PLoS Curr, 2011. **3**: p. RRN1210.
26. Wu, J.S. and L. Luo, *A protocol for dissecting Drosophila melanogaster brains for live imaging or immunostaining.* Nat Protoc, 2006. **1**(4): p. 2110-5.
27. Pichaud, F. and C. Desplan, *A new visualization approach for identifying mutations that affect differentiation and organization of the Drosophila ommatidia.* Development, 2001. **128**(6): p. 815-26.
28. Tenreiro, S., et al., *Phosphorylation modulates clearance of alpha-synuclein inclusions in a yeast model of Parkinson's disease.* PLoS Genet, 2014. **10**(5): p. e1004302.
29. Park, J., et al., *Mitochondrial dysfunction in Drosophila PINK1 mutants is complemented by parkin.* Nature, 2006. **441**(7097): p. 1157-61.

Chapter V

Testing the potential therapeutic effect of mannosylglycerate in *Drosophila* models for Parkinson's and Huntington's diseases

Contribution

This chapter contains unpublished data:

Poças, G.M.; Borges, N.; Faria, C.; Santos, H. and Domingos, P.M.

G.M. Poças declares to have actively contributed for the experimental design, data analyses and manuscript writing**.** G.M. Poças performed the *Drosophila* genetic crosses, confocal microscopy of *Drosophila* samples and immunoblot analysis. N. Borges carried out the TLC and NMR analysis.

5.1. Abstract

The accumulation of small organic molecules termed compatible solutes (CS) constitutes an efficient strategy, developed by organisms during biological evolution, to deal with extreme environmental and physiological changes, like fluctuations in the osmotic and/or temperature conditions. CS are efficient stabilizers, with potent chemical chaperone properties, protecting essential biomolecules from denaturation. Mannosylglycerate (MG) is one of the most common and efficient CS, widely found in hyperthermophile organisms. The biosynthesis of MG can be catalyzed by the bifunctional enzyme mannosylglycerate synthase (MGSD). The misfolding and aggregation of proteins constitutes a problem with strong biotechnological and medical relevance. In fact, the pathophysiology of several human neurodegenerative diseases, namely Parkinson's (PD) and Huntington's diseases (HD), is associated with the formation of protein aggregates containing misfolded proteins. Therefore, the strong stabilizer effects of CS on proteins have been investigated in order to explore the anti-aggregating and therapeutical potential uses of these compounds. The main aim of our study was to investigate the anti-aggregating and potential therapeutic effects of MG in *Drosophila* models for PD and HD expressing α-synuclein (α-syn) and huntingtin (Htt), respectively, and in a previously established model for Retinitis Pigmentosa (RP) expressing a mutant form of rhodopsin 1. We successfully generated transgenic lines expressing the bifunctional enzyme MGSD, but we could not detect the biosynthesis and accumulation of MG in *Drosophila* tissues.

5.2. Introduction

Living organisms are frequently subjected to extreme changes in the normal environmental or physiological conditions, namely changes in water activity. The ability to deal with these changes, in order to maintain the biomolecules in a functionally folded state, is a crucial prerequisite for cell survival. One of the strategies developed by organisms during biological evolution consists in the accumulation, by import or *de novo* synthesis, of small molecules termed osmolytes [1-3]. Besides fluctuations in the osmotic pressure, some organisms are also exposed to extreme changes in the temperature and salinity of the environment, like the hyperthermophile marine microorganisms that thrive at high temperatures. These forms of life accumulate in the cells high levels, even at molar concentrations, of small organic molecules to counteract the perturbations in the thermodynamic conditions that would otherwise induce a partial or complete loss in the activity of essential biomolecules. Although these organic compounds accumulate in the cells to very high levels, frequently becoming the most abundant organic components in the cytoplasm, they preserve the native biological function of macromolecules in the cell, thereby earning the name of compatible solutes (CS) [4, 5]. There are several different molecules belonging to the group of these curious organic compounds, some of them depicted on Figure 5.1. These special CS, naturally occurring in organisms growing at temperatures near 100 ºC and rarely found in organisms living in moderate environments, are usually negatively charged and are one of the most potent stabilizers for proteins, acting as chemical chaperones, with the ability to reverse the protein misfolding and/or aggregation [6]. These properties contribute to an increasing interest and investment in the research related with ionic CS, at the biotechnological and biomedical levels.

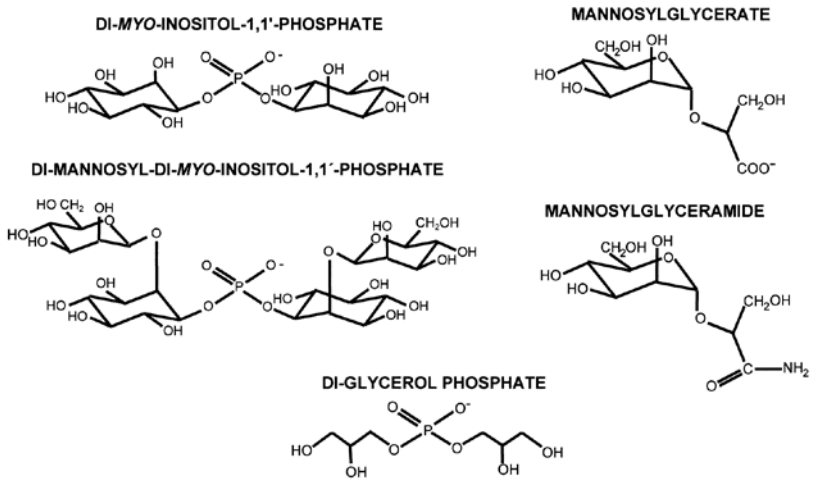

Figure 5.1. Examples of compatible solutes (CS) primarily restricted to hyperthermophile organisms. The molecular structures of these CS are shown.

Several human pathologies, including neurodegenerative diseases, such as Parkinson's (PD) and Huntington's diseases (HD), are associated with protein misfolding and accumulation in aggregates. Furthermore, it has been shown that the folding of proteins with intrinsically disordered conformations, as it is the case of PD's associated α-synuclein (α-syn), can be spontaneously induced by incubation with certain organic osmolytes, which promote the adoption of the native and functional form of these proteins [7, 8]. For these reasons, CS have been considered an attractive therapeutic target. There are some works in the literature stating for a potential therapeutic action of CS in the pathophysiology of some human diseases, as it is the case of trehalose (a disaccharide CS found in many microorganisms and invertebrates with the ability to protect the cell integrity against several environmental insults), which have shown promising therapeutic effects promoted by this CS on cellular and animal models of human neurodegenerative diseases [9, 10]. Mannosylglycerate (MG) is another very common CS produced by hyperthermophiles with a potent stabilizing effect on proteins, efficiently preserving the functional

protein structures against thermal denaturation [11-14]. A recent work from our collaborators has shown the beneficial effect of MG against α-syn aggregation in a yeast model for PD [15]. Previous studies have shown that the stabilization properties of MG are associated with a protein rigidification effect, induced by a generalized reduction of very fast backbone motions by this CS [16, 17]. The misfolding, aggregation and accumulation of α-syn in Lewy bodies, an hallmark in the pathophysiology of PD, involves the formation of amyloid oligomers with a distinctive antiparallel β-sheet structure [18, 19]. Therefore, it is very tempting to speculate that the beneficial effect induced by MG might come from an inhibition in the fibrillation of α-syn through rigidification and stabilization of these β-sheet oligomers. Our main goal with this work was to induce the *in vivo* biosynthesis and accumulation of MG in *Drosophila*, in order to test the anti-aggregating, re-folding and therapeutic properties of this CS in our *Drosophila* models for PD and HD, based on the expression of the prone-to-aggregate proteins α-syn and huntingtin (Htt), respectively. A previously established *Drosophila* model for Retinitis Pigmentosa (RP) was also used in our study [20]. Therefore, one of the main tasks of this work was to generate *Drosophila* transgenic lines expressing mannosylglycerate synthase (MGSD) [21], a bifunctional enzyme responsible for the synthesis of MG (Figure 5.2).

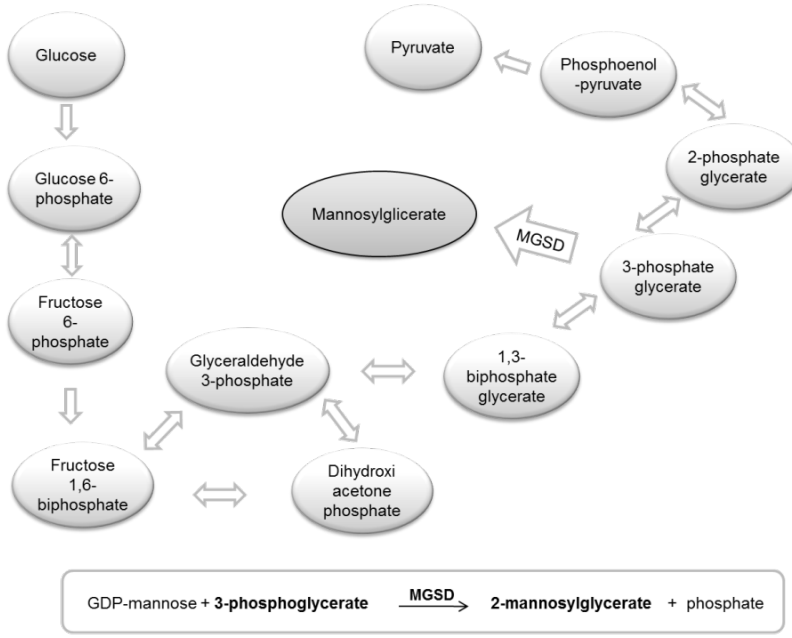

Figure 5.2. Mannosylglycerate synthase (MGSD) is a bifunctional enzyme that catalyzes a two steps reaction responsible for the biosynthesis of mannosylglycerate (MG). MGSD uses 3-phosphate glycerate, an intermediate metabolite of glycolysis, as substrate of the enzymatic reaction. All the intermediate metabolites from the glycolytic pathway are shown.

5.3. Results

5.3.1. Expression of MGSD in *Drosophila*

After the generation, by embryos transgenesis, of transgenic *Drosophila* lines for MGSD, we wanted to test if using the Gal4/UAS system we could induce the expression of this enzyme. By crossing the UAS MSGD lines with the pan-neuronal driver nSybGal4, we induced the expression of MGSD in the *Drosophila* nervous system. We proceeded with a protein extraction from these flies and we analyzed the expression of MGSD, at the protein level, by performing an immunoblot experiment, using a specific antibody for a homologue enzyme of MGSD [22].We successfully detected in the immunoblot a protein band with the expected molecular weight (77,9 kDa) for MGSD (Fig. 5.3).

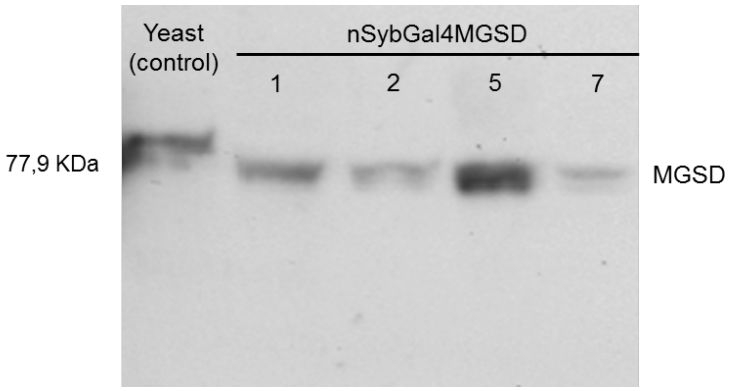

Figure 5.3. Expression of mannosylglycerate synthase (MGSD) in *Drosophila*, proved at the protein level by immunoblotting analysis. Protein extracts were obtained from four independent transgenic lines (numbered 1, 2, 5 and 7) expressing MGSD in the nervous system, under the control of the pan-neuronal nSybGal4 driver. For the immunoblotting we used a specific antibody for a homologue enzyme of MGSD [22]. The genotype of the transgenic *Drosophila* lines tested is indicated. Protein extracts from a genetically engineered yeast expressing MGSD were used as a positive control of the experiment.

We also tested the expression of MGSD protein, by performing an immunoflourescent assay in *Drosophila* eye imaginal discs. Using the lGMR Gal4 driver, we induced the expression of MGSD in the eye imaginal disc of third instar larvae and we proceeded with the immunostaining and confocal imaging of this tissue, using a specific antibody for a homologue enzyme of MGSD (and a secondary antibody conjugated with the Cy3 fluorescent die). We successfully detected the *in vivo* expression of MGSD in the *Drosophila* photoreceptors (Fig. 5.4).

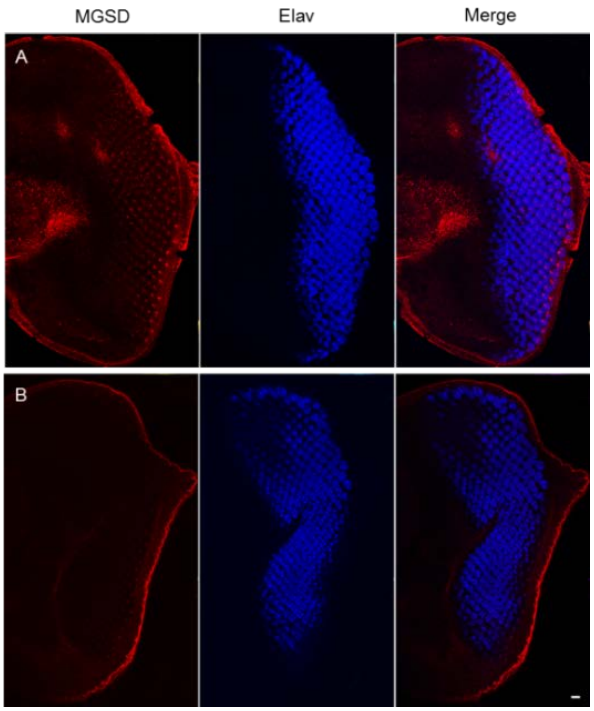

Figure 5.4. *In vivo* expression of mannosylglycerate synthase (MGSD) in the *Drosophila* photoreceptors. Immunoflourescent staining of third instar larvae eye discs, using a specific antibody for a homologue enzyme of MGSD [22] and a Cy3-conjugated secondary antibody. (A) MGSD expression was detected in the eye discs of flies expressing MGSD under the control of the lGMR Gal4 driver – Genotype: lGMR-GAL4, UAS-MGSD (B) MGSD was not detected in the eye discs of control flies expressing only Gal4 under the control of lGMR promoter (negative control) – Genotype: lGMR-Gal4. The nucleus of the photoreceptors was stained by the pan-neuronal marker anti-Elav. Scale bar represents 10 μm.

Therefore, by immunoblotting and immunostaining analysis, we could prove, at the protein level, that using the Gal4/UAS system, we can successfully induce the expression of the bifunctional enzyme MGSD in *Drosophila*.

5.3.2. The co-expression of MGSD reduced the ER stress levels in photoreceptors expressing ninaE^{G69D}

The point mutation G69D in ninaE, the gene that encodes Rhodopsin 1, causes accumulation of misfolded Rhodopsin 1 and leads to retinal degeneration. In a previous work [20], it was demonstrated that the expression of ninaE^{G69D} in the *Drosophila* photoreceptors induces retinal degeneration like in human patients suffering from Retinitis Pigmentosa, and causes ER stress and activation of the Ire1/Xbp1 branch of the unfolded protein response (UPR). Here, we investigated the ability of MG to reduce the ER stress levels and promote the correct folding of ninaE^{G69D}. We induced the co-expression of MGSD in the photoreceptors of third instar larvae expressing ninaE^{G69D}, under the control of the lGMR Gal4 driver, and we observed a reduction of the ER stress levels (Fig. 5.5). This reduction in the ER stress levels was assessed using the Xbp1-GFP reporter for Ire1 activation, previously generated [20].

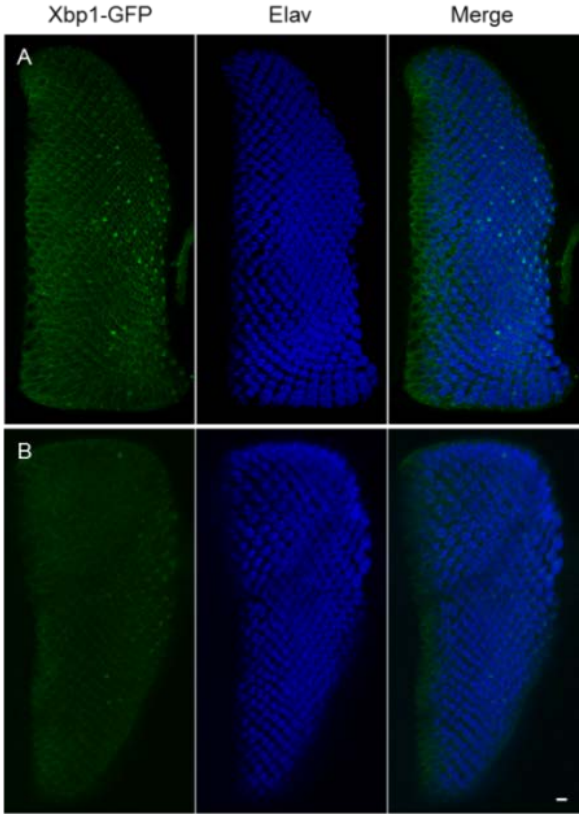

Figure 5.5. The expression of mannosylglycerate synthase (MGSD) in our model for Retinitis Pigmentosa (RP) reduces the ER stress levels in the *Drosophila* photoreceptors expressing ninaE^{G69D}. The ER stress levels were assessed using the Xbp1-GFP reporter. The activation of Xbp1-GFP was detected by the endogenous fluorescence of the GFP tag. The nucleus of the photoreceptors was stained by the pan-neuronal marker anti-elav. lGMR-GAL4 was the driver used in this experiment. (A) The expression of the mutant form of rhodopsin 1 (ninaE^{G69D}) causes ER stress and induces the activation of the Xbp1-GFP reporter. Genotype: lGMR-GAL4/ UAS-Xbp1-GFP, UAS-ninaE^{G69D} (B) The co-expression of MGSD in the photoreceptors expressing ninaE^{G69D} promoted a reduction in the ER stress levels, as indicated by a reduction in the activation of the Xbp1-GFP reporter. Genotype: lGMR-GAL4/ UAS-Xbp1-GFP, UAS-ninaE^{G69D}/UAS-MGSD. Scale bar represents 10 µm.

5.3.3. MG was not detected in cellular extracts from *Drosophila* tissues expressing MGSD

After confirming, by western blot and immunohistochemistry analysis, that we could successfully induce the expression of MGSD in our new transgenic UAS lines, and that the co-expression of MGSD alleviated the ER stress levels induced by the expression of ninaE^{G69D} in the photoreceptors, we wanted to prove that MG was being synthesized in *Drosophila*. The experimental approach we used was to analyze the presence of MG in Drosophila extracts by thin layer chromatography (TLC) and nuclear magnetic resonance (NMR). We induced the expression of MGSD in different *Drosophila* tissues, using distinct Gal4 drivers (elav Gal4 and nSyb Gal4, active in the nervous system and Actin Gal4, active in the whole organism). Thus, we analyzed several cellular extracts produced from these *Drosophila* lines expressing MGSD in different tissues. We could not detect MG expression in any of these extracts, neither by TLC nor by NMR analysis (Fig. 5.6 and 5.7).

We also performed an additional experiment where we co-expressed MGSD with a UAS RNAi line for phosphoglycero-mutase (Pglym78) in the *Drosophila* eye, using the sGMR-Gal4 driver. This experiment was done on the hypothesis that the genetic manipulation of the glycolytic pathway in order to increase the concentration 3-phosphate glycerate available in the cytoplasm to be enzymatically converted to MG by MGSD, would increase the chances of successfully produce MG in *Drosophila*. However, the analyses of the cellular extracts produced from this flies by TLC and NMR did not reveal the presence of MG (Fig. 5.8).

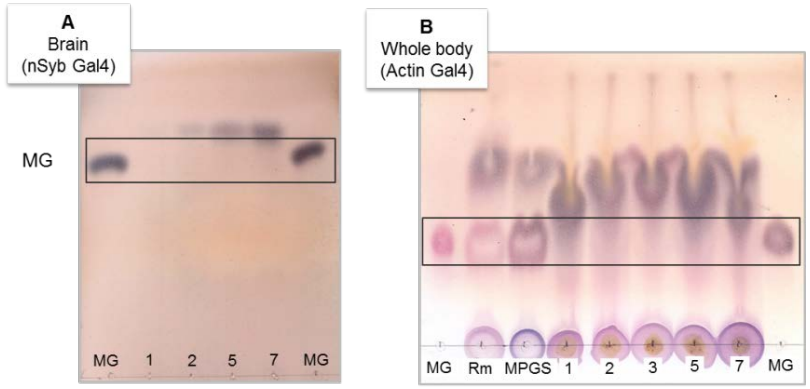

Figure 5.6. The presence of mannosylglycerate (MG) in cellular extracts from *Drosophila* tissues expressing mannosylglycerate synthase (MGSD) could not be detected by thin layer chromatography (TLC) analysis. (A) The TLC analysis of cellular extracts from *Drosophila* lines (1, 2, 5 and 7) expressing MGSD in the nervous system, under the control of the pan-neuronal nSybGal4 driver, could not detect the presence of MG – Genotype: nSyb-GAL4, UAS-MGSD. (B) The TLC analysis of cellular extracts from *Drosophila* lines expressing MGSD in the whole organism, under the control of the ubiquitous Actin Gal4 driver, could not detect the presence of MG – Genotype: Actin-GAL4, UAS-MGSD. A pure solution of MG, cellular extracts from *Rhodothermus marinus* (Rm) a hyperthermophile microorganisms which accumulates MG and cellular extracts from yeast genetically modified to express mannosyl-3-phosphoglycerate synthase (MGPS) and accumulate MG, , were used as positive controls for these experiments.

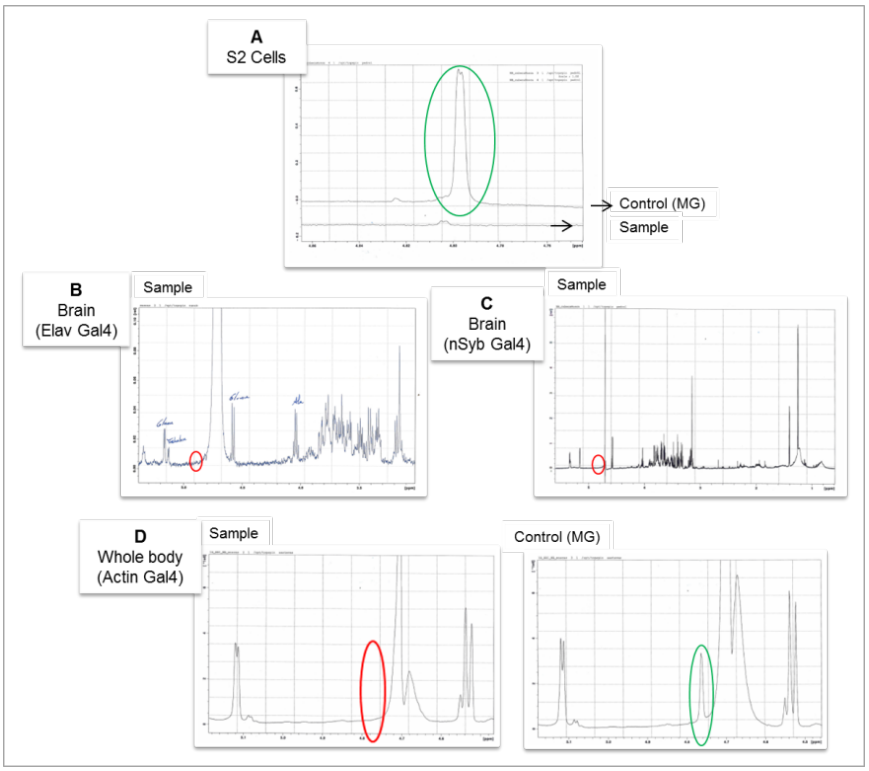

Figure 5.7. The presence of mannosylglycerate (MG) in cellular extracts from *Drosophila* tissues expressing mannosylglycerate synthase (MGSD) could not be detected by nuclear magnetic resonance (NMR) analysis. NMR analysis of *Drosophila* extracts was done for: (A) S2 cells transfected with the MGSD construct (pUAST MGSD), (B) *Drosophila* lines expressing MGSD in the nervous system, under the control of the pan-neuronal drivers elav Gal4, (C) *Drosophila* lines expressing MGSD in the nervous system, under the control of the pan-neuronal drivers nSyb Gal4 and (D) *Drosophila* lines expressing MGSD in the whole organism, under the control of the ubiquitous Actin Gal4 driver. The presence of MG could not be detected in none of the extracts tested. Genotypes: (A) pUAST MGSD, actin-Gal4 (B) elav-GAL4, UAS-MGSD, (C) nSyb-GAL4, UAS-MGSD (D) Actin-GAL4, UAS-MGSD. The green circles point for the detection of control MG, added to the extracts. The red circles point for the absence of detection of MG in the extracts tested.

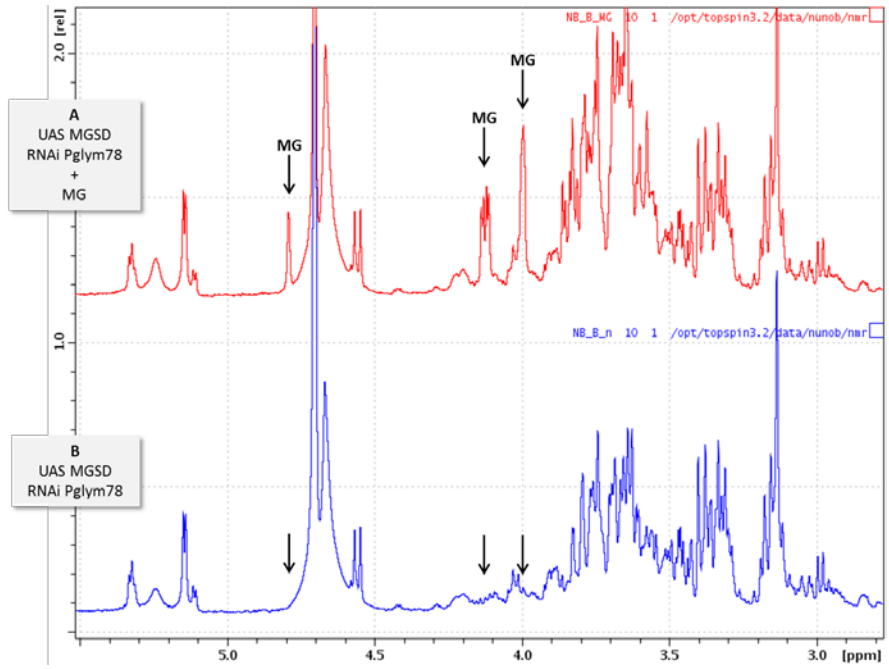

Figure 5.8. The presence of mannosylglycerate (MG) in cellular extracts from *Drosophila* tissues co-expressing mannosylglycerate synthase (MGSD) and RNAi for phosphoglycero-mutase (Pglmy78) could not be detected by nuclear magnetic resonance (NMR) analysis. (A) analysis of an extract produced from a *Drosophila* line co-expressing MGSD in the eye, under the control of sGMR-Gal4 driver with (A) or without (B) the addition of pure MG. The presence of MG could not be detected in the tested extract without the addition of pure MG. The arrows point for the detection of MG in the positive control, with the addition of pure MG to the extracts (in A). Genotype: sGMR-GAL4, UAS-MGSD/UAS-RNAi Pglmy78.

5.4. Discussion

In this work we successfully generated transgenic *Drosophila* lines expressing the bifunctional enzyme MGSD. The expression of MGSD, at the protein level, was proved by immunoblot and confocal imaging analysis, using a specific antibody for this enzyme. Additionally, we demonstrated that the co-expression of MGSD promoted a beneficial effect in the ER stress induced by the expression of ninaE^{G69D} in the photoreceptors. However, as we could not prove the *in vivo* biosynthesis and accumulation of MG in *Drosophila* tissues, we cannot conclude that MGSD is being expressed in a functionally active state. Also, we cannot be sure that the reduction of the ER stress levels promoted by the expression of MGSD was specifically induced by MG. The failure to prove the *in vivo* accumulation of MG did not allow us to proceed with the testing of the potential anti-aggregating and therapeutic properties of MG in *Drosophila* models for PD and HD.

We can speculate about some of the reasons that could have contributed for the expression of MGSD in a functionally inactive state and/or for the failure of MGSD, even if expressed in a functional state, in synthesizing MG in *Drosophila*. One of the factors to take into consideration is the temperature for MSGD optimum activity, which has been determined as being 50 ºC [21]. Additionally, the optimum growth temperature of *Dehalococcoides ethenogenes*, the microorganism where the bifunctional enzyme MSGD was identified, is approximately 35 ºC [23]. These temperatures are different from the range of temperatures normally used to maintain *Drosophila* lines (18 ºC – 25 ºC). In order to minimize this difference, the *Drosophila* lines expressing MGSD used in our study were maintained at 28 ºC, the highest possible temperature to maintain healthy flies. Although the temperature used to cultivate our fly lines may have contributed for the improper function of MGSD, we

believe this did not constitute the determinant factor for the non-functional state of this enzyme and consequent failure in the production and accumulation of MG. Actually, in a previous study [15], it has been described the successful MG *in vivo* accumulation, in a genetically engineered yeast expressing MGSD grown at 30 ºC. This fact reinforces our opinion that other factors, beyond temperature, would have been more decisive to the failure in the accumulation of MG by our *Drosophila* transgenic lines. A possible reason may be the lack of proper machinery and/or physiological conditions in *Drosophila* cells for the correct folding necessary to produce an enzymatically active form of this enzyme. Another plausible reason can be related with the low levels in the *Drosophila* cells of 3-phosphate glycerate, the necessary substrate for the biosynthesis of MG by MGSD. Although this substrate is an intermediate of glycolysis, a universal energy pathway present in all organisms, it is possible that the occurrence of substrate channeling and formation of a metabolon, a very common and well characterized metabolic phenomenon [24], could have contributed to an inadequate metabolic environment for the *in vivo* biosynthesis of MG in *Drosophila* cells. It is tempting to think that increasing the concentration 3-phosphate glycerate in the cytoplasm, for example through the genetic manipulation of the glycolytic pathway, would increase the quantity of this substrate available to diffuse to the active site of MGSD to be converted into MG. In order to test this hypothesis we induced the genetic knockdown of the enzyme involved in the immediately next step of the glycolytic pathway, in this case the phosphoglycero-mutase, by using a specific RNAi *Drosophila* line for this enzyme. We did this experiment in the *Drosophila* eye, by co-expressing MGSD with a UAS RNAi line for phosphoglycero-mutase (Pglym78). Unfortunately, once again, we could not detect the presence of MG in the cellular extracts produced from these flies, neither by TLC nor by NMR.

5.5. Material and Methods

Generation and maintenance of *Drosophila* stocks

To generate UAS-MGSD, we sub-cloned the MGSD cDNA into pUAST using the BglII and Acc65I restriction sites. The primers used for PCR amplification of MGSD insert were: Forward – GCGAAGAT CTATGCGCATTGAAAGCCTG; Reverse – CGGTACCCTTATTCCATGGGCAG TATTATATCG. The transgenic flies were generated by BestGene, USA. We obtained 7 different UAS-MGSD lines. Four different drivers were obtained from the Bloomington Stock Center (Indiana University, Bloomington, IN, USA): elav-GAL4 (active in the entire nervous system under the control of the embryonic lethal abnormal vision promoter), nSyb-GAL4 (active in the entire nervous system, under the control of the Synaptobrevin promoter), Actin-GAL4 (active in the whole body), lGMR-GAL4 (active in the eye, under the control of the glass multiple reporter). *Drosophila* stocks were maintained at 25 °C (or at 28 ºC for MGSD expression and MG production experiments) on standard cornmeal media in an incubator with a 12 h light/dark cycle.

Immunohistochemistry and microscopy

Eye imaginal discs preparations for confocal microscopy imaging were done as previously described [25]. Briefly, third instar larvae were collected and the eye imaginal discs were dissected and fixed in phosphate buffered saline (PBS) containing 4% paraformaldehyde.

The photoreceptors were stained by incubation for 24 h at 4°C with rat anti-elav antibody (7E8A10 - Developmental Studies Hybridoma Bank – IA, USA) diluted 1:40 in PBST (1× PBS + 0.3% Triton X-100) containing 5% (v/v) normal goat serum. Three 10-min washes with PBST were done before incubation with a secondary anti-rat Cy5 (Jackson

ImmunoResearch), also diluted in PBST-containing 5% (v/v) normal goat serum. Eye imaginal discs were analyzed and images were collected using a LSM 710 Meta Zeiss confocal microscope. Images were acquired with a resolution of 1024 × 1024, with a slice thickness of 1 µm and a line-average of 4. Z-projections were generated using ImageJ and the images were processed using Adobe Photoshop.

Western Blot analysis

Cell extracts from *Drosophila* heads (nSybGal4driver) were heated at 100 ºC for 10 min in Laemmili´s buffer (2% SDS). Protein separation was carried out by SDS-PAGE (10%). After electrophoresis, the proteins were transferred onto a polyvinylidene fluoride (PVDF) membrane (Millipore) with an electroblotting apparatus (Bio-Rad). The membranes were treated at room temperature with a blocking solution (TBS-T buffer: 0.1% (v/v) Tween-20, 150 mM NaCl, 50 mM Tris–HCl, pH 7.5 plus 5% (w/v) BSA) during 1 hour. After blocking, the membranes were treated with a washing solution (phosphate-buffered saline containing 0.5% of milk and 0.1% of tween 20) followed by incubation overnight with the appropriate dilution of primary antibody (1:27000 for anti-MGSD) at room temperature in washing solution. The anti-MGSD was kindly supplied by Prof. H. Santos [22]. After overnight incubation at 4 °C, the membrane was washed three times with TBS-T buffer and probed with the appropriate secondary antibodies (anti-rabbit conjugated with horseradish peroxidase, GE healthcare), for 1 h at room temperature. Signals were revealed with the ECL Plus detection kit (Millipore, USA) and visualized on a ChemiDoc system (BioRad).

Analysis of MG formation by thin layer chromatography

Fly tissues (isolated heads or whole bodies) were frozen in liquid nitrogen and triturated with a mortar and pestle. Subsequently we proceeded with an ethanol-chloroform extraction by the method previously described [26].

Thin layer chromatography was performed on Silica Gel 60 plates (Merck) with a solvent system composed of chloroform, methanol, acetic acid, and water (30:50:8:4, v/v/v/v). MG was visualized by spraying with α-naphtholsulfuric acid solution followed by charring at 120 ºC. Pure MG was used for comparison [27].

NMR spectroscopy

1H-NMR spectra were acquired on a Bruker Avance II 500 NMR spectrometer with a 5-mm broadband probe head with inverse detection.

5.6. References

1. Yancey, P.H., et al., *Living with water stress: evolution of osmolyte systems.* Science, 1982. **217**(4566): p. 1214-22.
2. Yancey, P.H., *Organic osmolytes as compatible, metabolic and counteracting cytoprotectants in high osmolarity and other stresses.* J Exp Biol, 2005. **208**(Pt 15): p. 2819-30.
3. Record, M.T., Jr., et al., *Responses of E. coli to osmotic stress: large changes in amounts of cytoplasmic solutes and water.* Trends Biochem Sci, 1998. **23**(4): p. 143-8.
4. Brown, A.D. and J.R. Simpson, *Water relations of sugar-tolerant yeasts: the role of intracellular polyols.* J Gen Microbiol, 1972. **72**(3): p. 589-91.
5. Brown, A.D., *Microbial water stress.* Bacteriol Rev, 1976. **40**(4): p. 803-46.
6. Lamitina, T., C.G. Huang, and K. Strange, *Genome-wide RNAi screening identifies protein damage as a regulator of osmoprotective gene expression.* Proc Natl Acad Sci U S A, 2006. **103**(32): p. 12173-8.
7. Kumar, R., et al., *The conformation of the glucocorticoid receptor af1/tau1 domain induced by osmolyte binds co-regulatory proteins.* J Biol Chem, 2001. **276**(21): p. 18146-52.
8. Kumar, R. and E.B. Thompson, *Transactivation functions of the N-terminal domains of nuclear hormone receptors: protein folding and coactivator interactions.* Mol Endocrinol, 2003. **17**(1): p. 1-10.
9. Davies, J.E., S. Sarkar, and D.C. Rubinsztein, *Trehalose reduces aggregate formation and delays pathology in a transgenic mouse model of oculopharyngeal muscular dystrophy.* Hum Mol Genet, 2006. **15**(1): p. 23-31.
10. Sarkar, S., et al., *Trehalose, a novel mTOR-independent autophagy enhancer, accelerates the clearance of mutant huntingtin and alpha-synuclein.* J Biol Chem, 2007. **282**(8): p. 5641-52.
11. Borges, N., et al., *Comparative study of the thermostabilizing properties of mannosylglycerate and other compatible solutes on model enzymes.* Extremophiles, 2002. **6**(3): p. 209-16.
12. Faria, T.Q., et al., *Protein stabilisation by compatible solutes: effect of mannosylglycerate on unfolding thermodynamics and activity of ribonuclease A.* Chembiochem, 2003. **4**(8): p. 734-41.
13. Faria, T.Q., et al., *Protein stabilization by osmolytes from hyperthermophiles: effect of mannosylglycerate on the thermal unfolding of recombinant nuclease a from Staphylococcus aureus studied by picosecond time-resolved fluorescence and calorimetry.* J Biol Chem, 2004. **279**(47): p. 48680-91.

14. Faria, T.Q., et al., *Design of new enzyme stabilizers inspired by glycosides of hyperthermophilic microorganisms.* Carbohydr Res, 2008. **343**(18): p. 3025-33.
15. Faria, C., et al., *Inhibition of formation of alpha-synuclein inclusions by mannosylglycerate in a yeast model of Parkinson's disease.* Biochim Biophys Acta, 2013. **1830**(8): p. 4065-72.
16. Pais, T.M., et al., *Relationship between protein stabilization and protein rigidification induced by mannosylglycerate.* J Mol Biol, 2009. **394**(2): p. 237-50.
17. Pais, T.M., et al., *Mannosylglycerate stabilizes staphylococcal nuclease with restriction of slow beta-sheet motions.* Protein Sci, 2012. **21**(8): p. 1126-37.
18. Pellarin, R. and A. Caflisch, *Interpreting the aggregation kinetics of amyloid peptides.* J Mol Biol, 2006. **360**(4): p. 882-92.
19. Cerda-Costa, N., et al., *Early kinetics of amyloid fibril formation reveals conformational reorganisation of initial aggregates.* J Mol Biol, 2007. **366**(4): p. 1351-63.
20. Ryoo, H.D., et al., *Unfolded protein response in a Drosophila model for retinal degeneration.* EMBO J, 2007. **26**(1): p. 242-52.
21. Empadinhas, N., et al., *A gene from the mesophilic bacterium Dehalococcoides ethenogenes encodes a novel mannosylglycerate synthase*. J Bacteriol, 2004. **186**(13): p. 4075-84.
22. Borges, N., et al., *Specialized roles of the two pathways for the synthesis of mannosylglycerate in osmoadaptation and thermoadaptation of Rhodothermus marinus.* J Biol Chem, 2004. **279**(11): p. 9892-8.
23. Maymo-Gatell, X., et al., *Isolation of a bacterium that reductively dechlorinates tetrachloroethene to ethene.* Science, 1997. **276**(5318): p. 1568-71.
24. Spivey, H.O. and J. Ovadi, *Substrate channeling.* Methods, 1999. **19**(2): p. 306-21.
25. Walther, R.F. and F. Pichaud, *Immunofluorescent staining and imaging of the pupal and adult Drosophila visual system.* Nat Protoc, 2006. **1**(6): p. 2635-42.
26. Santos, H., P. Lamosa, and N. Borges, *Characterization and Quantification of Compatible Solutes in (Hyper)thermophilic Microorganisms.* Methods in Microbiology, 2006. **35**: p. 171-198.
27. Silva, Z., et al., *Combined effect of the growth temperature and salinity of the medium on the accumulation of compatible solutes by Rhodothermus marinus and Rhodothermus obamensis.* Extremophiles, 1999. **3**(2): p. 163-72.

Chapter VI

Final discussion

6.1. Final discussion

Here we provide a discussion of the main findings described in the previous research chapters and we also highlight some future perspectives.

In this work, we developed new transgenic *Drosophila* models for PD and HD (Chapter I). The model for PD is based on the overexpression of EGFP-tagged versions of a wild-type and the A30P familiar mutant form of human α-syn. The HD model is based on the overexpression of mCherry-tagged versions of a wild-type (19Q) and a mutant (97Q) form of human Htt. Previous *Drosophila* models for PD based on the overexpression of human α-syn, express this protein without fluorescent tags [1]. To the best of our knowledge, our transgenic UAS lines for PD are the only ones encoding fluorescent-tagged versions of α-syn, which constitutes a significant improvement that allows an efficient imaging of these proteins in vivo, avoiding possible artifacts derived from fixation of tissues and the use of antibodies.

PD and HD are two common human neurodegenerative diseases with no cures available and associated to the malfunction of the basal ganglia, which clinically manifests in the motor dysfunction symptoms typically observed in patients. During the last two decades, the intense research in the genetic bases of these pathologies permitted the identification of loci that, when mutated, cause the disease. In PD, α-syn is one of the major molecular players, and in HD, Htt was identified as its monogenic cause. These proteins share some important molecular features, namely, they are both highly expressed in the brain and very prone-to-aggregate and to form intraneuronal protein inclusions. Furthermore, and very importantly, the exact biological function of α-syn and Htt remains unclear. In this study, using our *Drosophila* models, we were specifically interested in studying how the subcellular localization of α-syn and the N-terminal phosphorylation of mutant Htt may affect the

development of PD and HD, respectively. Additionally, we aimed to study how these neuronal proteins interact at the functional and genetic levels.

Using our newly established *Drosophila* model for PD, we investigated the molecular determinants of the subcellular localization of α-syn (Chapter II). Taking advantage of the Gal4/UAS system, we induced the targeted expression of the wild-type and the mutant A30P α-syn in the eye using the sGMR-Gal4 driver. We observed a differential phenotype for the two versions of α-syn, in terms of subcellular localization in the photoreceptors: while wild-type α-syn was enriched in pre-synaptic terminals, mutant α-syn was distributed throughout the cytoplasm of the photoreceptors, both in cell bodies and axons (Fig. 2.3). The synaptic enrichment of wild-type α-syn in *Drosophila* is consistent with the normal intracellular distribution of α-syn in the vertebrate nervous system [2-5]. Our observation that A30P α-syn loses this synaptic enrichment is coherent with a previous study observing a less efficient axonal transport of familiar mutant forms of α-syn in rat cortical neurons in culture [6]. The phenotypes observed in our *Drosophila* model were not a consequence of different expression levels (Fig. 2.4) or of different states and/or levels of aggregation (Fig. 2.5 and 2.6).

The subsequent experiments performed in our study were delineated under the basis the hypothesis that the A30P missense mutation, responsible for familiar cases of PD, induces its neurotoxicity both by loss-of-function and gain-of-toxicity mechanisms. The mislocalization and the depletion of mutant α-syn from the axonal terminals may hinder the normal biological functions of α-syn in the synapse, causing synaptic dysfunctions, namely abnormal neurotransmission. Additionally, gain-of toxicity mechanisms may be caused by an increase in the propensity of the A30P mutant form of α-syn to interact, co-aggregate and accumulate with

other neuronal proteins, changing its specific neuronal partners and consequently affecting the normal functions of other neuronal proteins.

In order to test our hypothesis we decided to identify the specific protein partners for the wild-type and A30P mutant versions of α-syn (Fig. 2.7). The results obtained were consistent with the eye phenotype observed in vivo. Most protein partners identified for wild-type α-syn, which we found to mainly accumulate in the synapse, were synaptic proteins and proteins involved in neurotransmission, while the interactome of the A30P mutant, which we found to lose this synaptic enrichment, was mostly associated to mitochondria and/or ribosomes (Table 2.1).

Taking advantage of the list of specific protein partners for wild-type and mutant α-syn, we decided to test the effect of the specific removal of these protein interactors in the differential localization of wild-type and A30P α-syn. The experimental approach chosen was to perform a reverse genetic RNAi screen in the genetic background of flies expressing the A30P mutant version of α-syn in the eye. Based on this genetic screen, we identified 3 candidate modulators of the subcellular localization of A30P α-syn: Tomosyn, Spaghetti Squash and Synaptotagmin 4 (Fig. 2.8). By demonstrating the existence of different specific neuronal partners for the wild-type and mutant version of α-syn and that some of these protein interactors can modulate the subcellular localization of α-syn, we could confirme the pertinence of our hypothesis, previously mentioned.

However, and despite our work, a very important question persists: is the mislocalization of α-syn an early event contributing to the neurodegeneration associated to PD or a consequence of this neurodegenerative process? The answer to this question is still unclear and more studies are needed to clarify this issue. The study and validation of Tomosyn, Spaghetti Squash and Synaptotagmin 4 as modulators of α-syn localization could be an interesting continuation of our work. The first step

would be to prove the physical interaction between these proteins and A30P α-syn. Also, the modulatory effects of α-syn partners should be further evaluated in additional functional assays, such as climbing and survival assays, where the motor ability and mortality of flies would be evaluated. Additionally, we would like to expand this study to other neuronal populations, such as DA neurons, in order to determine if A30P mislocalization is universal – and therefore dependent on the A30P mutation – or if it depends on the cellular context – and therefore can be modulated by genetic or environmental factors.

We believe the continuing of our work could contribute to the knowledge of the molecular mechanisms involved in PD, both in the familiar and in the sporadic forms. Also, this study could help to clarify the role of α-syn's subcellular localization and the possibility of defective axonal transport of this protein being involved in PD pathogenesis.

With our new *Drosophila* model for HD, we studied the role of the phosphorylation of the N-terminal domain of Htt in HD (Chapter III).

We presented evidence suggesting that single phosphorylation events in the first 17 amino acids of the N-terminal domain (NT17) of Htt can modulate mutant Htt aggregation and neurotoxicity, depending on the biological context (Fig. 3.5, 3.6 and 3.7). Most of the studies on the therapeutic potential of NT17 phosphorylation have investigated the protective effect of double phosphorylation events at S13 and S16 residues [7, 8]. However, single phosphorylation events are more common than double phosphorylation events [9]. By demonstrating that single NT17 phosphorylation events are sufficient to reduce the toxicity of mutant Htt, we provide evidences that a simpler and, probably more effective, approach may also have a therapeutic value. Because, the approach based on the double phosphorylation events would imply the overexpression of specific kinases [10], we believe our study could constitute a positive

contribution in the complex path towards the discovery of an effective drug against HD.

Furthermore, we aimed to identify some of the phosphatases involved in the dephosphorylation of NT17 residues, which may constitute a more promising therapeutic target in HD than the kinases.We found that the inhibition of specific protein phosphatases resulted in lower aggregation of mutant Htt (Fig. 3.3). Namely, the inhibition of Cdc25 promoted a reduction of mutant Htt aggregation, both in human H4 cells and in *Drosophila* dopaminergic neurons (Fig. 3.3 and 3.4). We are currently interested in identifying the specific residues in the NT17 domain which are substrates of specific phosphatases that modulate mutant Htt aggregation. The reduction of mutant Htt aggregation induced by the downregulation of Cdc25 is not coherent with our results obtained with the phosphomimic mutants. At this point, we are not able to justify these discrepancies, but we think that one possible explanation could be related with the differences in the experimental approaches used. The overexpression of mutant Htt containing phosphomimic mutations simulates the extreme situation in which the whole pool of mutant Htt is constitutively phosphorylated, while the genetic knockdown of Cdc25 inhibits the dephosphorylation promoted by this specific phosphatase, increasing the fraction of mutant Htt in the phosphorylated state but maintaining a mixed pool of mutant Htt in the phosphorylated and unphosphorylated states. The cell machinery involved in the maintenance of protein homeostasis, such as the ubiquitin–proteasome system, may be sensitive to these differences and induce different responses with different final outcomes, namely by targeting or not misfolded proteins to degradation and/or to form protein inclusions.

We believe the findings described in this thesis may be relevant in the context of HD pathogenesis, since a single NT17 phosphorylation

event could provide a simpler and more efficient molecular target from a therapeutic point of view. We hope the continuing of this study and the successful identification of the specific phosphatases and the exact residues involved in the modulation of mutant Htt aggregation and neurotoxicity could consistently establish the NT17 as a very promising target in the search for new drugs for HD.

Taking advantage of our new *Drosophila* models for PD and HD, we investigated the possible crosstalk between these neuropathologies (Chapter 4). This study arose from the hypothesis that the cellular and molecular mechanisms underlying PD and HD may overlap in the same neuronal cells, of the same patient. Proteins associated to human neuropathologies, which are very prone-to-aggregate, show the tendency to co-aggregate and sequester other neuronal proteins [11-13].

We studied the functional and genetic interaction of α-syn and Htt and besides showing that α-syn and mutant Htt can interact and co-aggregate when co-expressed in vivo (Fig. 4.1, 4.2, 4.3 and 4.4), we demonstrated the occurrence of synergistic deleterious actions of these proteins. Flies co-expressing α-syn and mutant Htt in the same neuronal tissues, showed an increased and more premature neurodegeneration (Fig. 4.5), accompanied by a strong deterioration of the motor function and a significant decrease in the life span (Fig. 4.6).

Our results support the hypothesis that the co-occurrence of α-syn and mutant Htt in neuronal cells could affect disease progression and constitute a real risk for the triggering and co-evolution of pathogenic molecular mechanisms associated with PD and HD.

Consistent with our results, postmortem analyses of HD brains showed that Htt inclusions were also immunoreactive for α-syn [14]. In fact, we believe a patient suffering from HD that an individual harboring an expanded polyQ tract in Htt gene, may have an increased risk of

co-developing some neuropathology related with the malfunction of α-syn. Htt aggregation could affect the normal function of aggregation-prone proteins like α-syn by sequestering them in HD inclusions. The observation that wild-type α-syn is mostly soluble in *Drosophila* neuronal tissues and only aggregates in the presence of mutant Htt further supports this hypothesis.

Our results could explain why some patients diagnosed with HD or other neurodegenerative disease frequently show symptoms typically associated with other neuropathologies, such as PD or AD.

Although the dysfunction of molecular pathways like the autophagy/lysosomal pathway or the disturbance of the normal axonal transport were not investigated in our *Drosophila* models for PD and HD, we think they should be addressed in future works. These mechanisms are involved in the development of neuropathologies associated with the accumulation of misfolded-proteins and it would be important to investigate if they have a causative relation with the phenotypes observed in our fly models.

Finally, in this work, we aimed to demonstrate the utility of our *Drosophila* models for PD and HD in testing potential therapeutic compounds for these pathologies (chapter 5).

The in vivo testing of candidate therapeutic compounds using animal models for human neurodegenerative may help not only in the selection of the most promising compounds for clinical trials, but also guide and inspire the design of new more effective drugs.

A previous study from our collaborators demonstrated the protective effect of MG in a yeast model for PD [15]. We wanted to expand this study by investigating if we could reproduce the protective effect of MG in our *Drosophila* models for PD and HD.

We successfully generated transgenic *Drosophila* lines expressing the bifunctional enzyme MGSD (Fig. 5.3) and demonstrated a beneficial effect of this enzyme in ninaE^{G69D}-mediated ER stress (Fig. 5.4). However, we failed to prove the biosynthesis of MG in *Drosophila* in vivo, making impossible to conclude about the specificity of the MG effect.

The substrate for MGSD is 3-phosphate glycerate, an intermediate of the universal energy pathway glycolysis. Because it is universal, we believe it could be possible to induce the in vivo biosynthesis of MG in *Drosophila* cells. However, several factors could have contributed for the non-accumulation of MG in *Drosophila*. The differences between the optimum temperature for the activity of MGSD (50 ºC) and the normal temperatures to cultivate flies (25 ºC), may be one of these factors. Alternative causes may be related with genetic and molecular determinants specific of *Drosophila* cells, which may lack the proper conditions for the correct folding of MGSD or may have low levels of some metabolites (namely, 3-phosphate glycerate) available to be converted into MG.

Based on the tempting hypothesis that by manipulating the cellular concentration of metabolites involved in the biosynthesis of MGSD, such as 3-phosphate glycerate, we could increase the chances of successfully accumulate MG in *Drosophila*, we decided to genetically modify the glycolytic pathway. We knocked down phosphoglycero-mutase, the enzyme responsible for the catalysis of the glycolytic intermediate 3-phosphate glycerate, the MGSD substrate, to 2-phosphate glycerate. This experiment was performed in the eye, using the sGMR-Gal4 driver. In future experiments, this same experimental approach should be tested in different tissues, which may offer specific genetic and molecular determinants that can be more advantageous for the biosynthesis of MG.

We think our study supports a view where the mechanisms associated to different human neuropathologies could be very significantly

overlapped, at the cellular and molecular levels. In fact, from a list of top-ranked protein interactors of Htt in the mammalian brain, constituted by 17 proteins, 9 were also identified in our study as being α-syn's interactors, further supporting the view of a possible strong proteomic crosstalk between PD and HD [16]. The continuing of the study of the interactomes associated to particular human neurodegenerative diseases, namely by characterizing the protein networks established in the neuronal cells affected, may help to clarify if and how the crosstalk between these pathologies occurs, as well as its relevance in their etiology and evolution.

We hope our new *Drosophila* models for PD and HD may constitute one more useful platform available to scientific community working on PD and HD.

6.2. References

1. Feany, M.B. and W.W. Bender, *A Drosophila model of Parkinson's disease.* Nature, 2000. **404**(6776): p. 394-8.
2. Maroteaux, L., J.T. Campanelli, and R.H. Scheller, *Synuclein: a neuron-specific protein localized to the nucleus and presynaptic nerve terminal.* J Neurosci, 1988. **8**(8): p. 2804-15.
3. Iwai, A., et al., *The precursor protein of non-A beta component of Alzheimer's disease amyloid is a presynaptic protein of the central nervous system.* Neuron, 1995. **14**(2): p. 467-75.
4. Jakes, R., M.G. Spillantini, and M. Goedert, *Identification of two distinct synucleins from human brain.* FEBS Lett, 1994. **345**(1): p. 27-32.
5. Withers, G.S., et al., *Delayed localization of synelfin (synuclein, NACP) to presynaptic terminals in cultured rat hippocampal neurons.* Brain Res Dev Brain Res, 1997. **99**(1): p. 87-94.
6. Saha, A.R., et al., *Parkinson's disease alpha-synuclein mutations exhibit defective axonal transport in cultured neurons.* J Cell Sci, 2004. **117**(Pt 7): p. 1017-24.
7. Gu, X., et al., *Serines 13 and 16 are critical determinants of full-length human mutant huntingtin induced disease pathogenesis in HD mice.* Neuron, 2009. **64**(6): p. 828-40.
8. Mishra, R., et al., *Serine Phosphorylation Suppresses Huntingtin Amyloid Accumulation by Altering Protein Aggregation Properties.* J Mol Biol, 2012.
9. Bustamante, M.B., et al., *Detection of huntingtin exon 1 phosphorylation by Phos-Tag SDS-PAGE: Predominant phosphorylation on threonine 3 and regulation by IKKbeta.* Biochem Biophys Res Commun, 2015. **463**(4): p. 1317-22.
10. Thompson, L.M., et al., *IKK phosphorylates Huntingtin and targets it for degradation by the proteasome and lysosome.* J Cell Biol, 2009. **187**(7): p. 1083-99.
11. Sajjad, M.U., et al., *DJ-1 modulates aggregation and pathogenesis in models of Huntington's disease.* Hum Mol Genet, 2014. **23**(3): p. 755-66.
12. Blum, D., et al., *Mutant huntingtin alters Tau phosphorylation and subcellular distribution.* Hum Mol Genet, 2014.
13. Badiola, N., et al., *Tau Enhances alpha-Synuclein Aggregation and Toxicity in Cellular Models of Synucleinopathy.* PLoS One, 2011. **6**(10): p. e26609.
14. Charles, V., et al., *Alpha-synuclein immunoreactivity of huntingtin polyglutamine aggregates in striatum and cortex of Huntington's disease patients and transgenic mouse models.* Neurosci Lett, 2000. **289**(1): p. 29-32.

15. Faria, C., et al., *Inhibition of formation of alpha-synuclein inclusions by mannosylglycerate in a yeast model of Parkinson's disease.* Biochim Biophys Acta, 2013. **1830**(8): p. 4065-72.
16. Shirasaki, D.I., et al., *Network organization of the huntingtin proteomic interactome in mammalian brain.* Neuron, 2012. **75**(1): p. 41-57.